Complete inference of causal relationships in dynamical systems

Zoltán Somogyvári

Research Centre for Physics

Department of Computational Sciences
Theoretical Neuroscience and Complex Systems Research Group

Determination of causal effects in time series

Is there any possibility to identify directed causal relationships from two observed data series, without experimental intervention?

We surely can measure correlation, but correlation and causality are different things. Moreover correlation is an asymmetrical relation while causality can be unidirectional.

Is there a way to distinguish directional and bidirectional (circular) causality or to reveal hidden common cause?

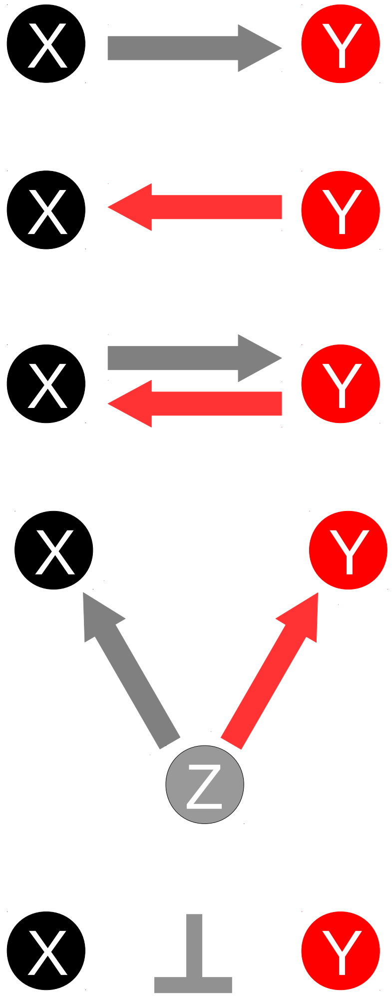

Personalized medicine:
Causality analysis in epilepsy

Is there a (multiple) Seizure Onset Zone (SOZ) or rather an epileptic network?

The SOZ is causal source during the seizure?

What about during interictal periods?

Sabesan, S., Good, L.B., Tsakalis, K.S., Spanias, A., Treiman, D.M., Iasemidis, L.D.: Information flow and application to epileptogenic focus localization from intracranial EEG. IEEE Trans Neural Syst Rehabil Eng 17(3), 244–253 (2009)

Epstein, C.M., Adhikari, B.M., Gross, R., Willie, J., Dhamala, M.: Application of high-frequency Granger causality to analysis of epileptic seizures and surgical decision making. Epilepsia 55(12), 2038–2047 (2014)

Seizure onset zone

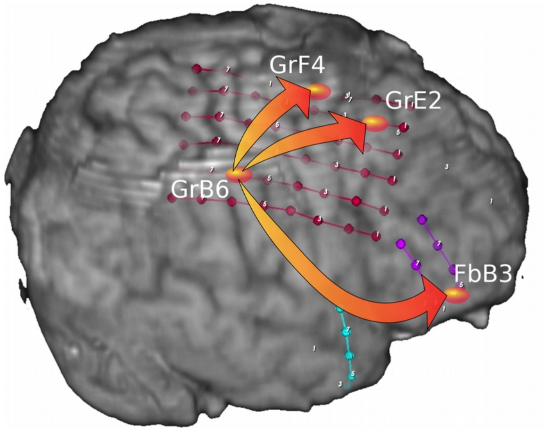

Epileptic network

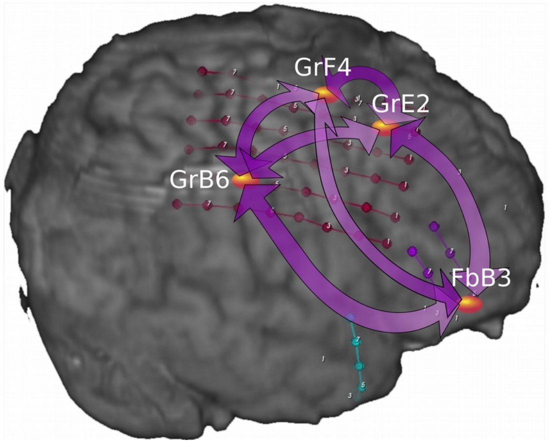

With interventions: Bayesian networks, graphical models, Conditional independence

RAIN	SPRINKLER T	SPRINKLER F
F	0.4	0.6
T	0.01	0.99

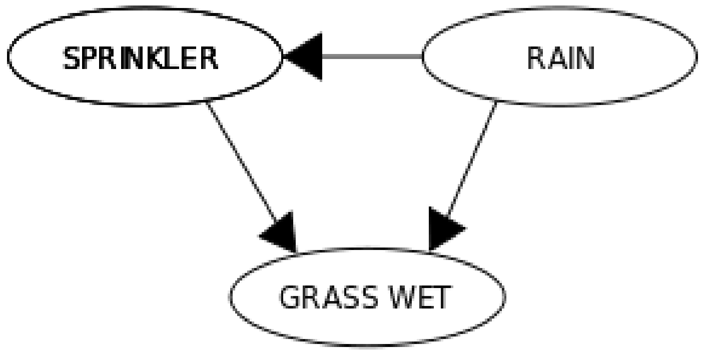

RAIN T	RAIN F
0.2	0.8

SPRINKLER	RAIN	GRASS WET T	GRASS WET F
F	F	0.0	1.0
F	T	0.8	0.2
T	F	0.9	0.1
T	T	0.99	0.01

Judea Pearl

The theory allows to reveal the direction of the dependencies only in specific cases or the direction of the relationships assumed a priory!

Bayesian networks with just observations

Observed dependencies

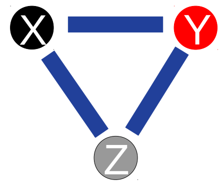

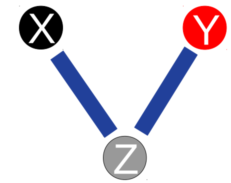

Truth

Forks

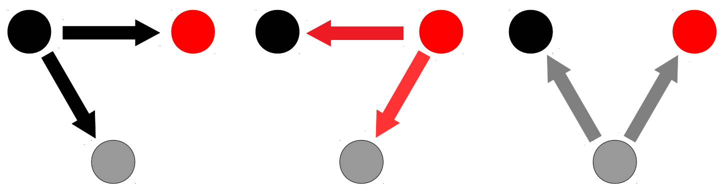

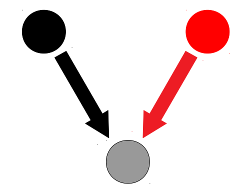

Collider

Chains

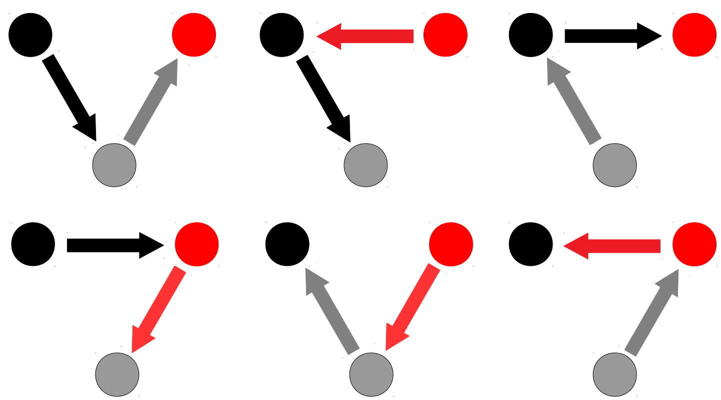

Combined

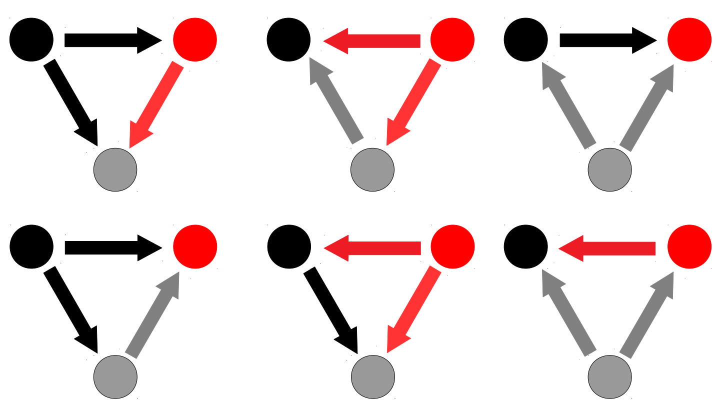

Times series: predictive causality

The original idea of predictive causality came from ***Norbert Wiener***

x → ***y***, if the inclusion of past ***x*** values improves the prediction quality on ***y***

Assuming time delay via the concept of prediction helps to reveal direction!

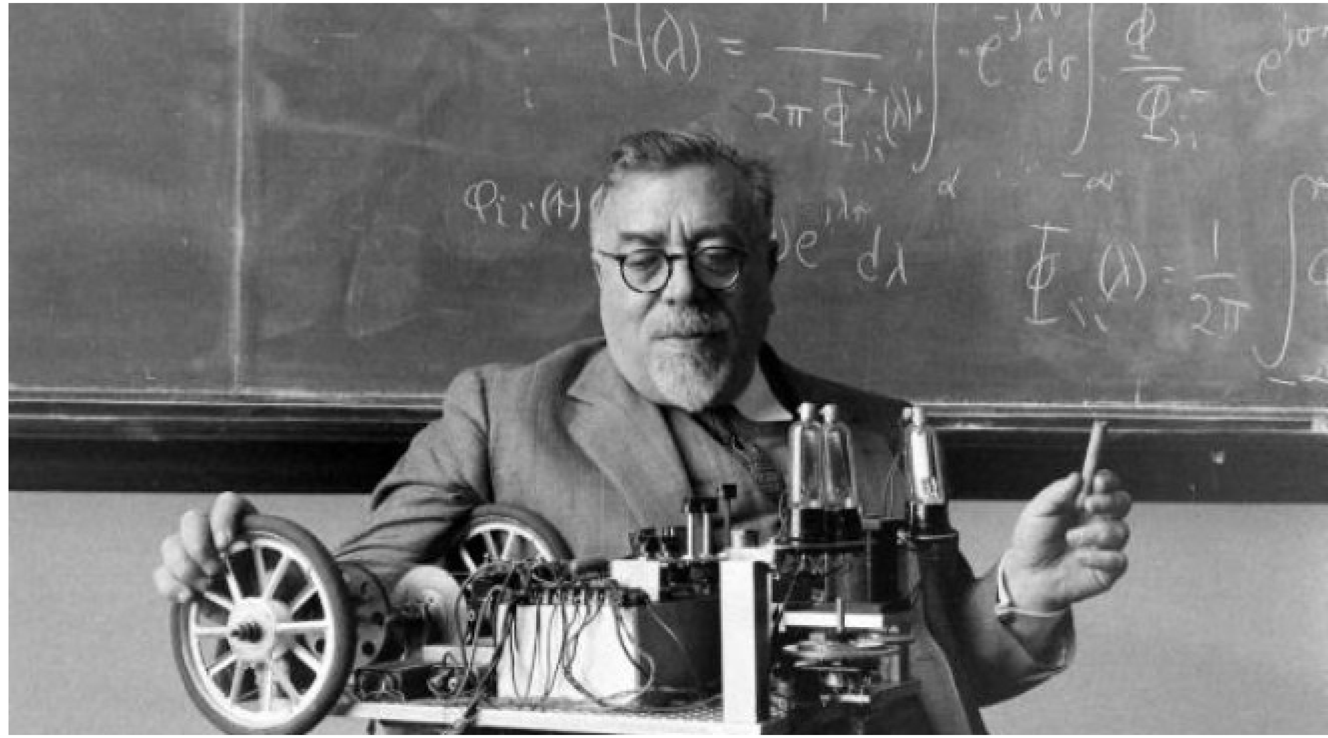

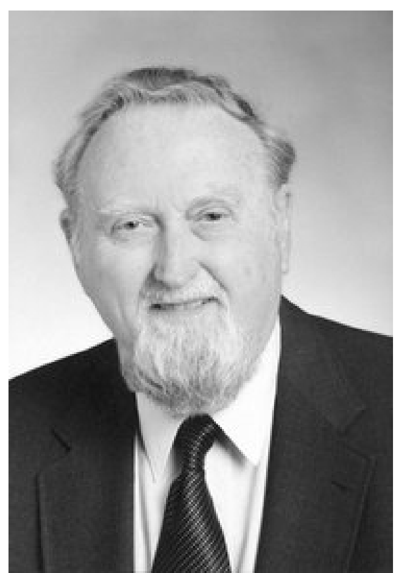

Clive Granger implemented it via autoregressive linear models in 1969

Nobel price in Economic Sciences 2003

Granger- causality

Linear autoregression:

$$x_t = \sum_i a_i x_{t-i} + \varepsilon_1 \qquad x_t = \sum_i c_i x_{t-i} + \sum_i d_i y_{t-i} + \varepsilon_3$$

$$y_t = \sum_i b_i y_{t-i} + \varepsilon_2 \qquad y_t = \sum_i e_i x_{t-i} + \sum_i f_i y_{t-i} + \varepsilon_4$$

$$F_{y \to x} = \ln\left(\frac{var(\varepsilon_1)}{var(\varepsilon_3)}\right)$$

$$F_{x \to y} = \ln\left(\frac{var(\varepsilon_2)}{var(\varepsilon_4)}\right)$$

Evaluation F test:

$$F_{X \to Y} = \frac{\dfrac{var(\epsilon_1) - var(\epsilon_3)}{m}}{\dfrac{var(\epsilon_3)}{T - 2m - 1}}$$

It is sensitive to the model used for the prediction. The limitations of linear autoregressive models can be ameliorated by using nonlinear extensions, kernel solutions or model free transfer entropy method.

The model-free predictive causality: Transfer Entropy

$$T_{X\to Y} = H(y_i|y^{(l)}_{i-t}) - H(y_i|y^{(l)}_{i-t'}, x^{(k)}_{i-\tau})$$

$$= \sum_{y_i, y^{(l)}_{i-t}} p(y_i, y^{(l)}_{i-t}) \log \frac{p(y^{(l)}_{i-t})}{p(y_i, y^{(l)}_{i-t})} - \sum_{y_i, y^{(l)}_{i-t'}, x^{(k)}_{i-\tau}} p(y_i, y^{(l)}_{i-t'}, x^{(k)}_{i-\tau}) \log \frac{p(x^{(k)}_{i-\tau}, y^{(l)}_{i-t})}{p(y_i, y^{(l)}_{i-t'}, x^{(k)}_{i-\tau})}.$$

The framework of Judea Pearl (Bayesian nets) can not handle circular causal relationships.

Neither the Bayesian nets nor the predictive causality principle can not reveal the existence of unobserved hidden common causes

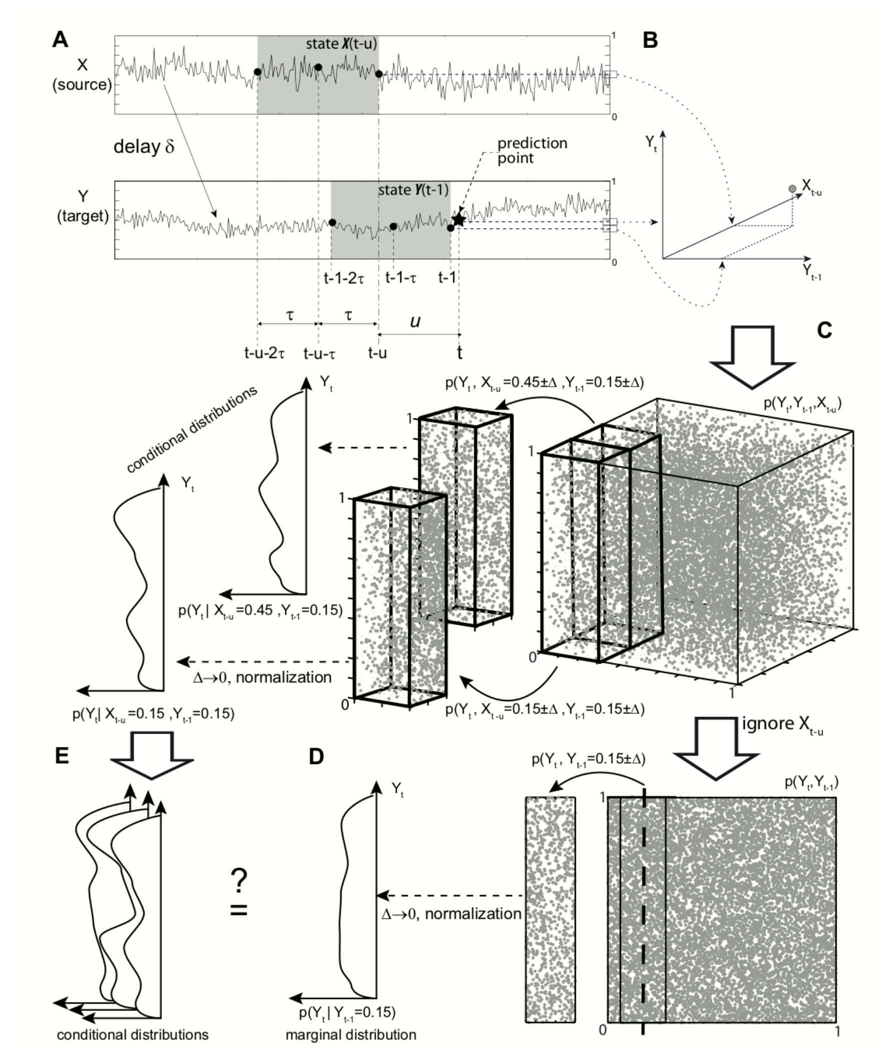

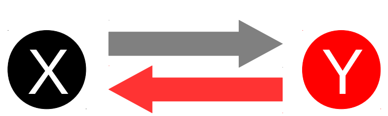

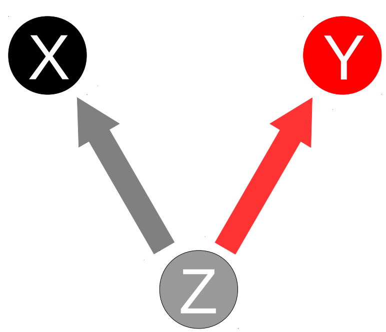

Cross Convergence Map:
A new framework for causality analysis

A new model-free approach, promising:

- Detection of circular causality
- Detection of nonlinear coupling

Detecting Causality in Complex Ecosystems

George Sugihara,[1*] Robert May,[2] Hao Ye,[1] Chih-hao Hsieh,[3*] Ethan Deyle,[1] Michael Fogarty,[4] Stephan Munch[5]

Science **338**, 496 (2012)

It utilizes the Taken's time delay embedding theorem:

The trajectory reconstructed in the state space is topologically equivalent With the trajectory of the system's original trajectory in its real space.

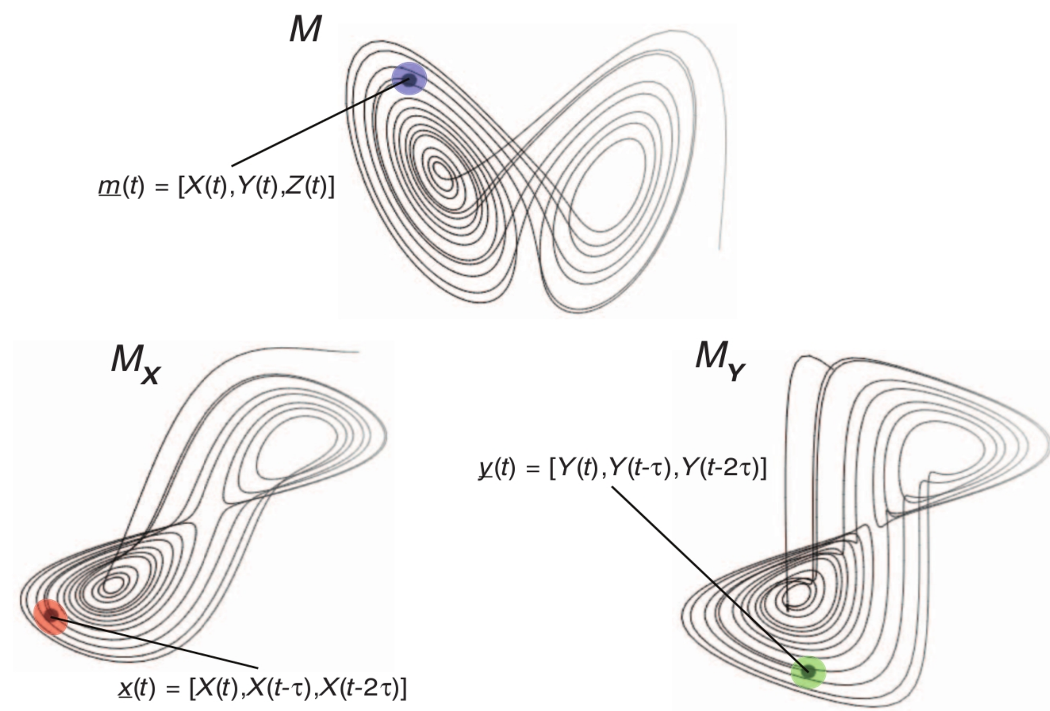

Cross Convergence Map:
A new framework for causality analysis

- Sugihara's method is based on that the consequence is an observation of the cause, thus the cause can be reconstructed from the consequence.
- Points that are neighbors in the state-space of the consequence should be neighbors in the state space of the cause as well.
- This topology preserving property can be tested by the cross mapping method.

Detecting Causality in Complex Ecosystems

George Sugihara,[1*] Robert May,[2] Hao Ye,[1] Chih-hao Hsieh,[3*] Ethan Deyle,[1] Michael Fogarty,[4] Stephan Munch[5]

Science **338**, 496 (2012)

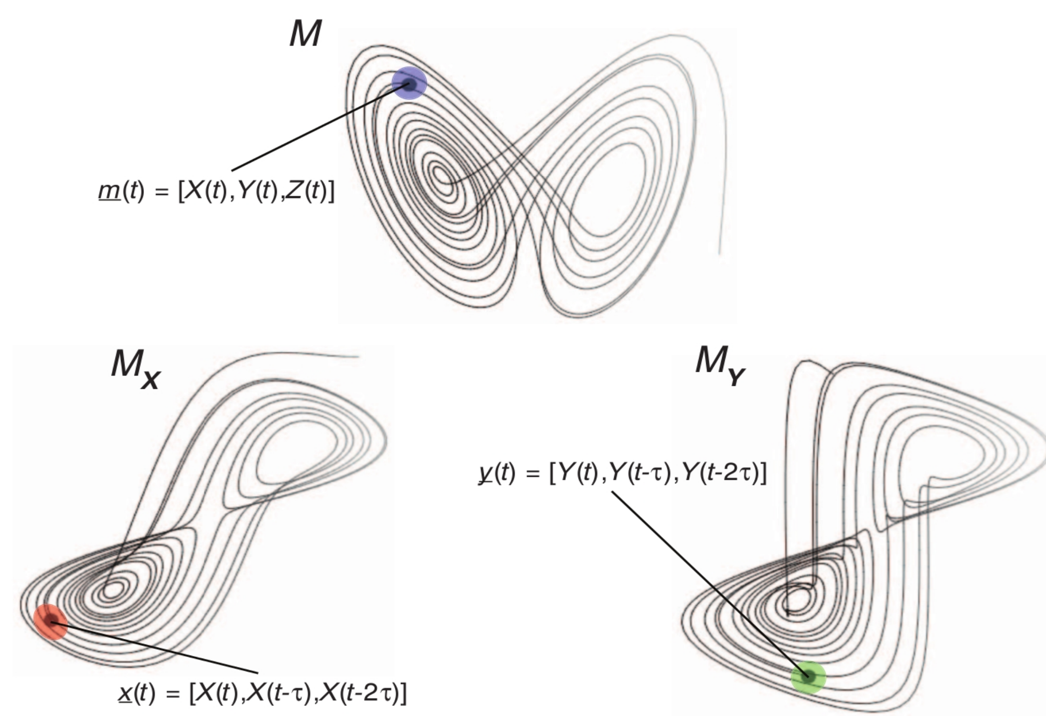

Our first model system: The logistic map

$$x_{t+1}=r\,x_t(1-x_t)$$

A one dimensional, discreet-time dynamical system implementing stretching an folding transformations.

It can exhibit different dynamical behavior, from stable fixpoint, through periodic oscillations to chaos, depending on the parameter r.

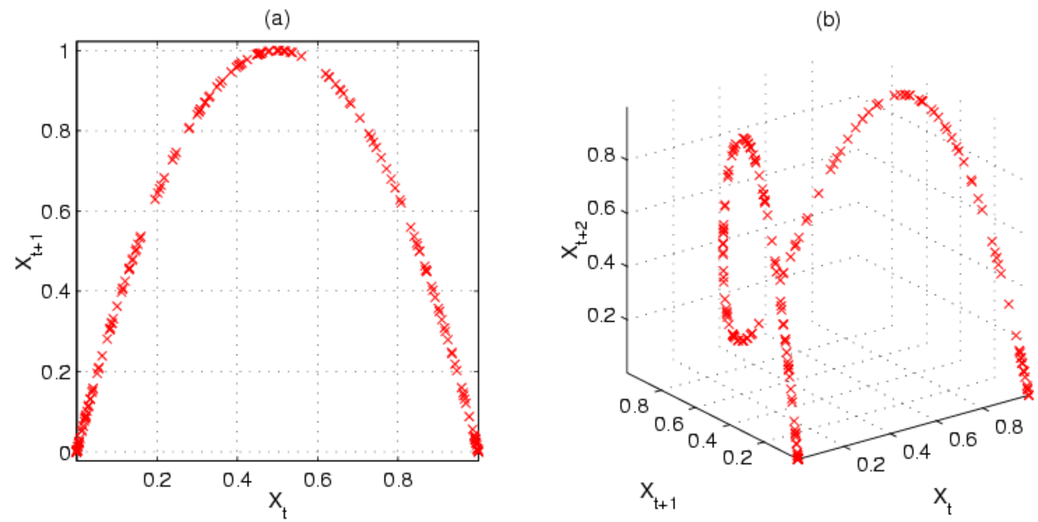

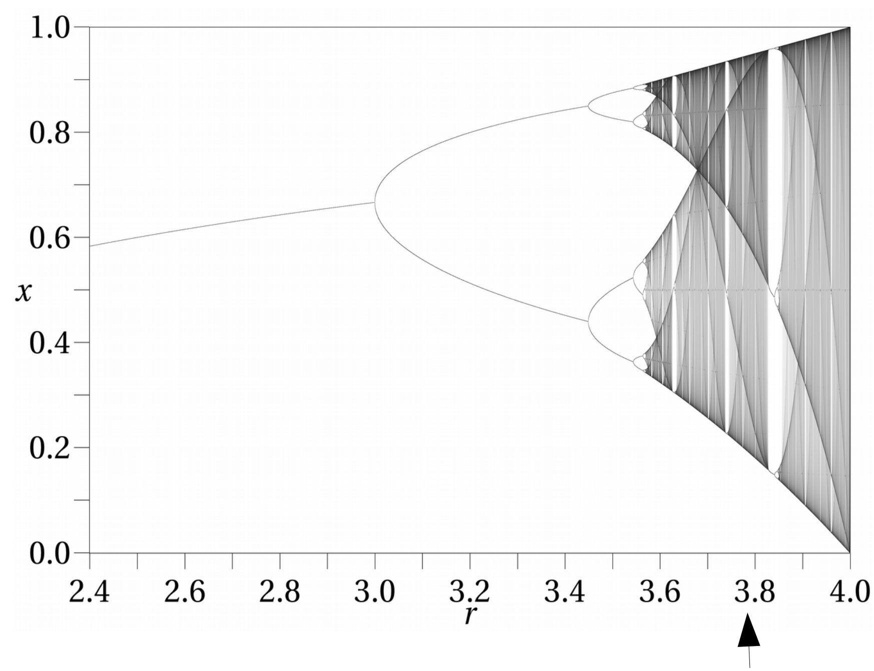

We choose r = 3.8 which ensures chaotic behavior.

Two coupled logistic maps

Case I.: Circular, nonlinear coupling

$x_{n+1}=r_x x_n((1-x_n)+b_{yx}y_n)$

$y_{n+1}=r_y y_n((1-y_n)+b_{xy}x_n)$

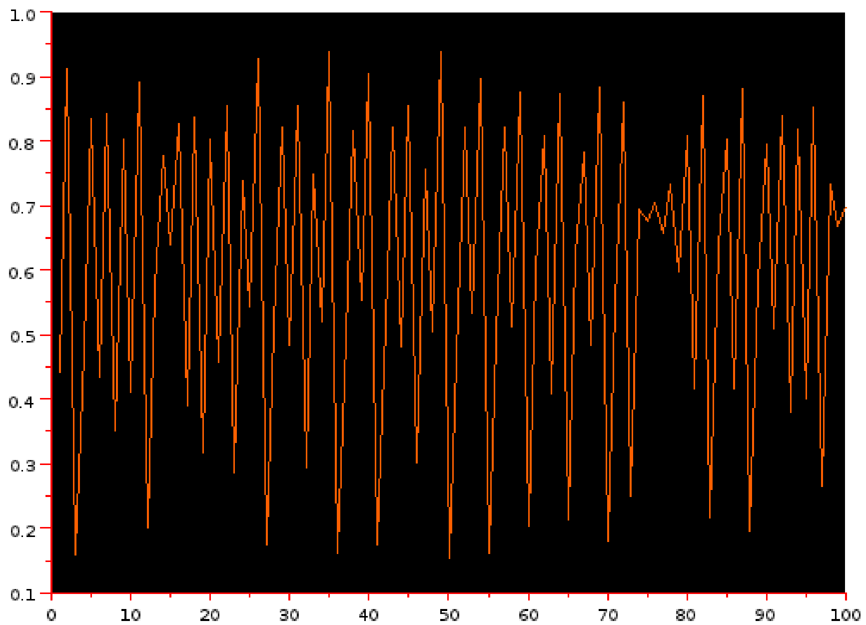

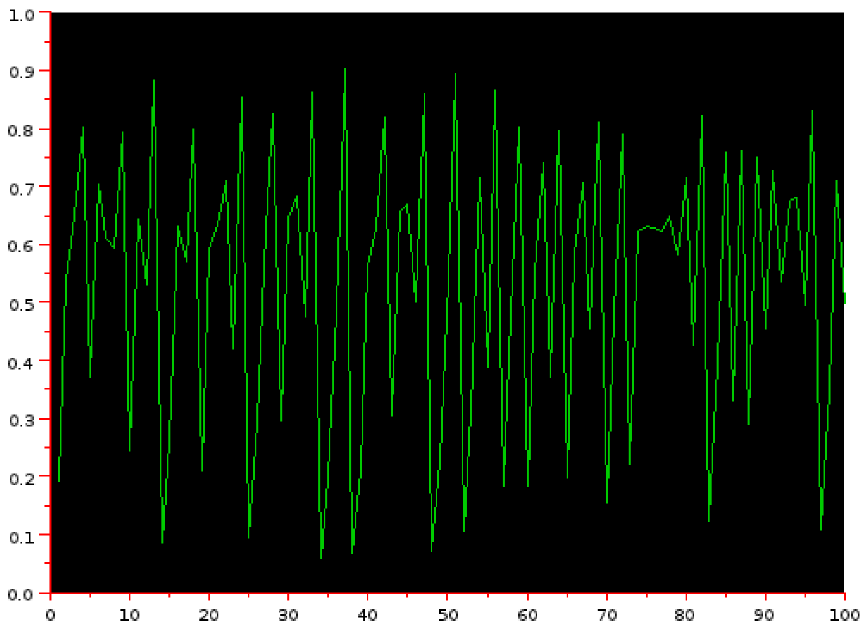

$r_x=r_y=$**3.8** so both maps are in the chaotic regime

Phase-space reconstruction based on delayed maps

$x_{n+1}=r_x x_n((1-x_n)+b_{yx}y_n)$

$y_{n+1}=r_y y_n((1-y_n)+b_{xy}x_n)$

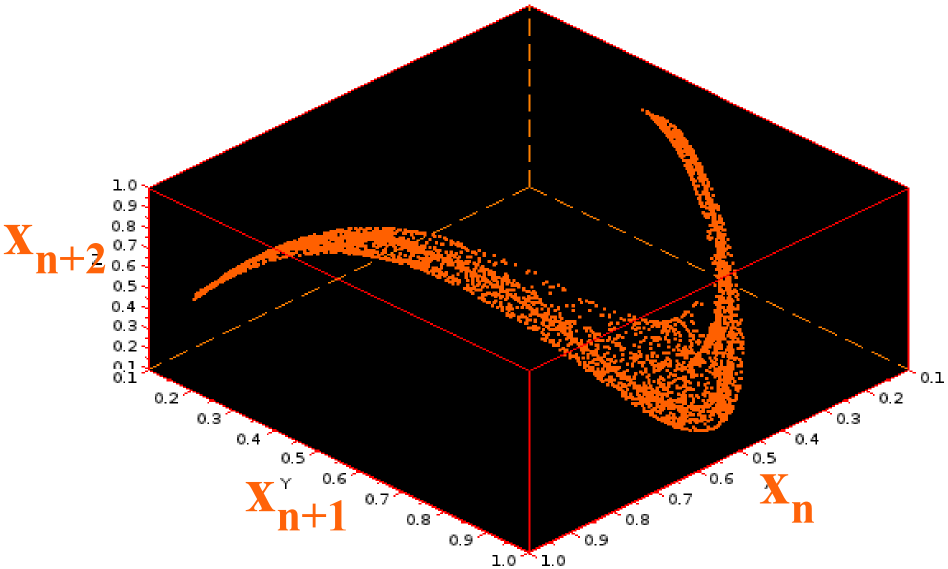

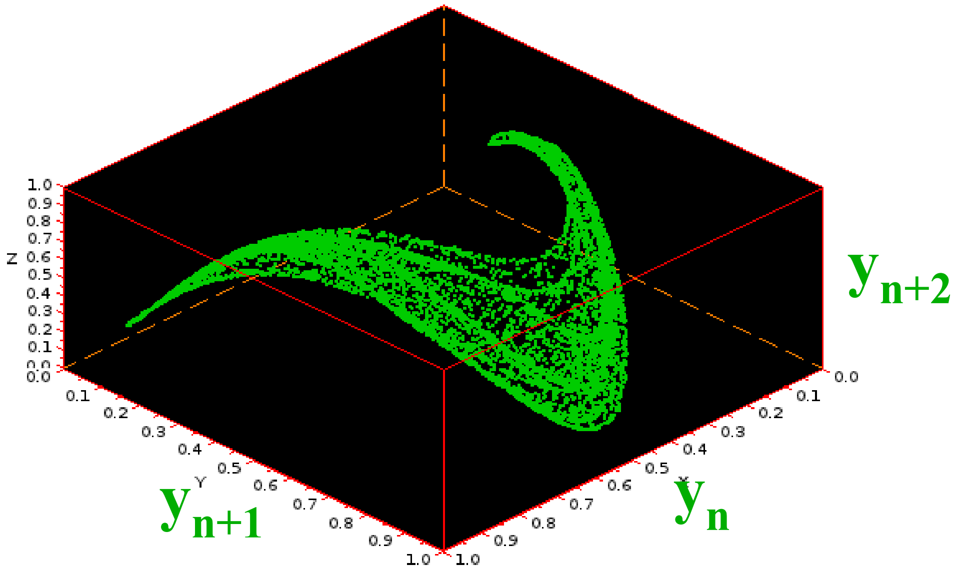

Reconstructed state-space from the first data series in 3 embedding dimension

Reconstructed state-space from the second data series in 3 embedding dimension

Both dataset formed a 2D manifold in the 3D embedding space.

Phase-space reconstruction based on delayed maps

$x_{n+1}=r_x x_n((1-x_n)+b_{yx}y_n)$

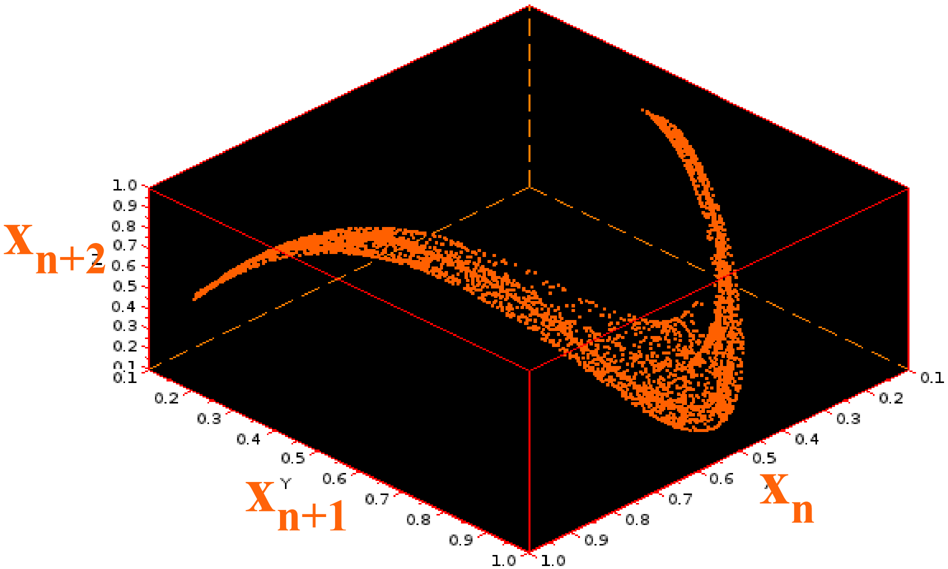

Reconstructed state-space from the first data series in 3 embedding dimension

$y_{n+1}=r_y y_n((1-y_n)+b_{xy}x_n)$

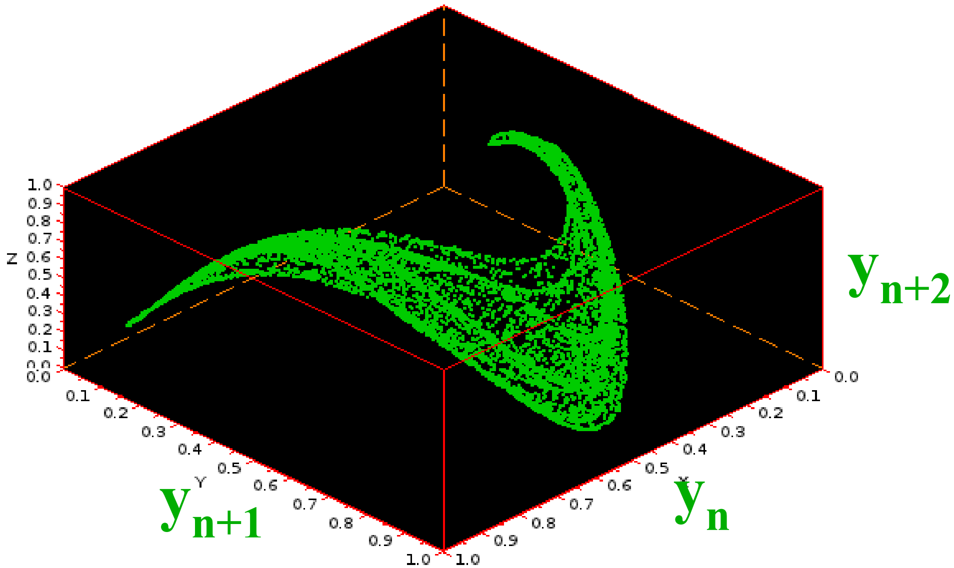

Reconstructed state-space from the second data series in 3 embedding dimension

Both dataset formed a 2D manifold in the 3D embedding space.

Existence of a diffeomorphism

In case of causal connections, the reconstructed manifold sholud be topologically equivalent according to the Takens' theorem. But, how to test it?

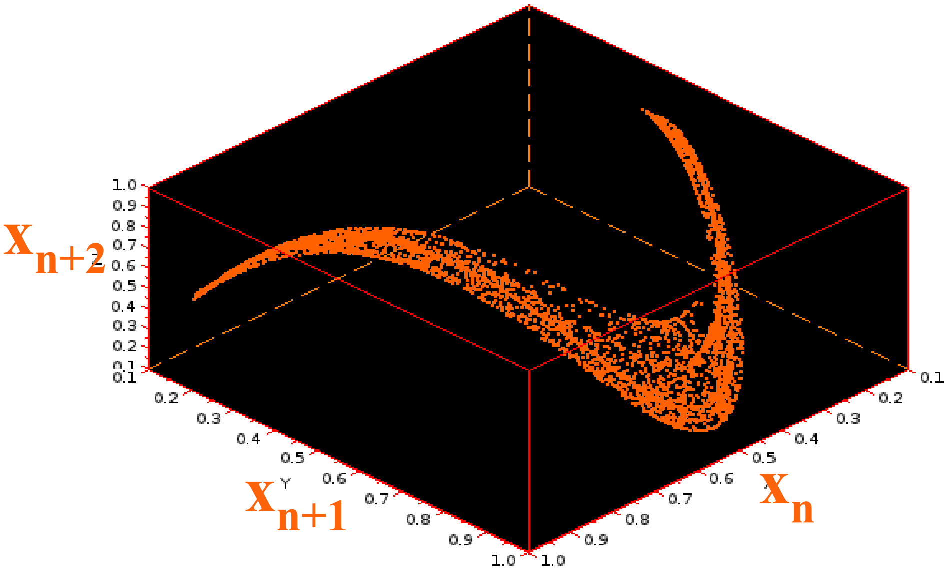

Reconstructed state-space from the first data series in 3 embedding dimension

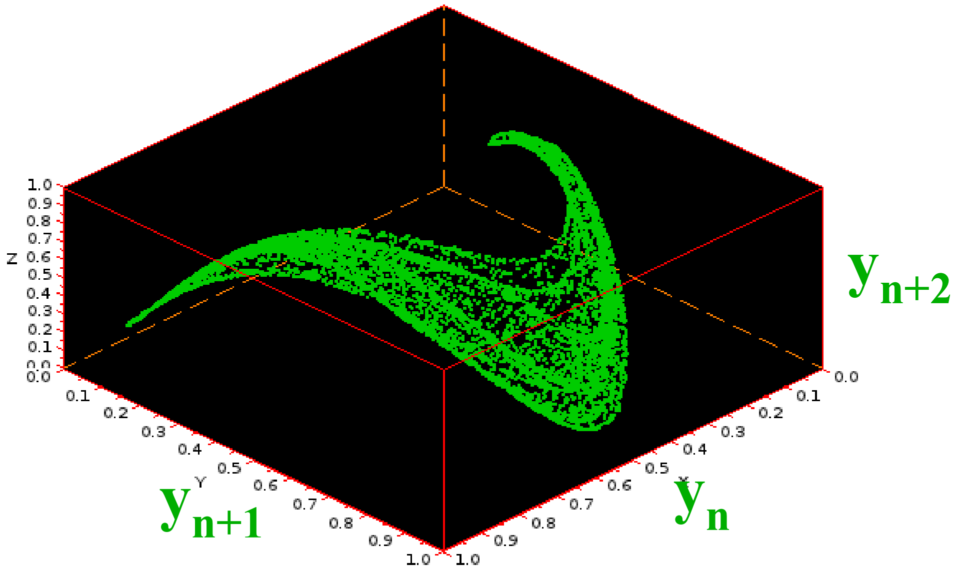

Reconstructed state-space from the second data series in 3 embedding dimension

Both dataset formed a 2D manifold in the 3D embedding space.

Sugihara's method: Convergent Cross mapping

Choose a point!

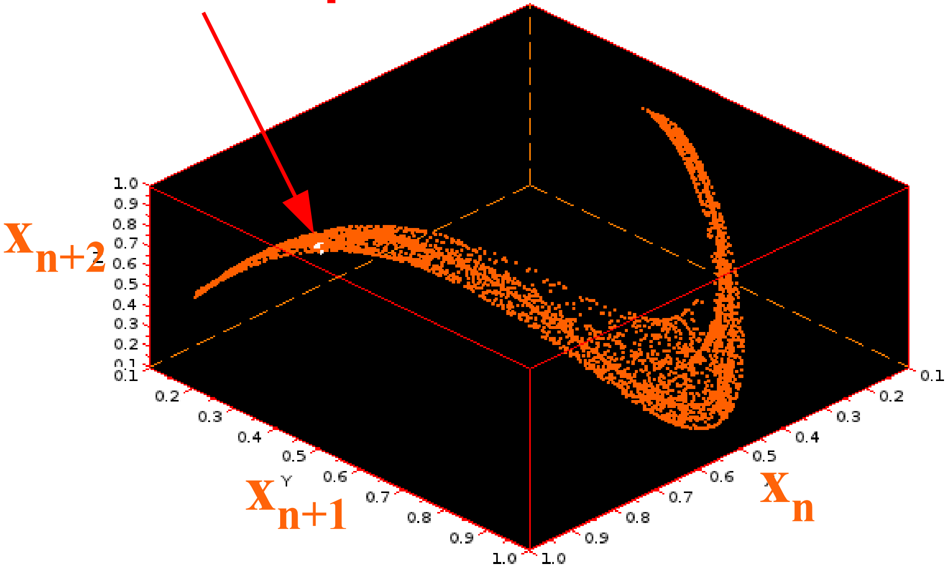

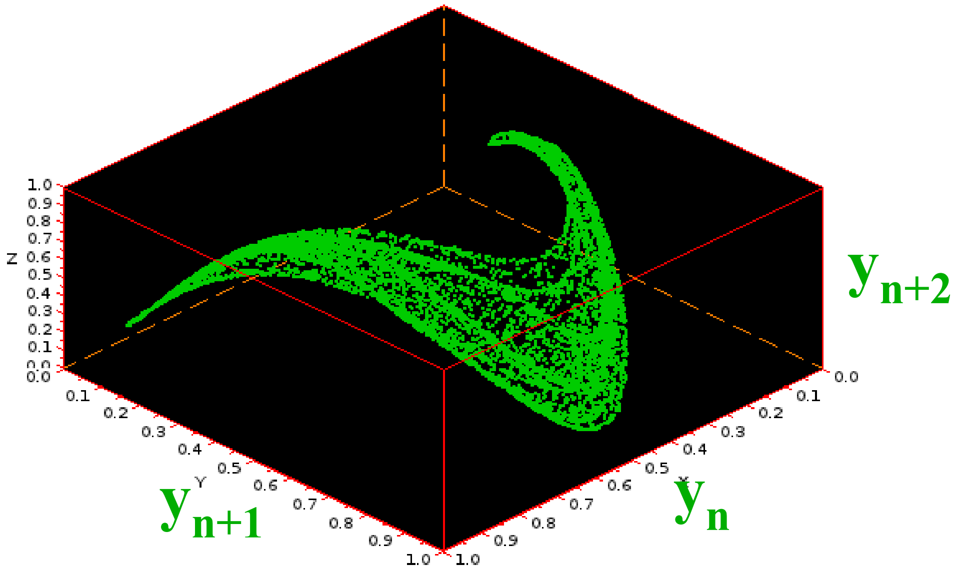

Reconstructed state-space from the first data series in 3 embedding dimension

Reconstructed state-space from the second data series in 3 embedding dimension

Both dataset formed a 2D manifold in the 3D embedding space

Sugihara's method: Convergent Cross mapping

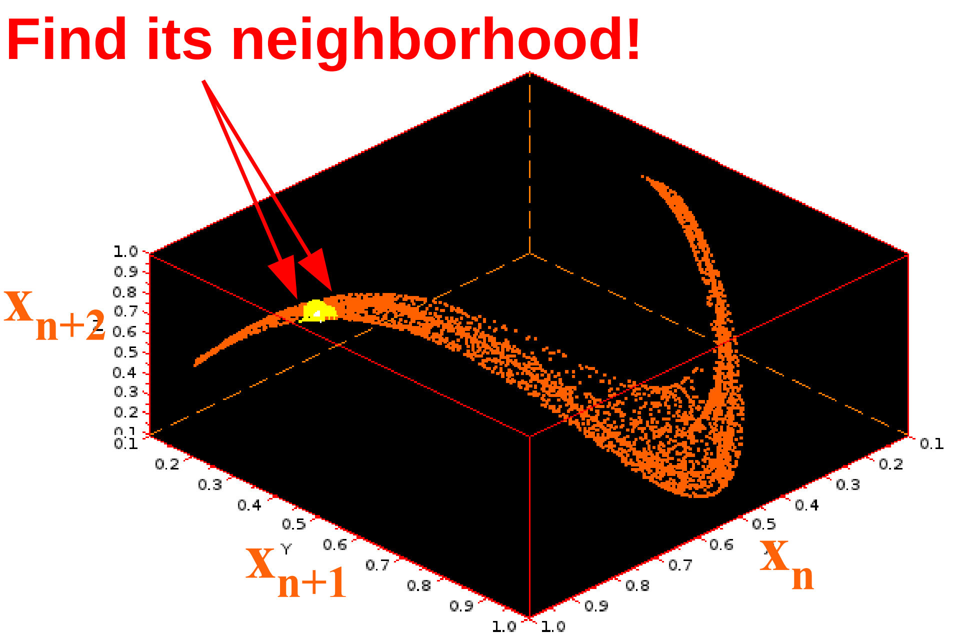

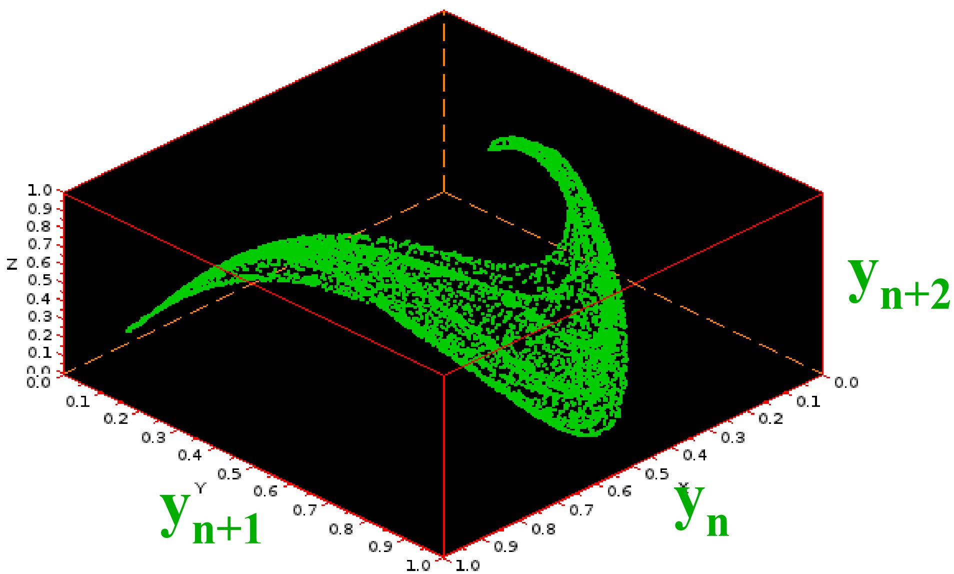

Reconstructed state-space from the first data series in 3 embedding dimension

Reconstructed state-space from the second data series in 3 embedding dimension

Both dataset formed a 2D manifold in the 3D embedding space.

Sugihara's method: Convergent Cross mapping

The images of the neighbors remained close to each other and to the image of the original point

Find the same time points in the other state space

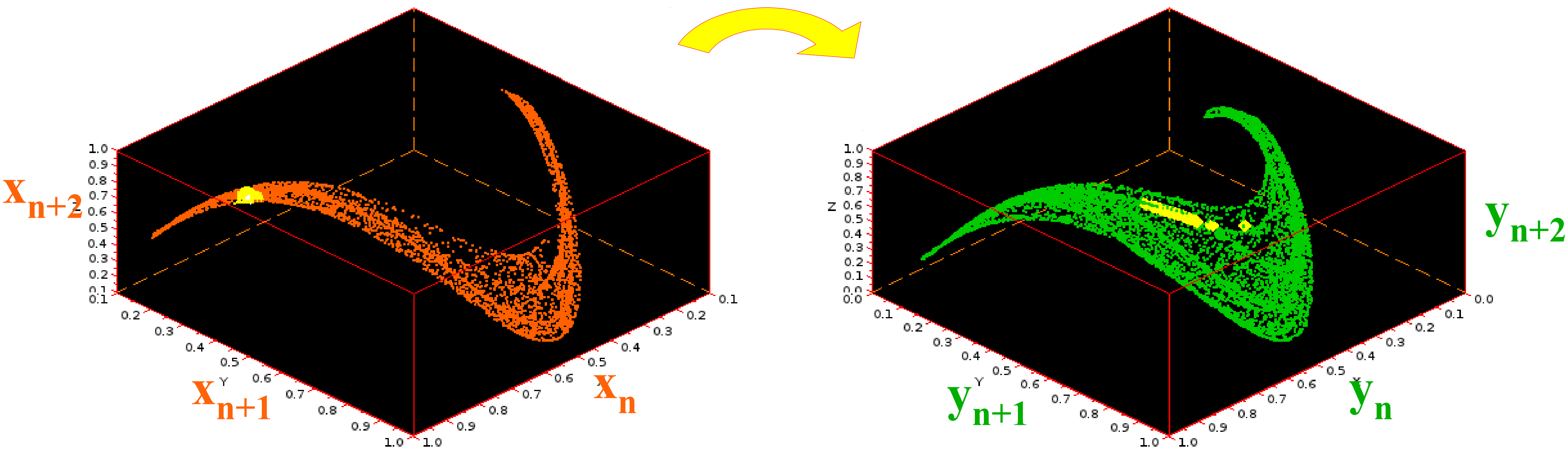

Reconstructed state-space from the first data series in 3 embedding dimension

Reconstructed state-space from the second data series in 3 embedding dimension

Lets do it for many points! If the neighbors in the first space are neighbors in the the second space as well, then the second variable is causal to the first one.

Sugihara's method: Convergent Cross mapping

In case of circular causality the mapping should work in both directions!

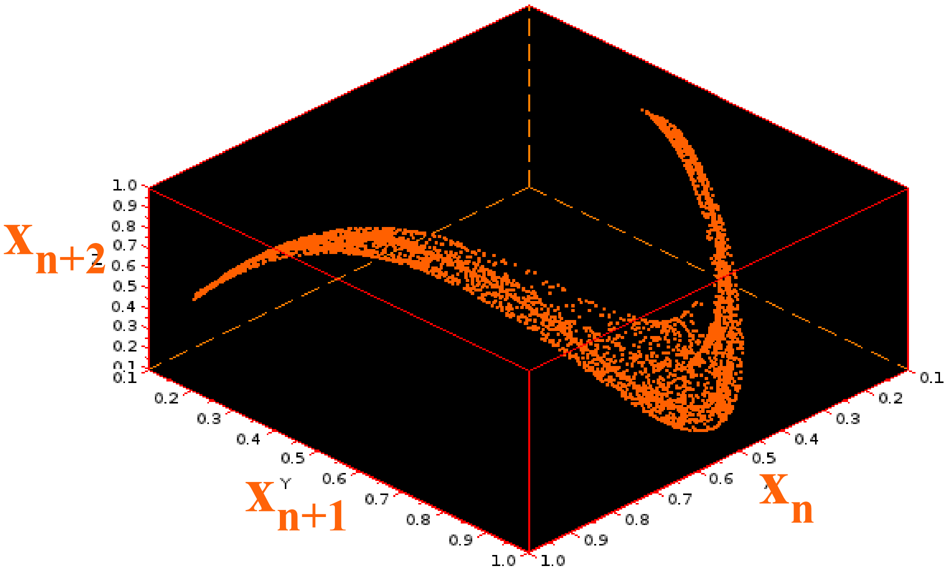

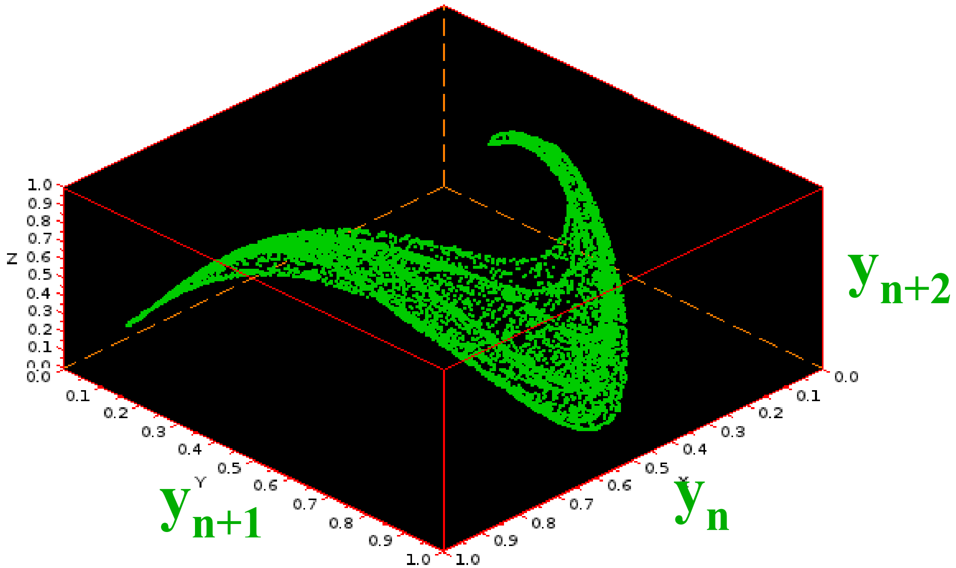

Reconstructed state-space from the first data series in 3 embedding dimension

Reconstructed state-space from the second data series in 3 embedding dimension

Let us do it into the other direction!

Sugihara's method: Convergent Cross mapping

Let us do it into the other direction!

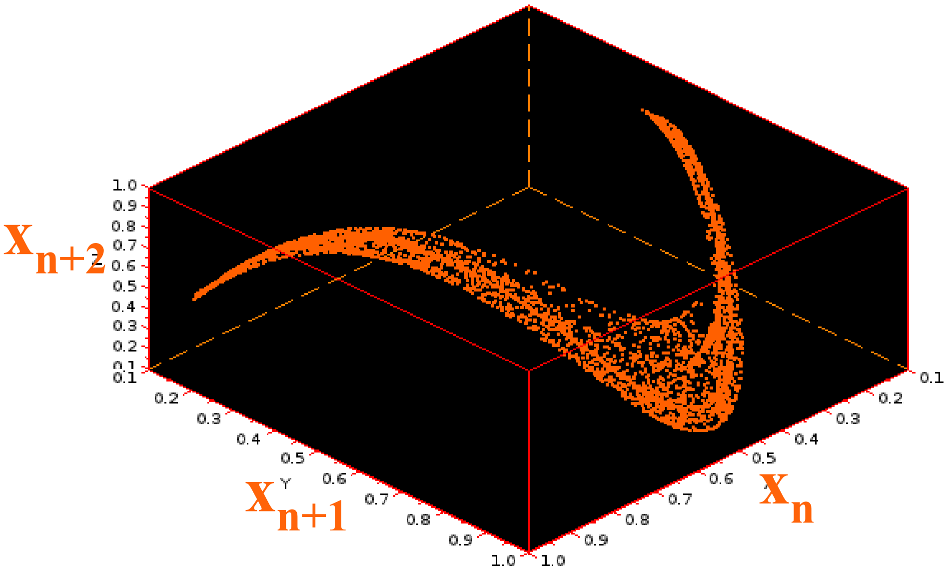

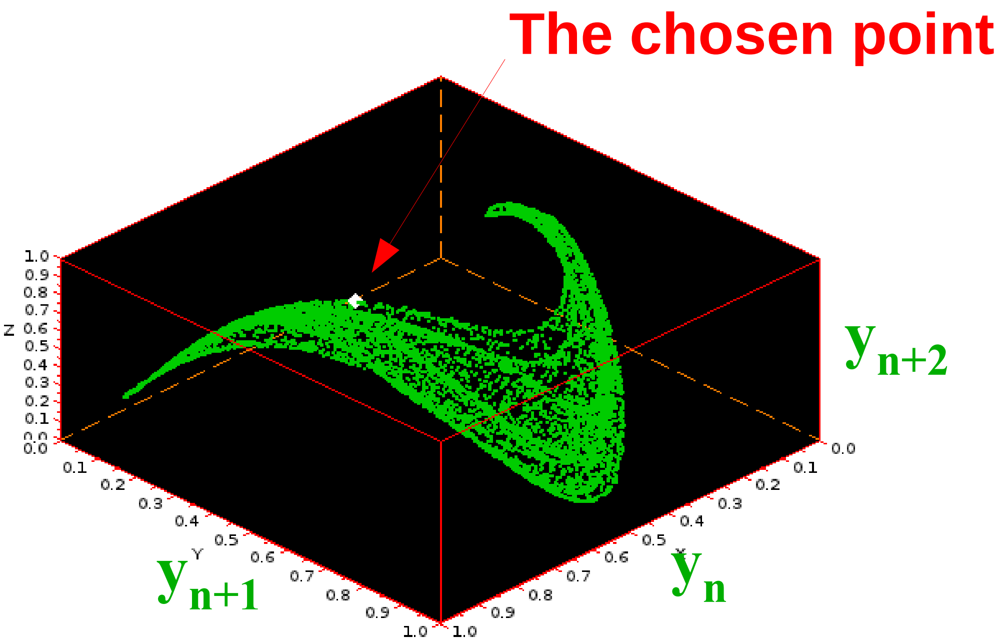

Reconstructed state-space from the first data series in 3 embedding dimension

Reconstructed state-space from the second data series in 3 embedding dimension

Sugihara's method: Convergent Cross mapping

Let us do it into the other direction!

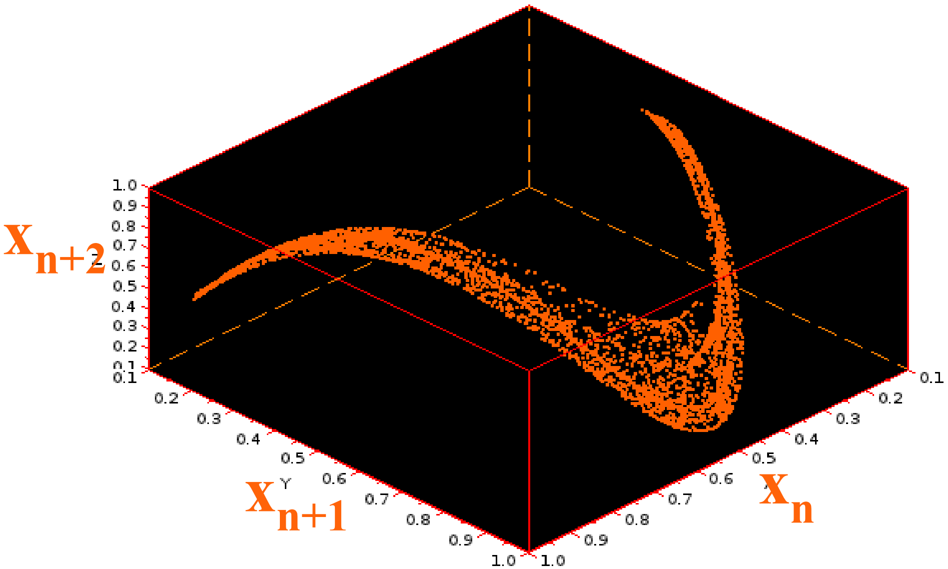

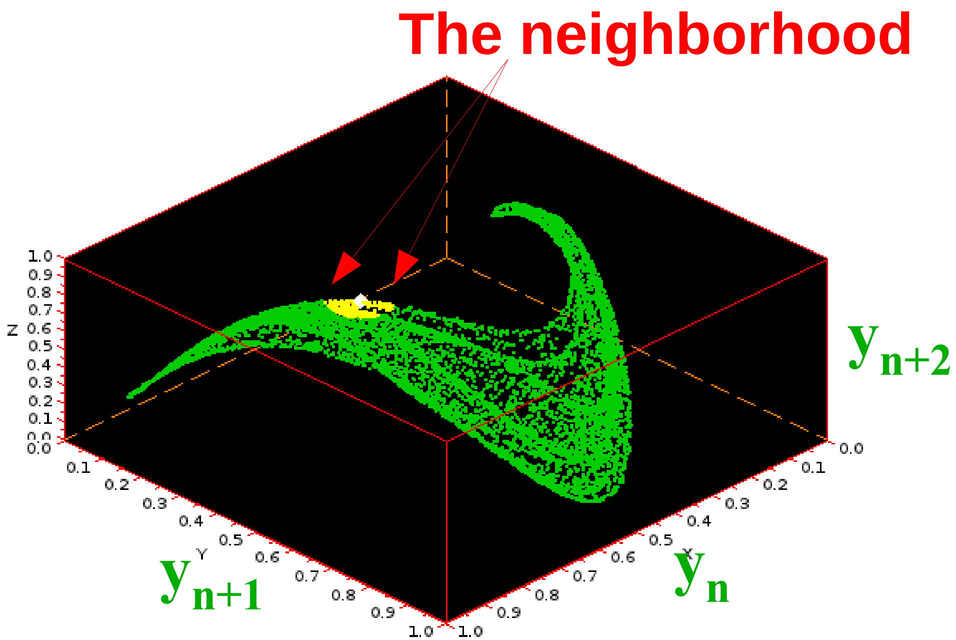

Reconstructed state-space from the first data series in 3 embedding dimension

Reconstructed state-space from the second data series in 3 embedding dimension

Sugihara's method: Convergent Cross mapping

The mapping worked well into both directions!
This is the sign of circular causality.

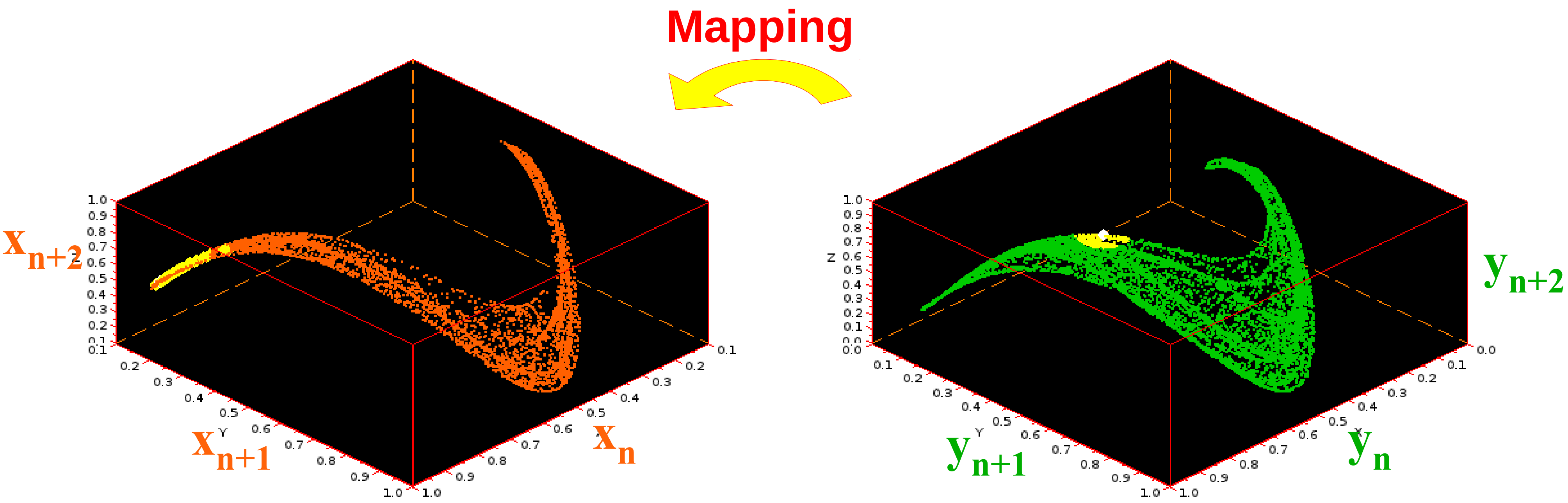

Reconstructed state-space from the first data series in 3 embedding dimension

Reconstructed state-space from the second data series in 3 embedding dimension

Cross mapping in case of unidirectional interactions

Case II.: Unidirectional, nonlinear coupling

$x_{n+1}=r_x x_n((1-x_n)+b_{yx}y_n)$ $\quad$ $y_{n+1}=r_y y_n(1-y_n)$

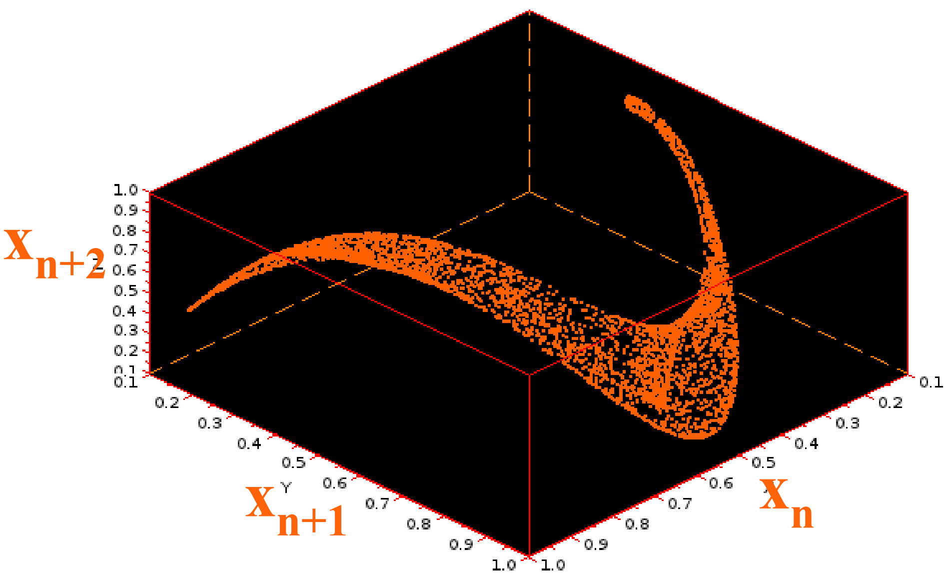

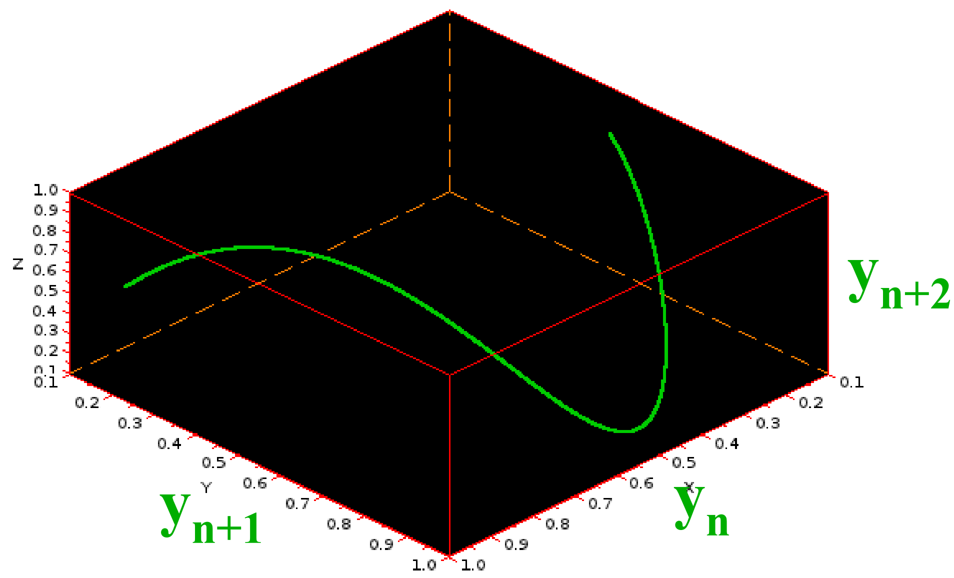

The consequence $\quad$ **The cause**

While the consequence formed a 2D manifold, the cause resulted an only 1D manifold in the 3D embedding space!

Cross mapping in case of unidirectional interactions

Mapping works well from consequence to cause

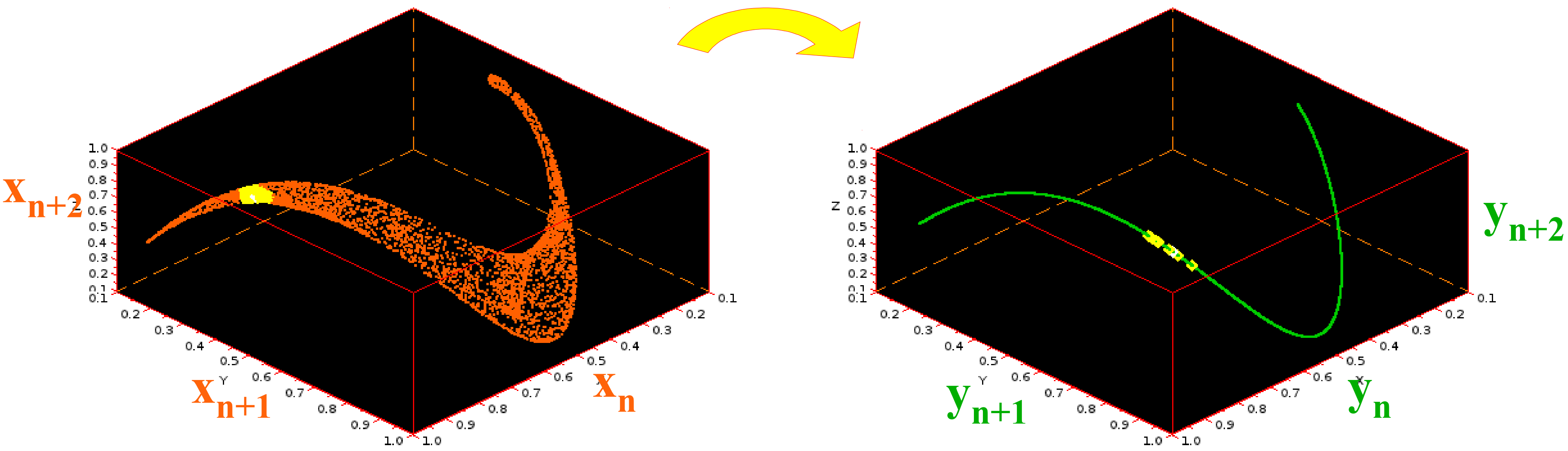

The consequence

The cause

While the first dataset formed a 2D manifold, the second dataset resulted an only 1D manifold in the 3D embedding space!

Cross mapping in case of unidirectional interactions

But spread out in the other direction!

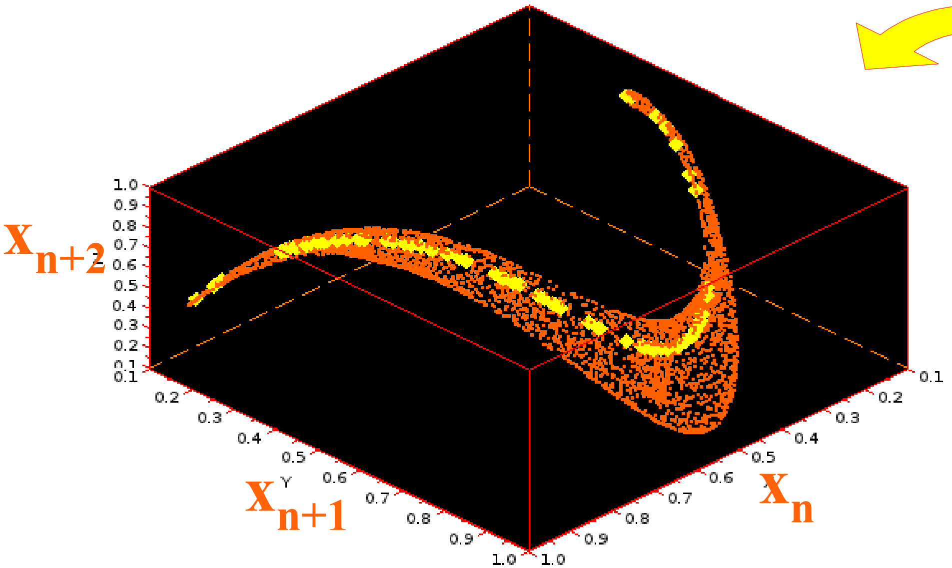

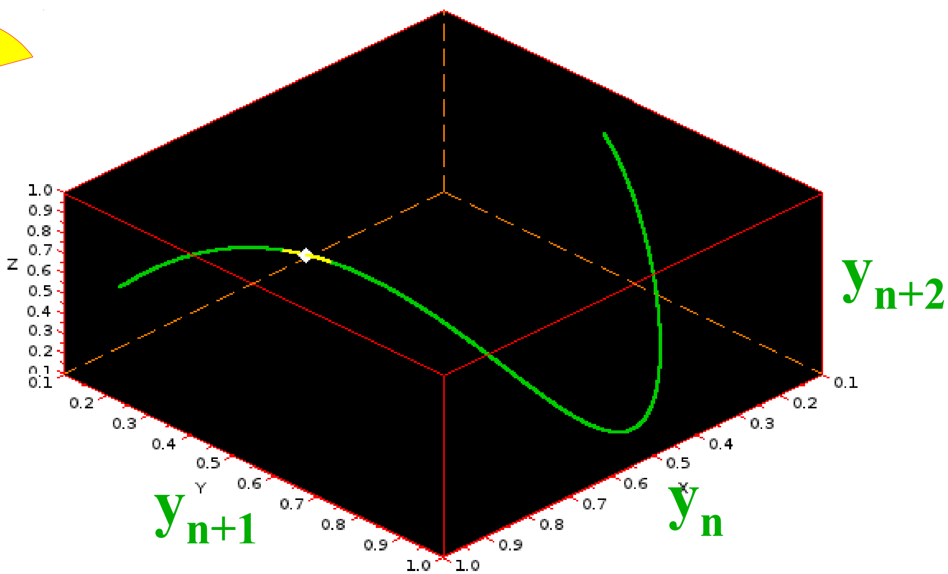

The consequence

The cause

The mapping worked well from x to y but failed from y to x, showing, that y is causal to x but x is not causal to y.

Detecting causality based on the quality of the cross convergence map

Based on the weighted average of the mapped neighborhood, and estimation for the second variable is generated. As the length of the data series increases, the neighborhood (the closest simplex) shrinks to the base point (of which neighborhood is mapped).

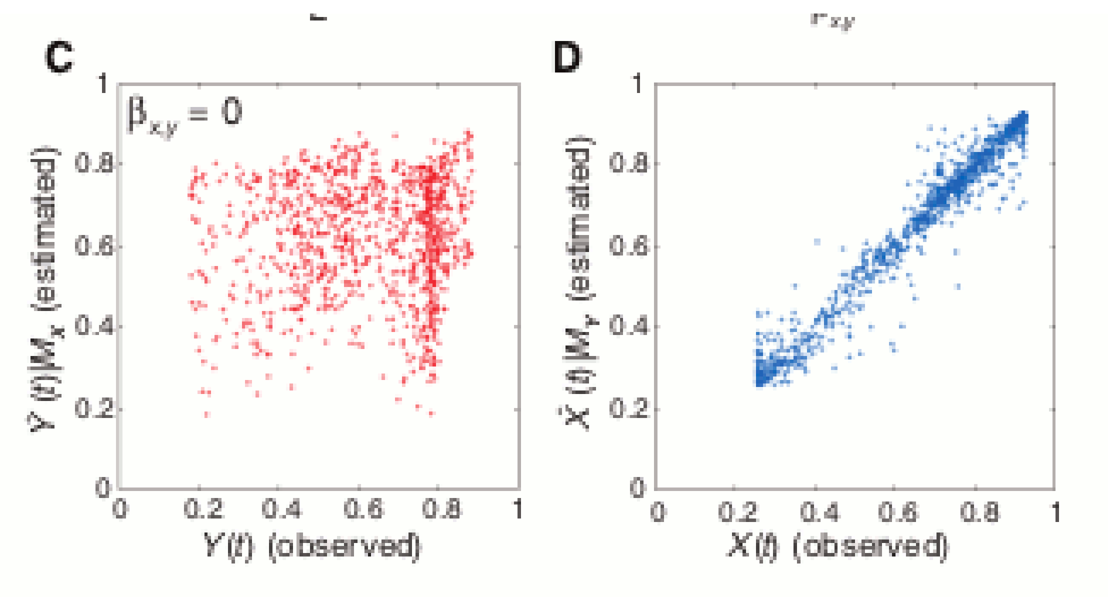

Quality of crossmapping described by the linear correlation coefficient between the estimated and the observed variable

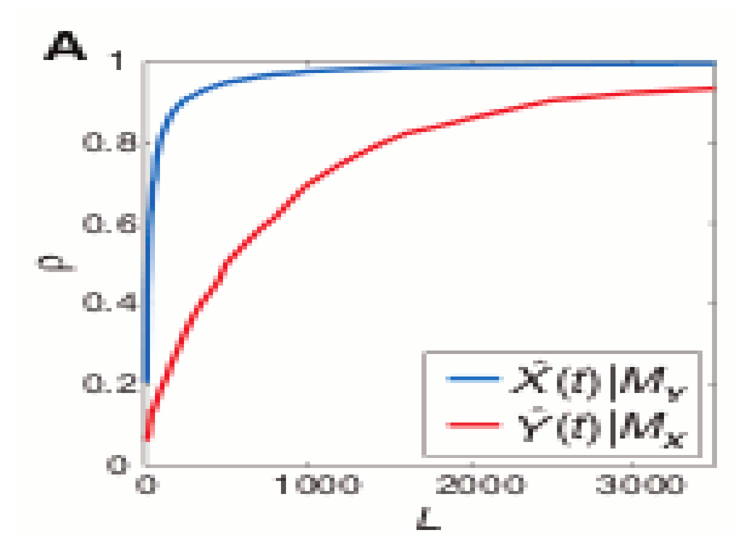

Causality appears as convergence of correlation coefficient as the length of data increases.

Comparison between 3 methods

Sugihara's CCM, Granger causality and transfer entropy (TE) were tested on coupled logistic maps.
1000 simulated systems, random parameters.

Neither method can reveal hidden common causes.

Concluding CCM is Problematic in the unidirectional case, no statistical test, false positive circular detections

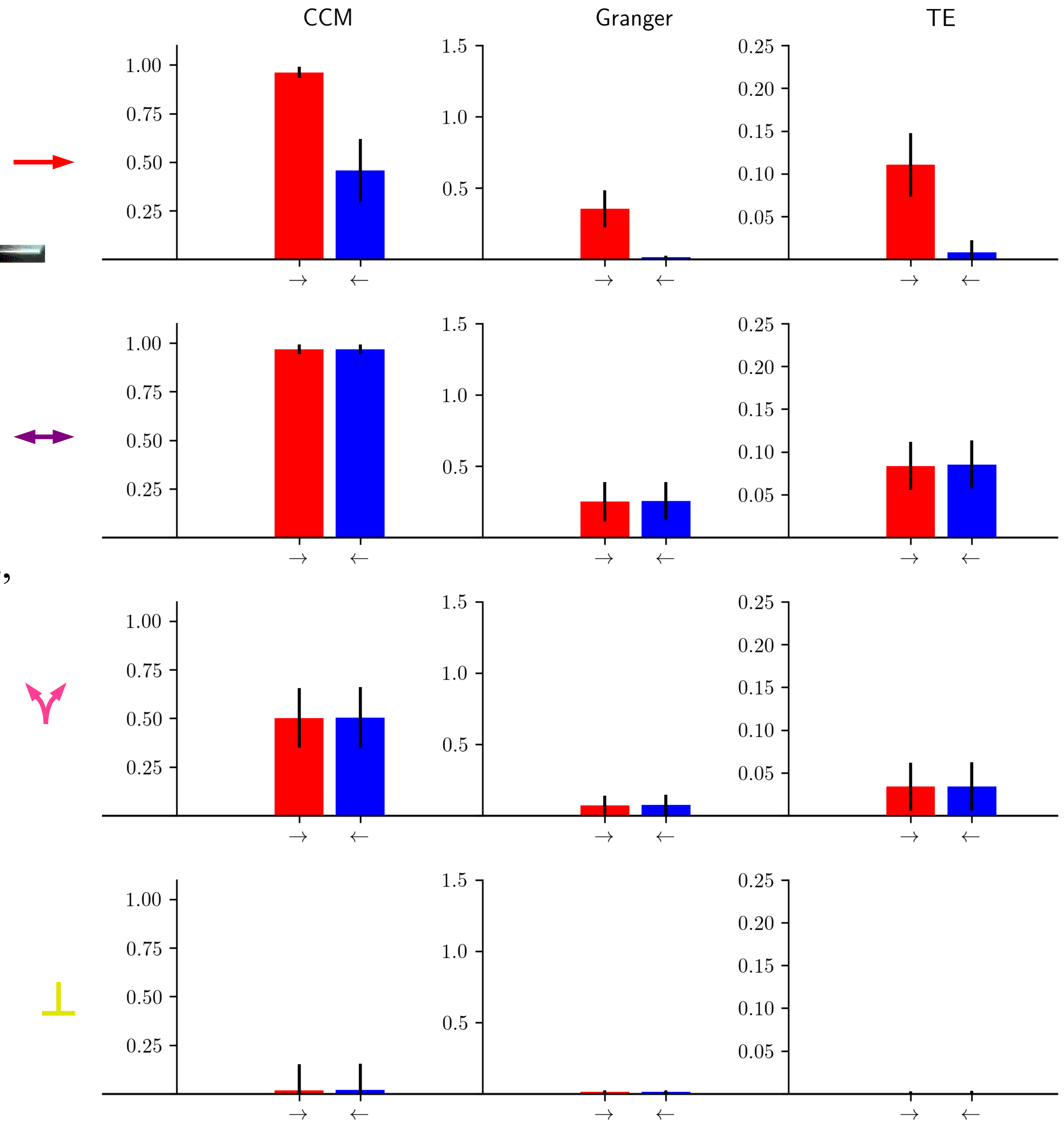

LFP vs IOS

Epileptiform activity was evoked by low Mg+ environment in vivo slice preparation. The local field potential was recorded together with the intrinsic optical signal (IOS), which is possibly a result of swelling of cells during over excitation.

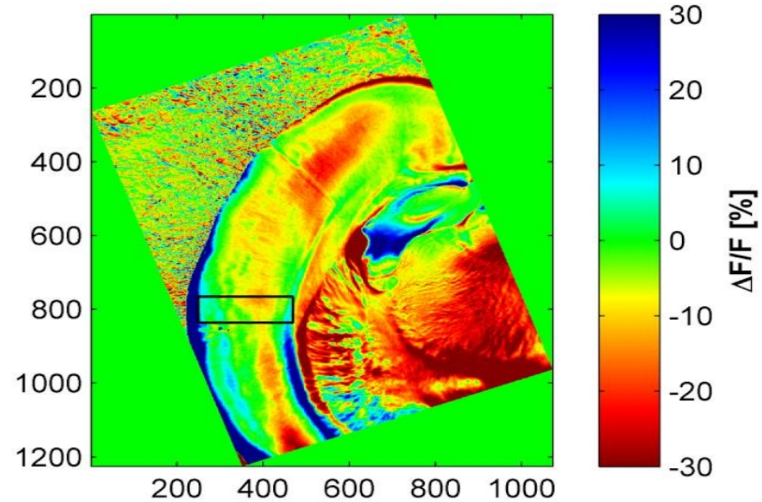

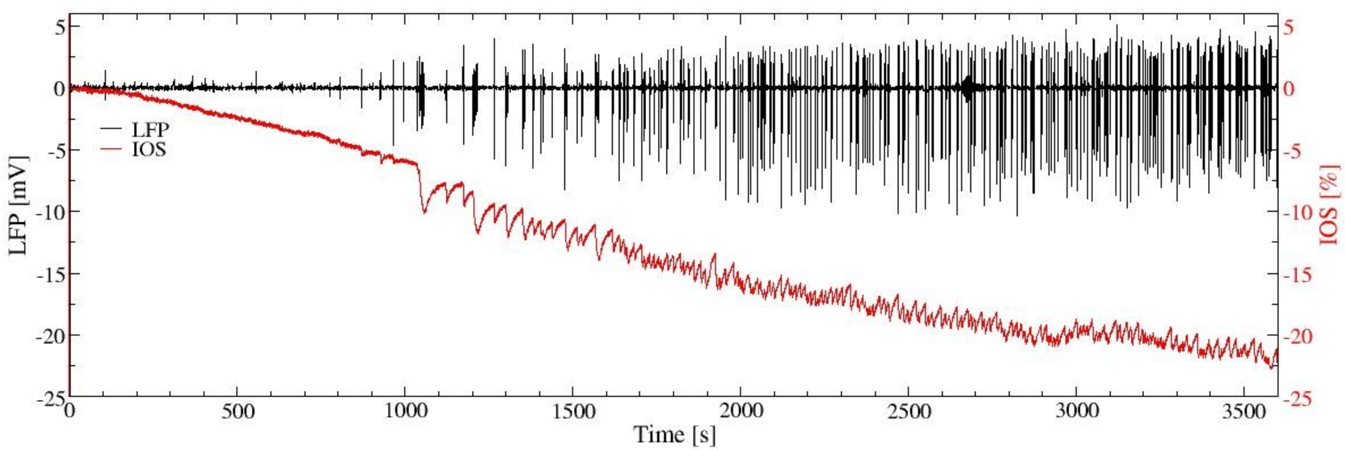

During the long (1 hour) recording, epileptiform bursts appeared with increasing frequency. Parallel, the optical reflectance (and the transmittance) of the tissue changes for visible light, without any additional dying. The process is clearly activity dependent, but slow.

Ildikó Világi

Sándor Borbély

Kinga Moldován

Eötvös Loránd University Department of Physiology and Neurobiology

LFP vs IOS

The faster component were inverted comparing reflected and transmitted light, while the slow component was negative both cases.

Different mechanisms:

IOS low → absorbtion

IOS high → transmittance

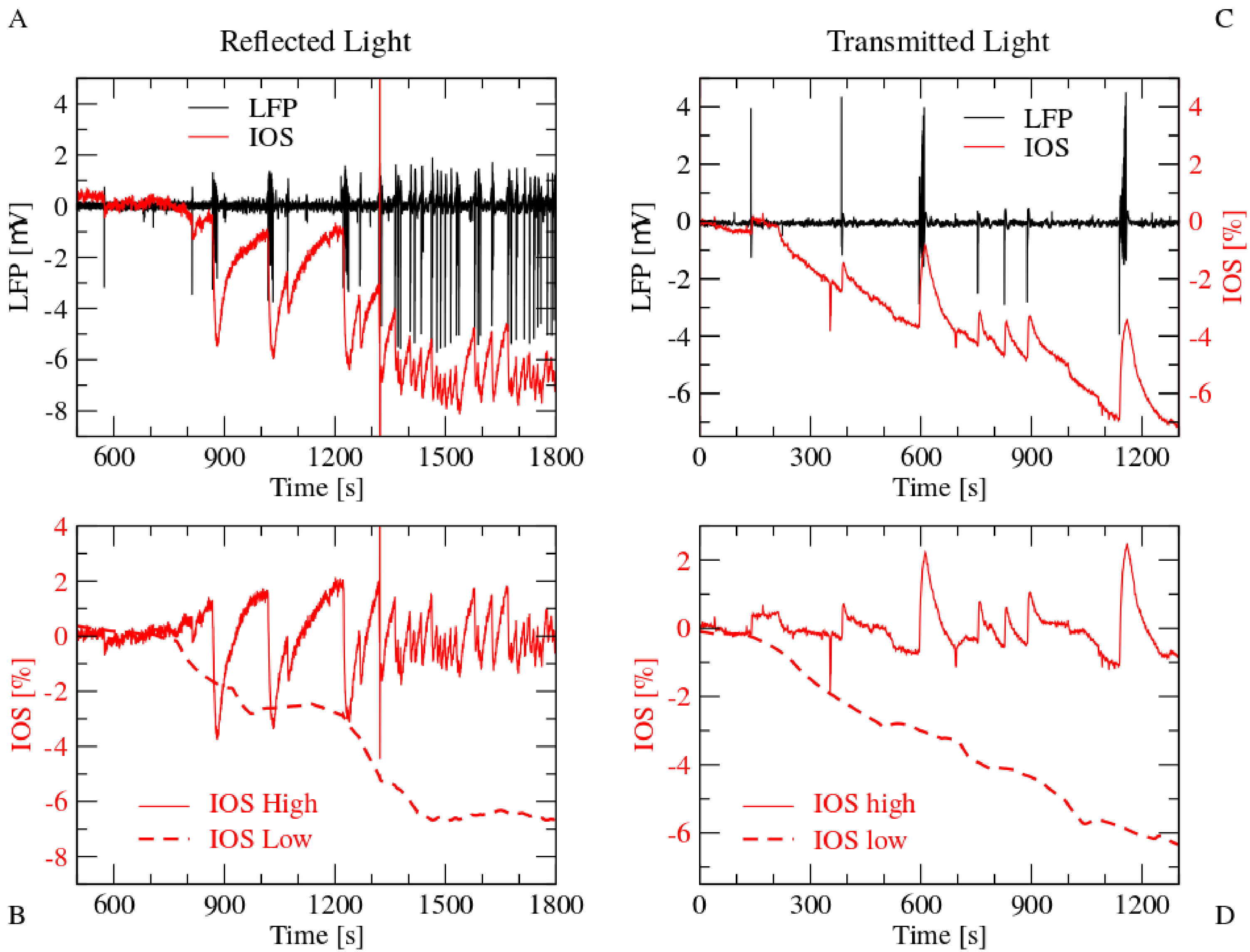

LFP vs IOS

The sampling frequency of the IOS was only 2Hz, much lower than the 1kHz of the LFP!!!

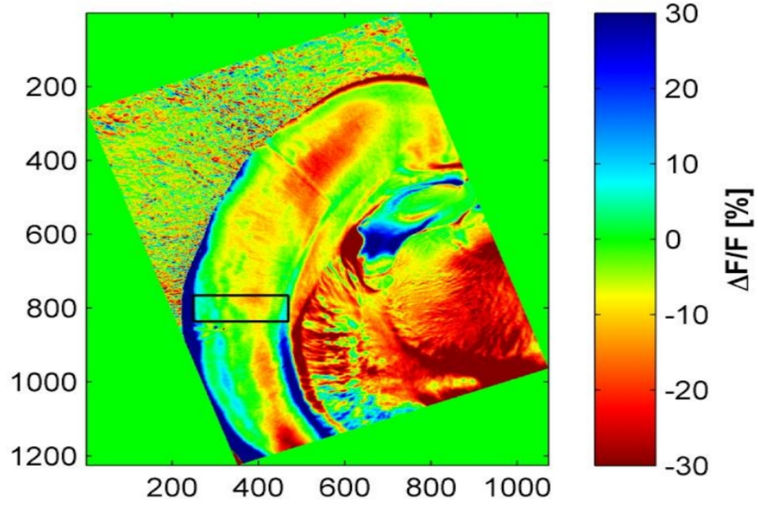

In order to make the causality analysis applicable:

The faster and slow component of the IOS were divided by subtracting a moving window average,to get stationary time series.

The LFP has been downsampled by summing up the V^2 for every 500 ms

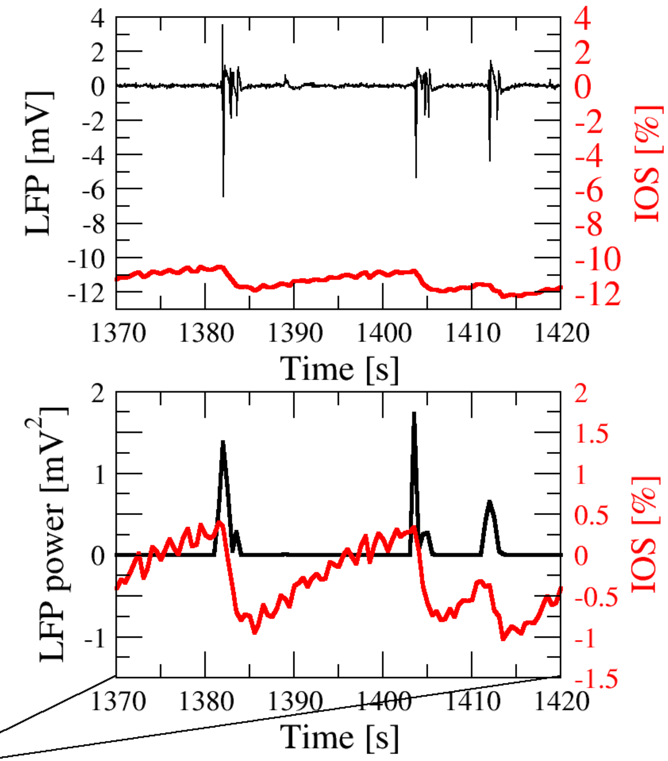

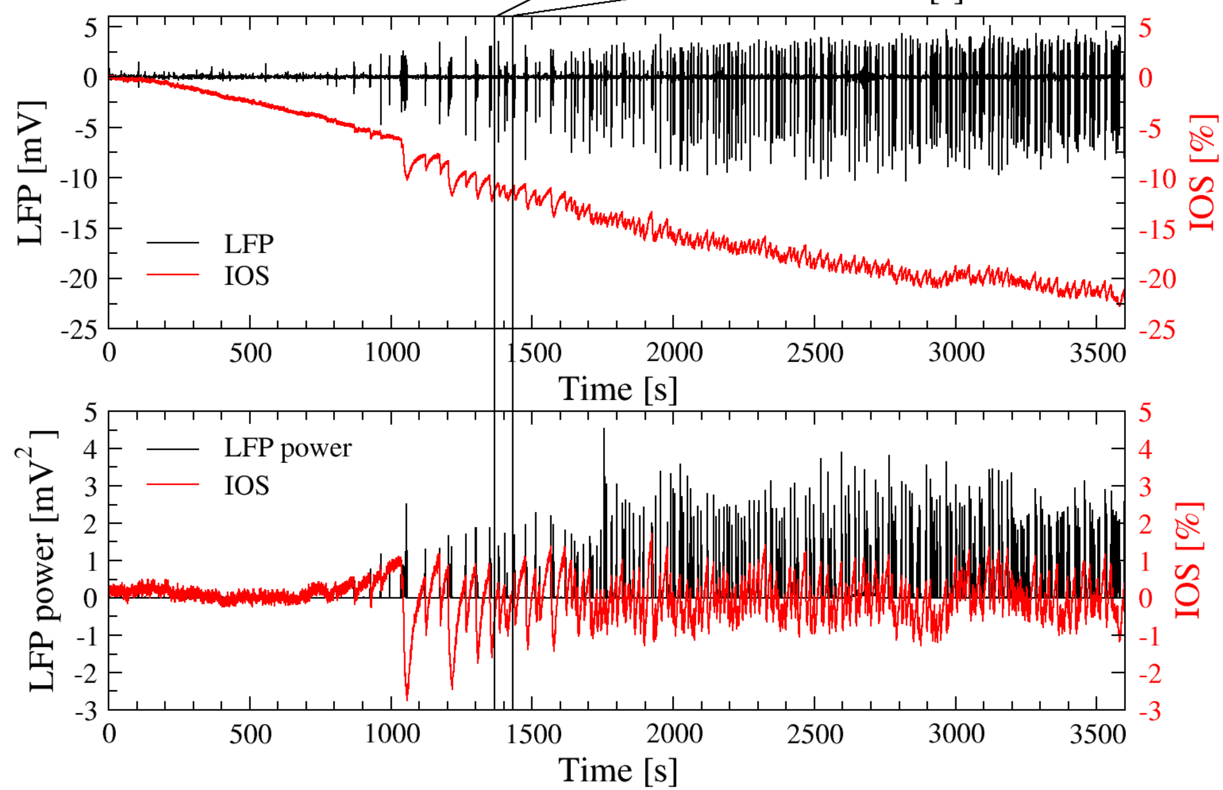

LFP-IOS cross correlation

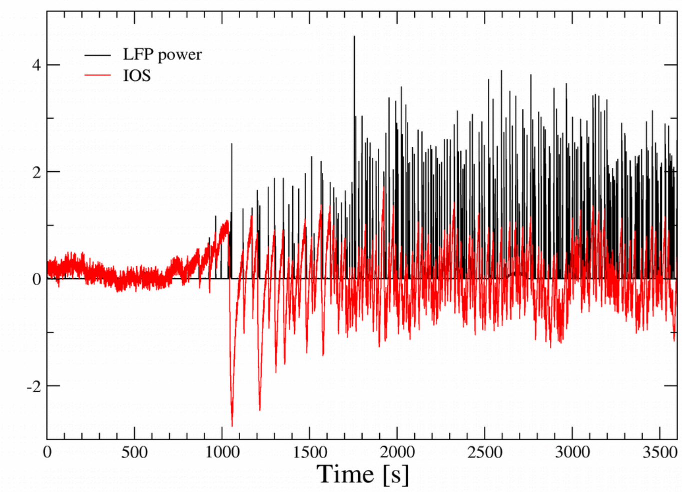

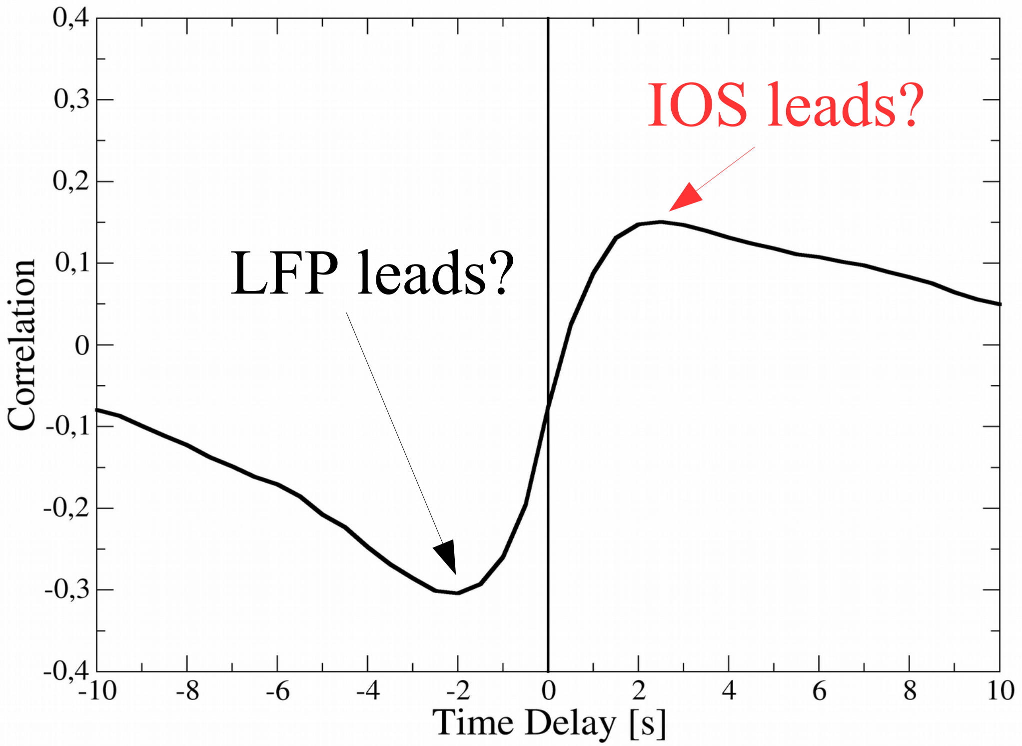

The instantaneous correlation is nearly zero, the cross correlation function has two significant peaks: a higher negative one at -2s (LFP leads) and a smaller positive one at +2.5s (IOS leads). This could be the sign of a well delayed interaction.

Delayed cross map function

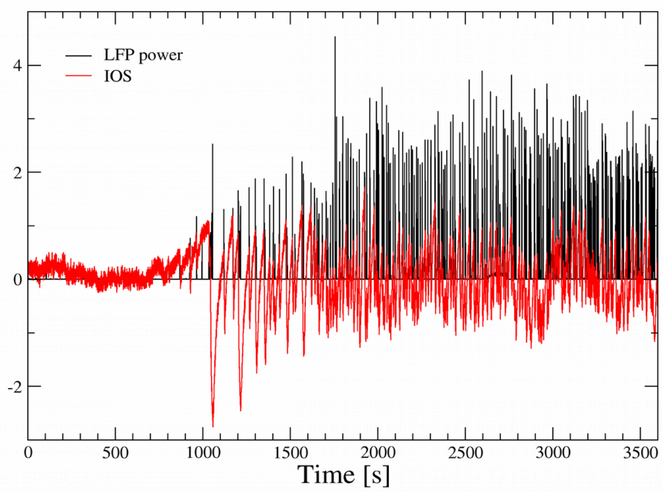

Instead:
Delayed Cross Map function shows a causal effect from LFP to IOS with 500ms delay, corresponding to 1 sample time for IOS.
Although, the time scale of the two signals were very different, the unidirectional causal effect was revealed.

LFP → IOS Delay: 500 ms

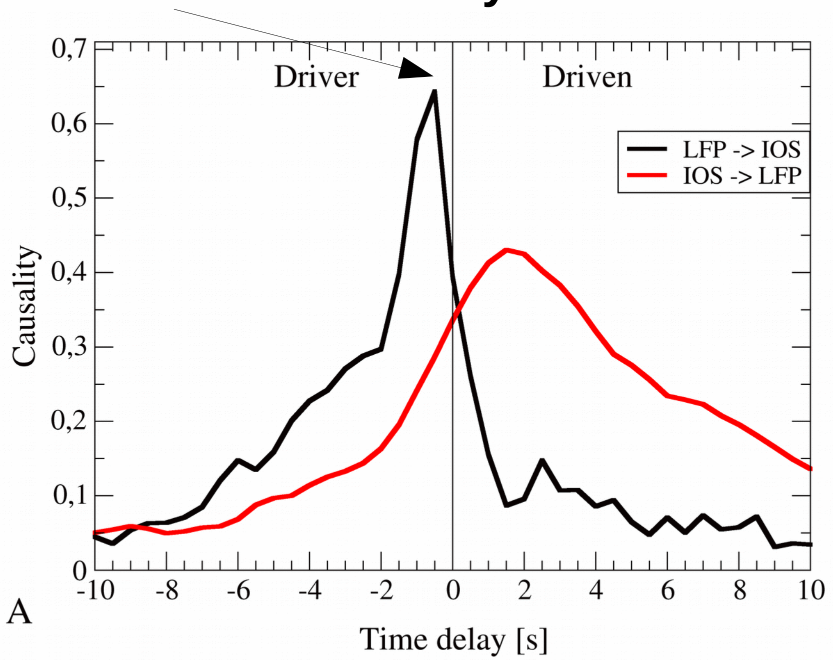

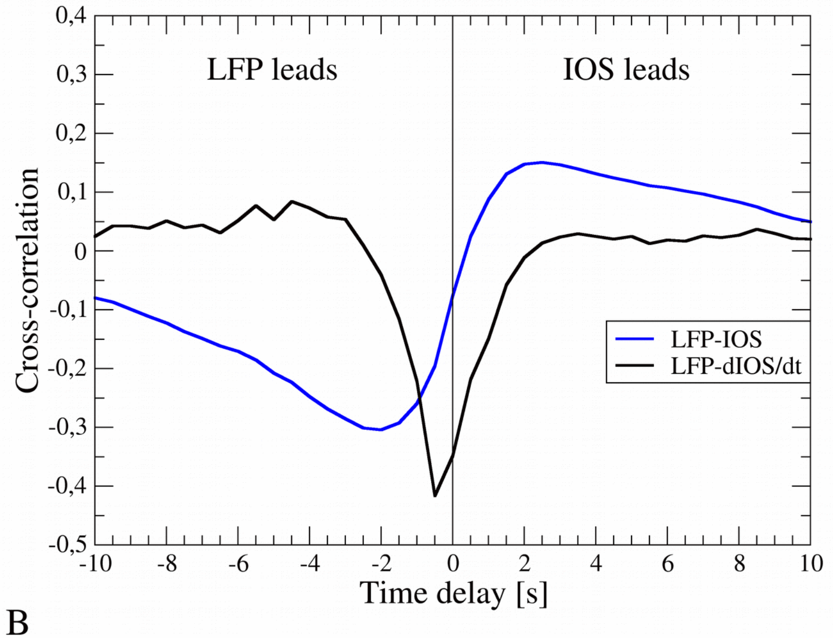

Delayed cross map function

The causal relationship was significant and independent from the form of evoking the epileptic activity.

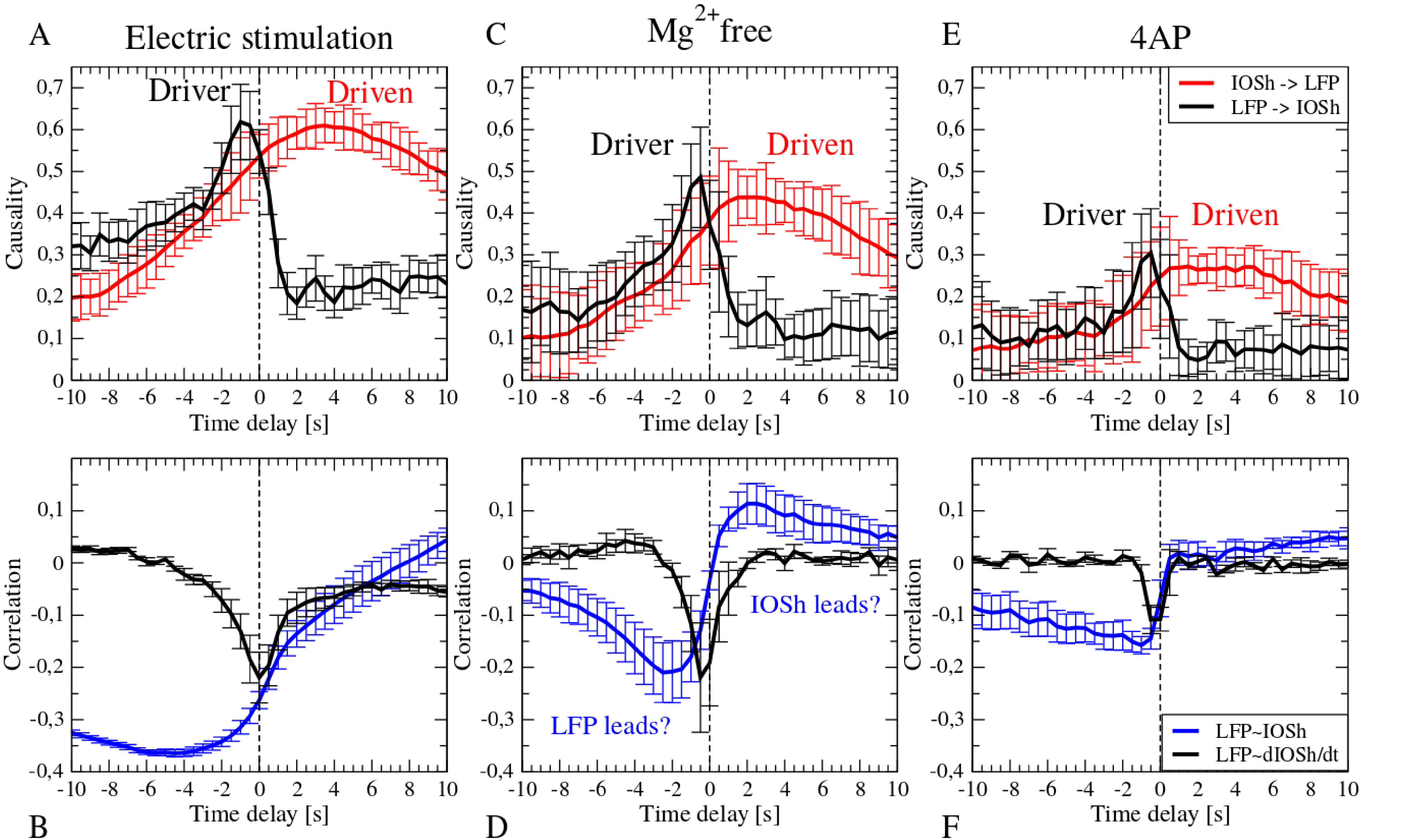

Autonomous dynamics between epileptic bursts

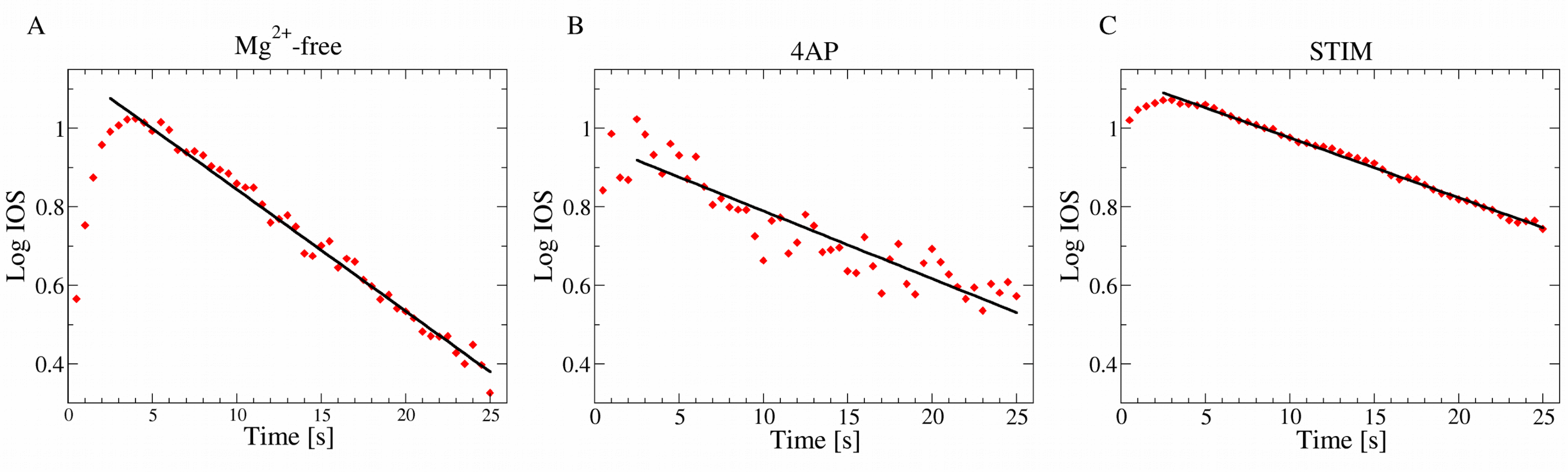

In lack of detectable epileptic activity, the amplitude of the IOS decay exponentially in all the three cases.

From this observation, a simple linear differential equation can describe the autonomous dynamics of IOS:

$$dIOSh = \frac{-IOSh(t)}{\tau_1}$$

Reverse engineering

$$\frac{dIOSh}{dt} = W(t) * LFP^2 - \frac{IOSh(t)}{\tau_1}$$

Where:

$$W(t) = W_0 * e^{\frac{-t}{\tau_2}}$$

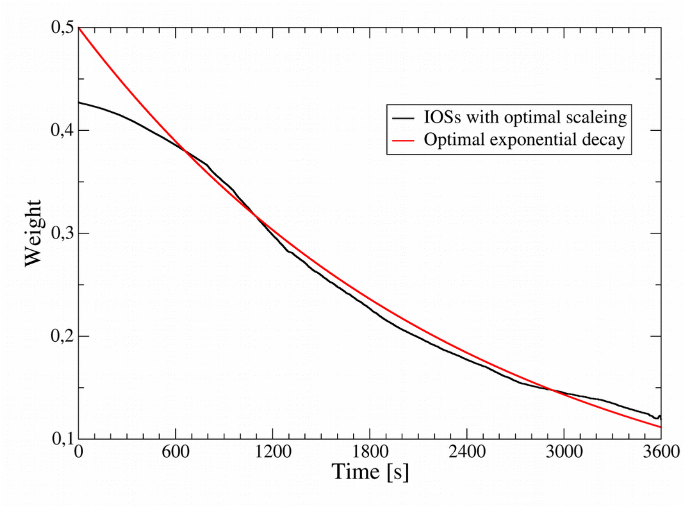

The IOS time series was reconstructed, based on the LFP recording with high precision during the 1h long session.

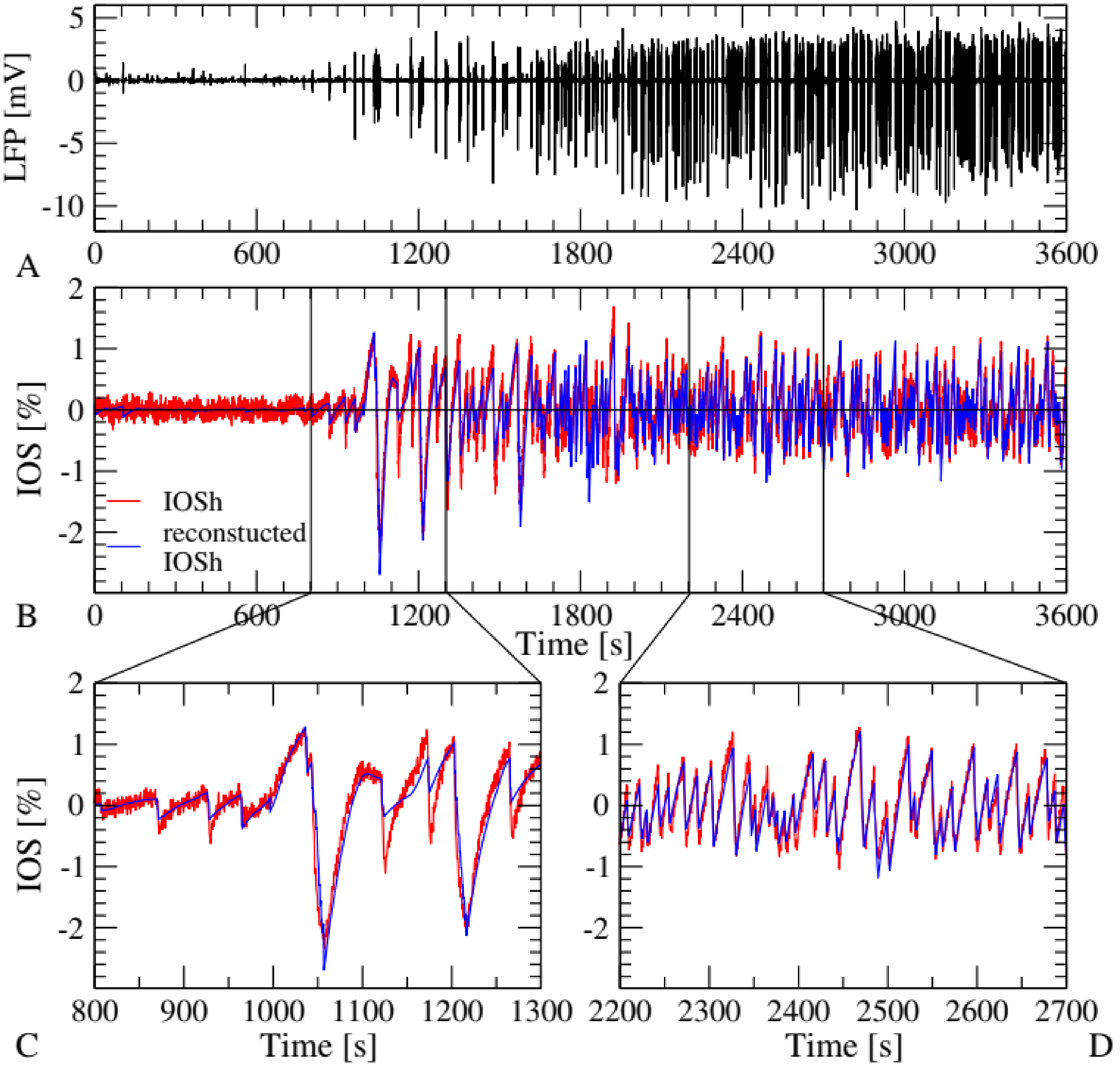

Reverse engineering

$$\frac{dIOSh}{dt} = W(t) * LFP^2 - \frac{IOSh(t)}{\tau_1}$$

Where:

$$W(t) = W_0 * e^{\frac{-t}{\tau_2}}$$

The same model, with different parameters describes the 4AP activity as well.

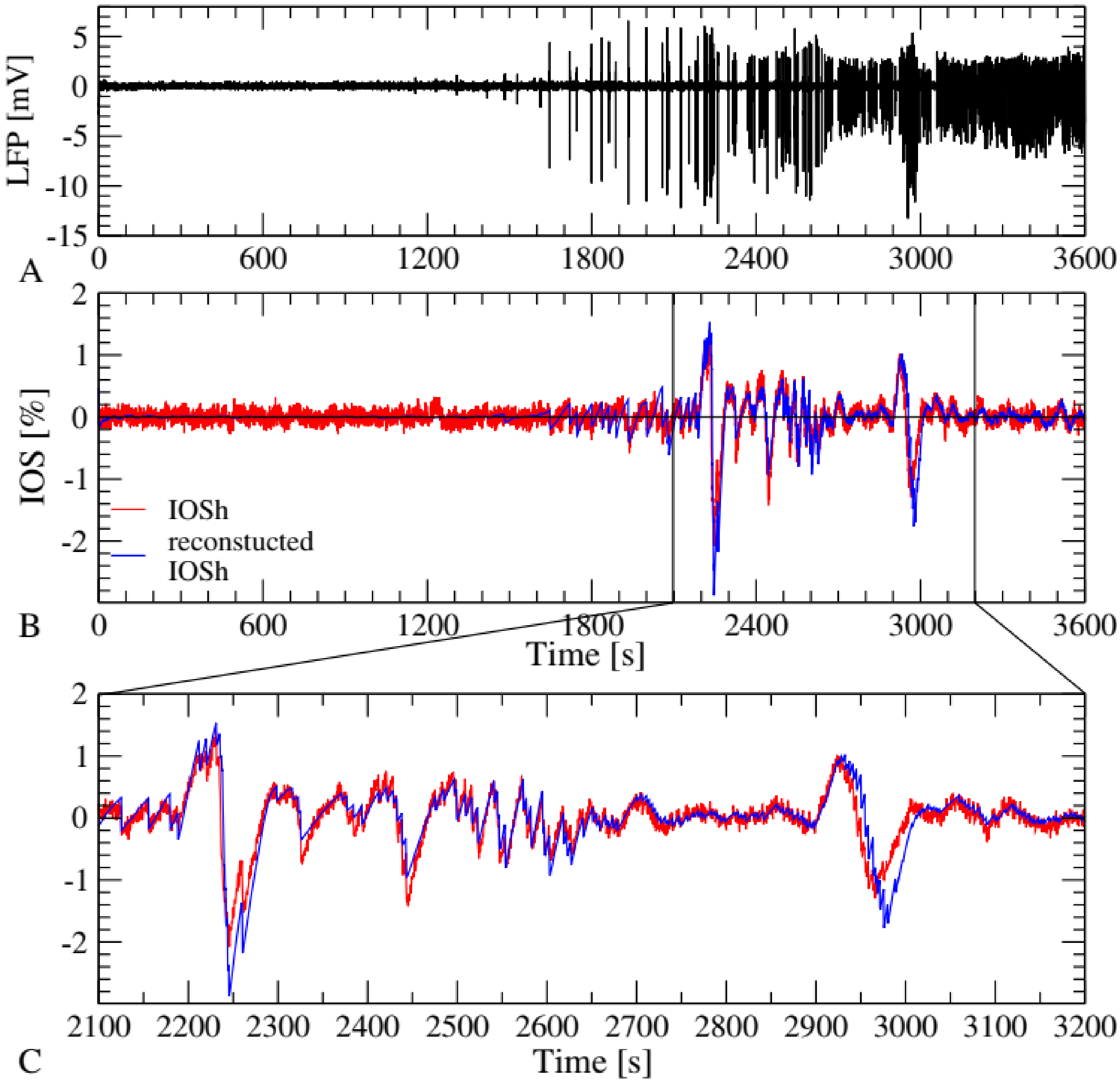

Delayed cross map function

We have extended Sugihara's method for time-dependent and delayed connections. The method was tested on simulated coupled dynamical systems. Peaks positions on the negative axis mark the correct delay times.

Zsigmond Benkő

Case I:
Unidirectional coupling

The method precisely:
identified the direction and
the delay of the coupling: **X → Y**
Delay: 0

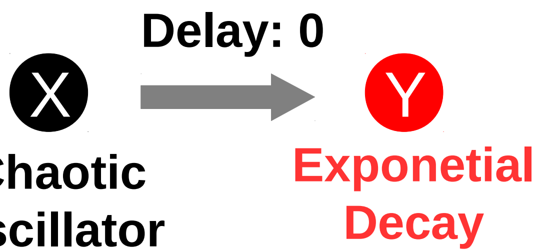

X(t+1)=3.8X(t)(1-X(t))

Y(t+1)=0.8Y(t)+*F*(X(t-delay))

$F(X)=e^{(1-X)^{10}}$ Non-linear coupling

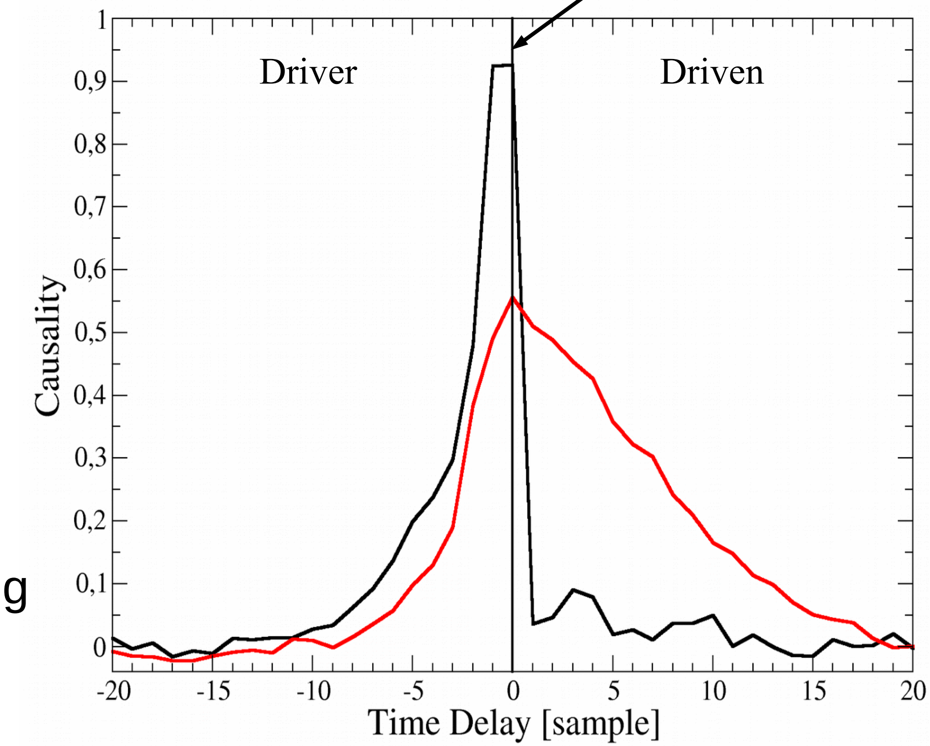

Delayed cross map function

The peak of the cross map functions follows precisely the delay of the effect

Case I:
Unidirectional coupling

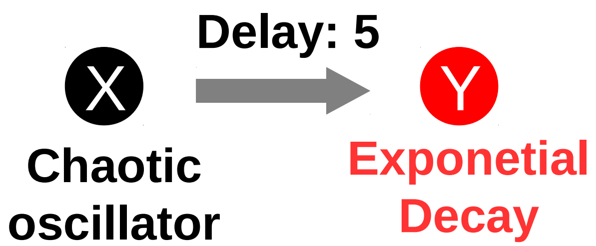

X(t+1)=3.8X(t)(1-X(t))

Y(t+1)=0.8Y(t)+*F*(X(t-delay))

$F(X)=e^{(1-X)^{10}}$ Non-linear coupling

X → Y
Delay: 5

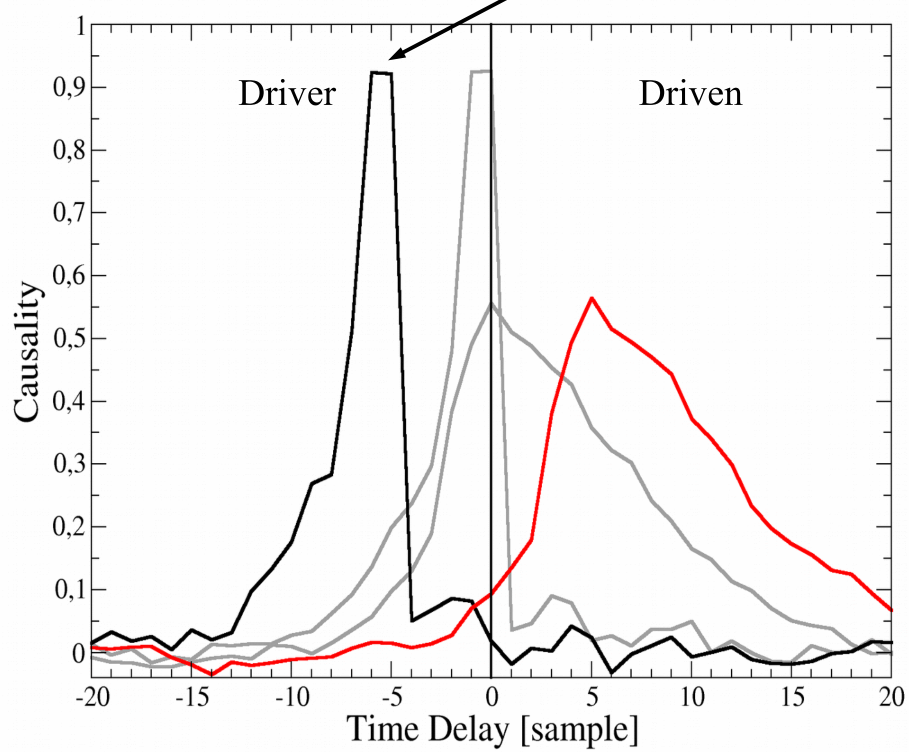

Delayed cross map function

The positive axis marks the anti-causal direction of the time shifts. This effect is stronger in deterministic systems and in case of strong couplings. In these cases, the future of the driven system can be predicted from the cause as well.

Case I: Unidirectional coupling

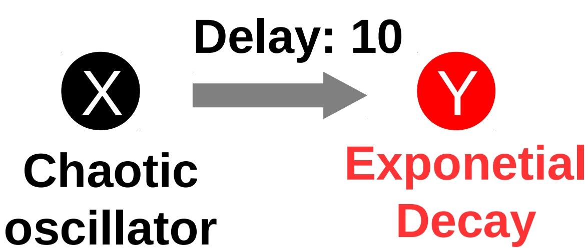

$X(t+1)=3.8X(t)(1-X(t))$

$Y(t+1)=0.8Y(t)+F(X(t-\text{delay}))$

$F(X)=e^{(1-X)^{10}}$ Non-linear coupling

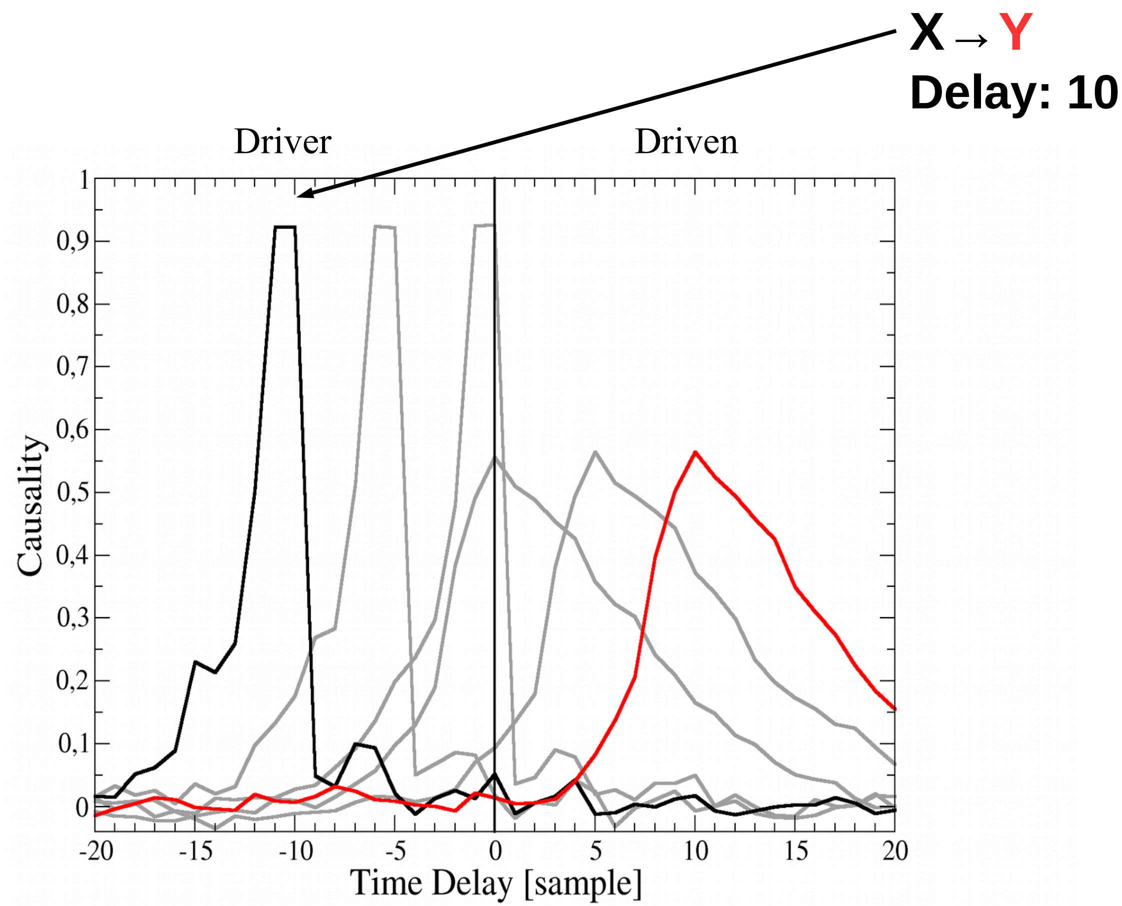

Delayed cross map function

In case of bidirectional coupling, the peak positions mark the correct delay times in both directions. The coupling coefficients could be different, and the delays could be the same or different into the two directions.

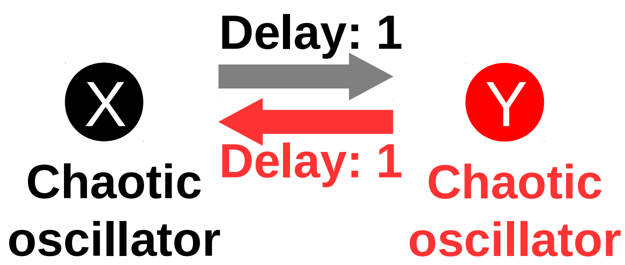

$$X(t+1)=3.8X(t)(1-X(t)+Y(t-delay))$$

$$Y(t+1)=3.8Y(t)(1-Y(t)+X(t-delay))$$

Non-linear coupling

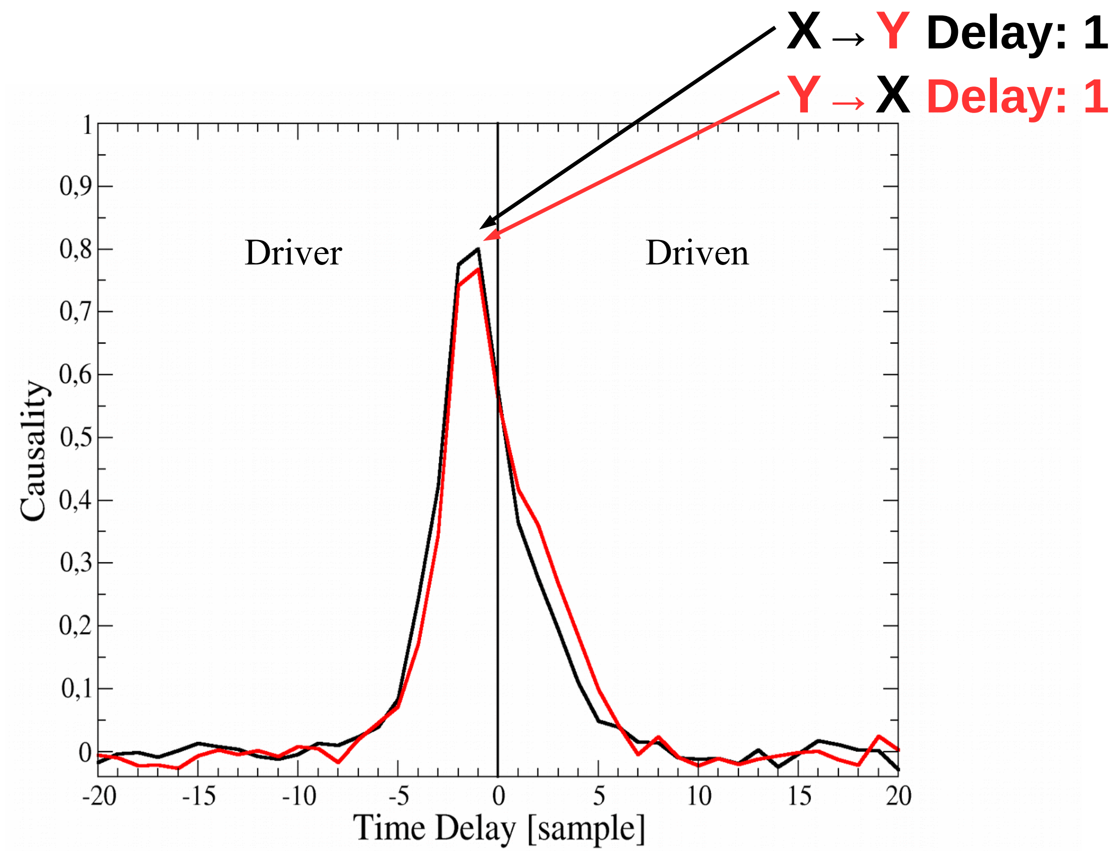

Delayed cross map function

In case of bidirectional coupling, the peak positions mark the correct delay times in both directions. The coupling coefficients could be different, and the delays could be the same or different into the two directions.

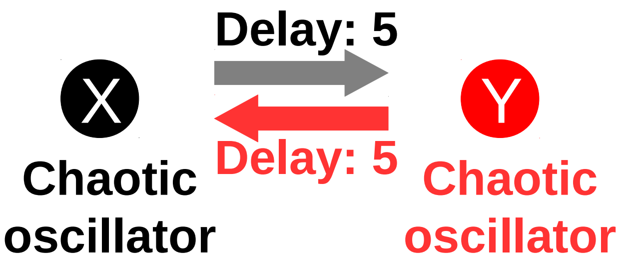

$X(t+1)=3.8X(t)(1-X(t)+Y(t-delay))$

$Y(t+1)=3.8Y(t)(1-Y(t)+X(t-delay))$

Non-linear coupling

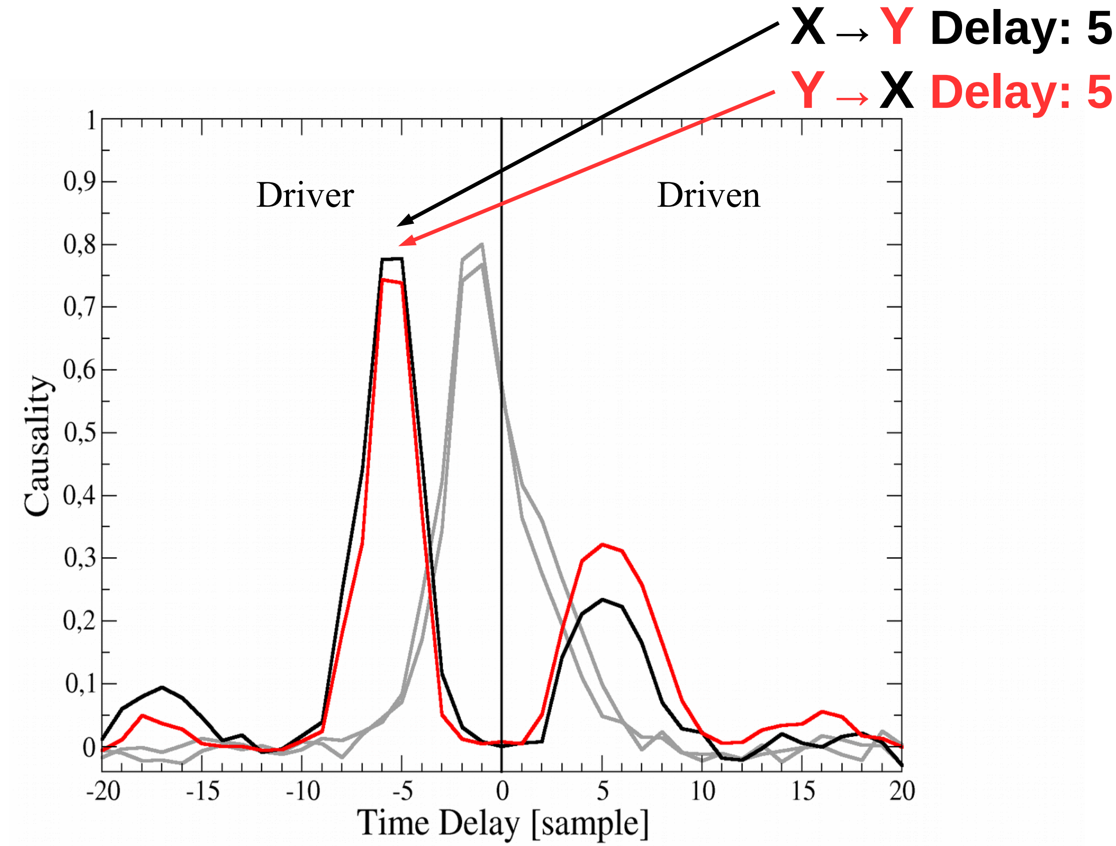

Delayed cross map function

In case of bidirectional coupling, the peak positions mark the correct delay times in both directions. The coupling coefficients could be different, and the delays could be the same or different into the two directions.

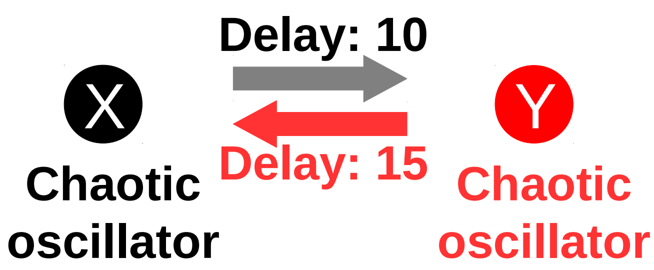

$$X(t+1)=3.8X(t)(1-X(t)+Y(t-delay))$$

$$Y(t+1)=3.8Y(t)(1-Y(t)+X(t-delay))$$

Non-linear coupling

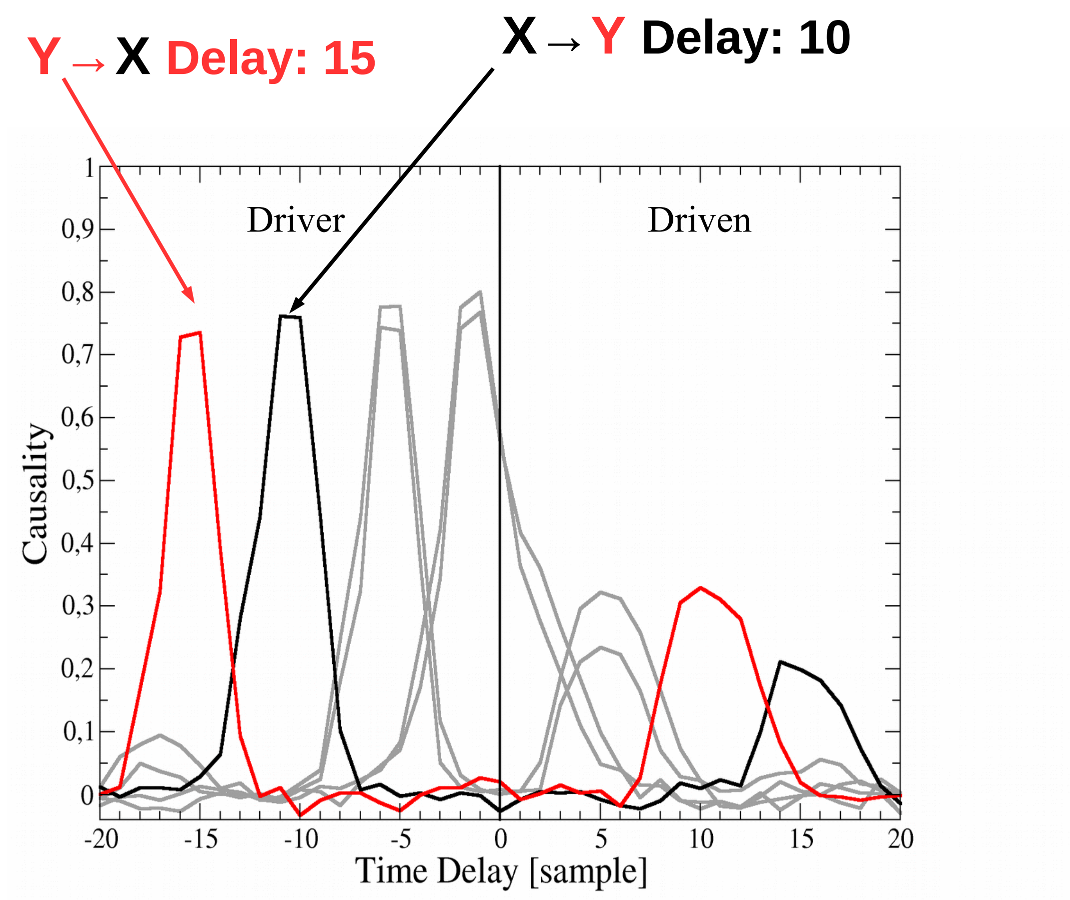

Task dependent causal connectivity networks based on fMRI dataseries

1. **Visuo-Motor task:**
Fingertapping in the rhythm of the flashing light stimulus (with different frequencies)

2. **Working memory task**:
N-Back (now N=2) push the button if the actual picture is the same as the one 2 stimuli before.

Vaibhav Diwadkar
Wayne State University

The data: fMRI records from 20-20 patients with obsessive-compulsive disorder at 0.5 Hz sampling rate.

The causal connections were calculated for 8 ROIs corresponding to brain areas:
V1, SPC, SMA, M1, dACC, dLFPC, BG, Hip

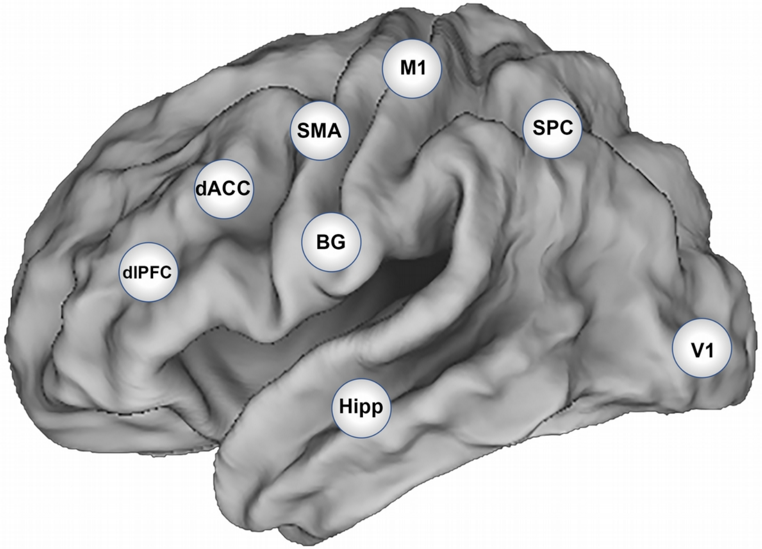

Task dependent causal connectivity networks based on fMRI dataseries

1. **Visuo-Motor task:**

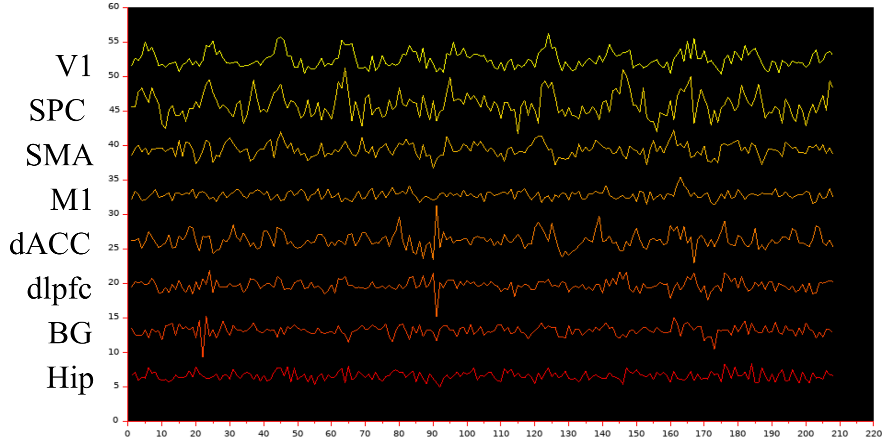

Each time series contains only 208-289 samples

Vaibhav Diwadkar
Wayne State University

2. **Working memory task:**

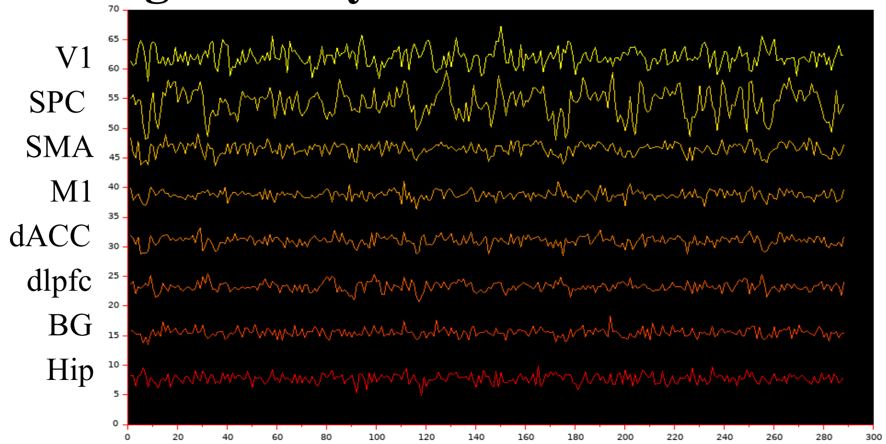

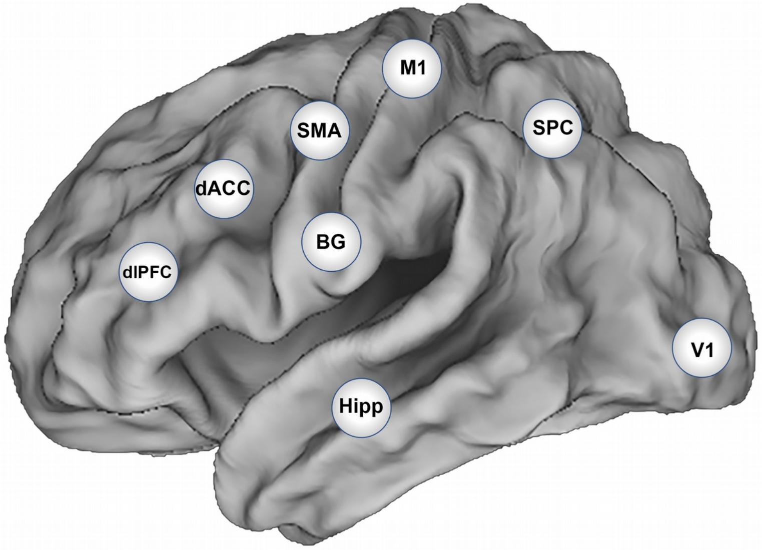

Causal network during visuo-motor task, delay 0s

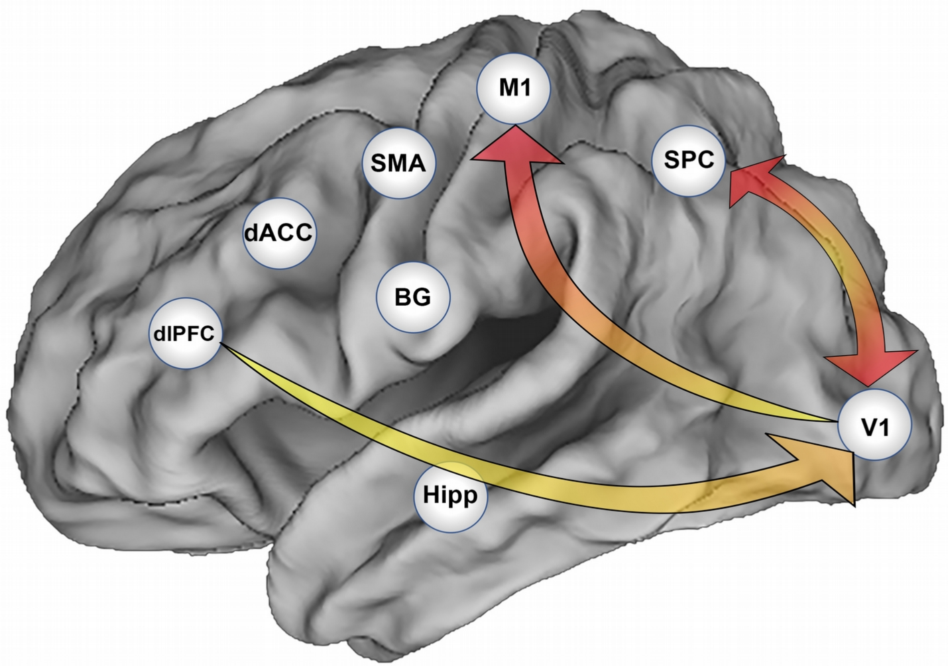

During the visuo-motor task, only three significant causal interactions were revealed: V1 → M1, and a bidirectional, circular connection V1↔ SPC and a weaker one: dLFPC → V1.

Causal network during working memory task, delay 0s

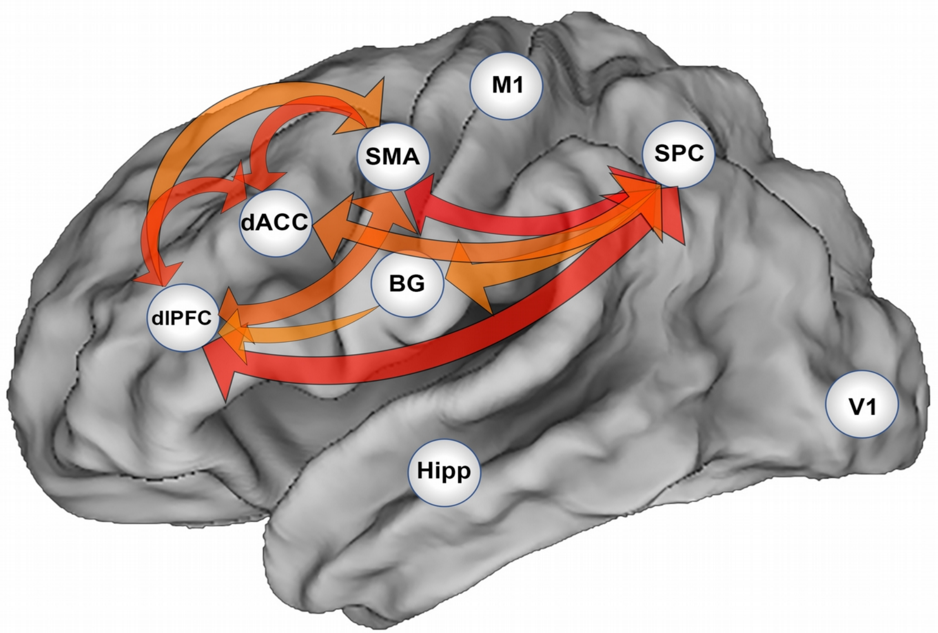

The working memory task induced much richer functional structure, revealing a more extended cortical network of significant uni- and bi-directional causal interactions between regions including the SPC, dLFPC SMA and dACC, while strong unidirectional interactions were observed from the SPC to BG, from BG to dLFPC and from SMA to dLFPC.

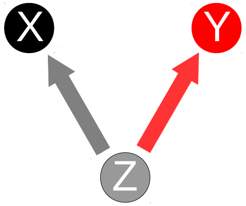

Revealing hidden common cause

Neither Granger's nor Sugihara's method is able to detect the existence of a hidden common cause or distinguish it from the direct interaction.

We have developed a new method which can!

It is based on the joint dimension measure:

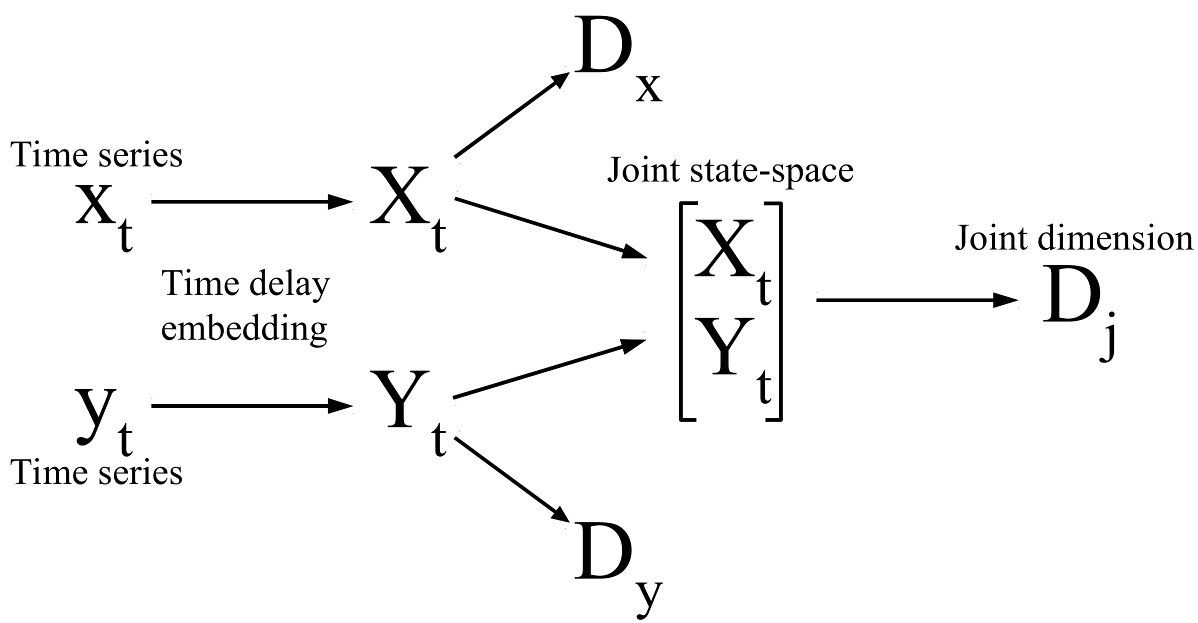

Zsigmond Benkő

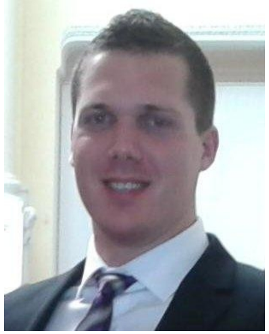

Ádám Zlatniczky

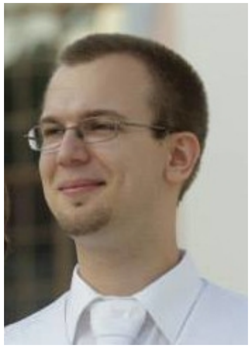

Marcell Stippinger

András Telcs

Revealing hidden common cause

Key point: the cause does not increases the dimension of the consequence in the joint space, the information is already there!

$x_{n+1}=r_x x_n((1-x_n)+b_{yx}y_n)$ $y_{n+1}=r_y y_n(1-y_n)$

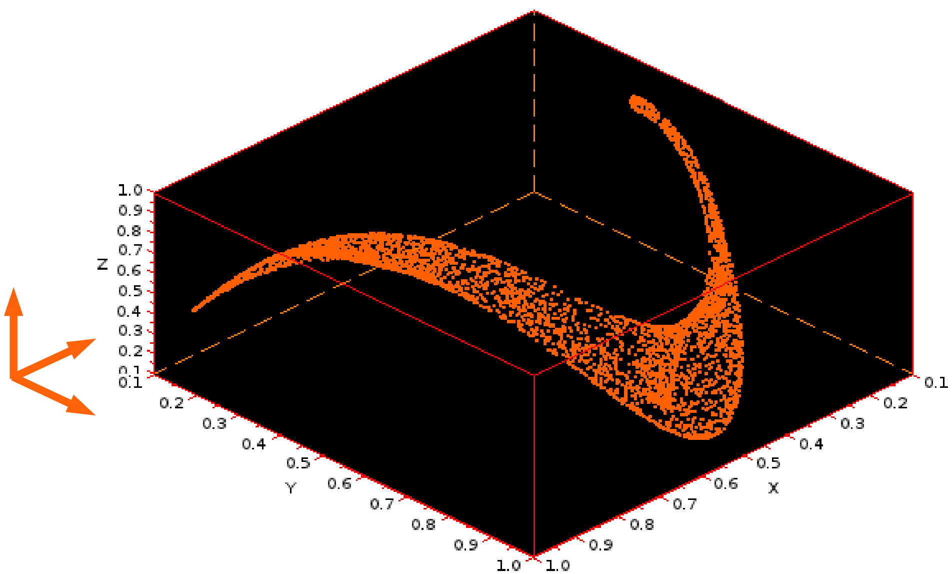

$[x_n;x_{n+1};x_{n+2}]$

The consequence

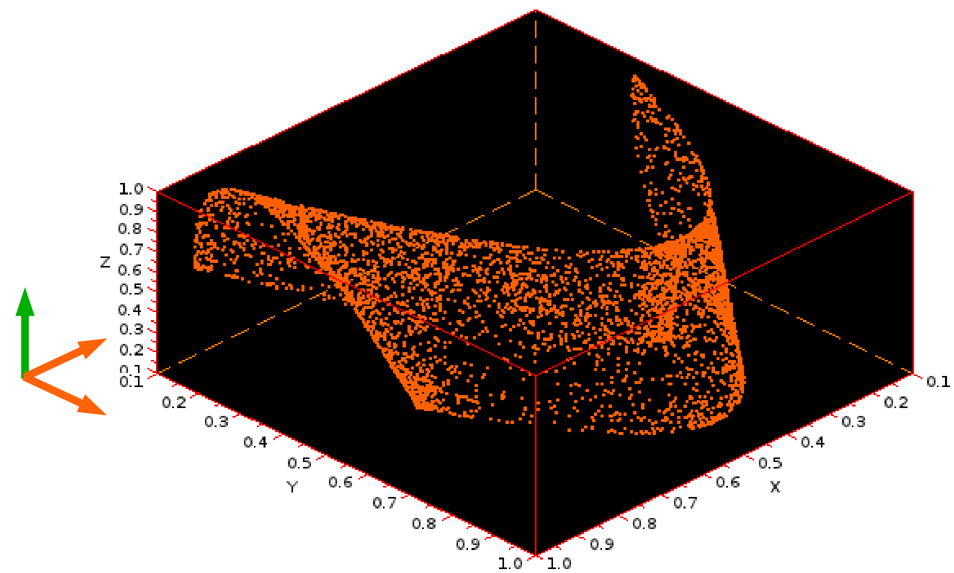

$[x_n;x_{n+1};y_n]$

The cause and the consequence together in the joint space

The consequence formed a 2D manifold both in its own and the together with the cause in the joint state space. The lack of dimensionality increase in the joint dimension is the sign of the existing causal link (x depends on y).

Revealing hidden common cause

$x_{n+1}=r_x x_n((1-x_n)+b_{yx}y_n)$

$y_{n+1}=r_y y_n(1-y_n)$

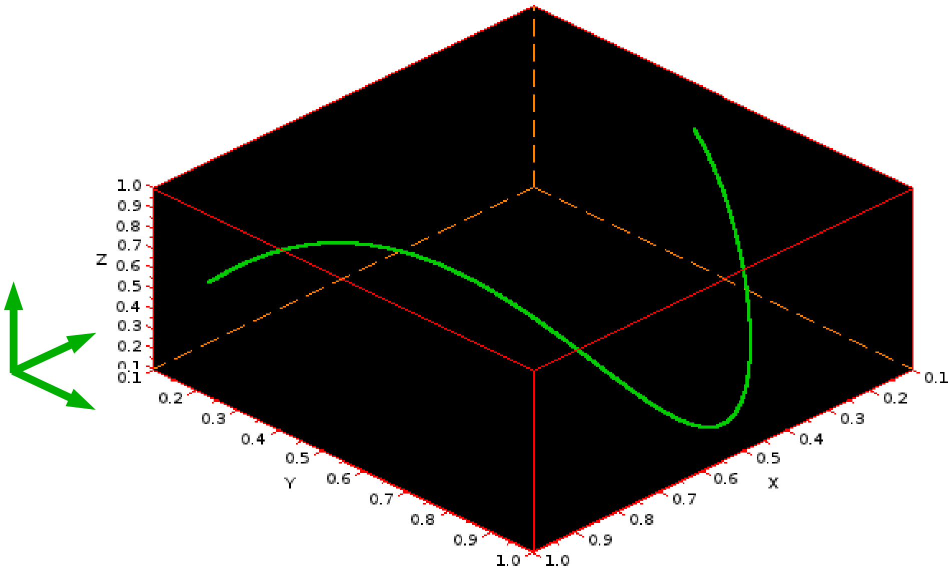

$[y_n;y_{n+1};y_{n+2}]$

The cause

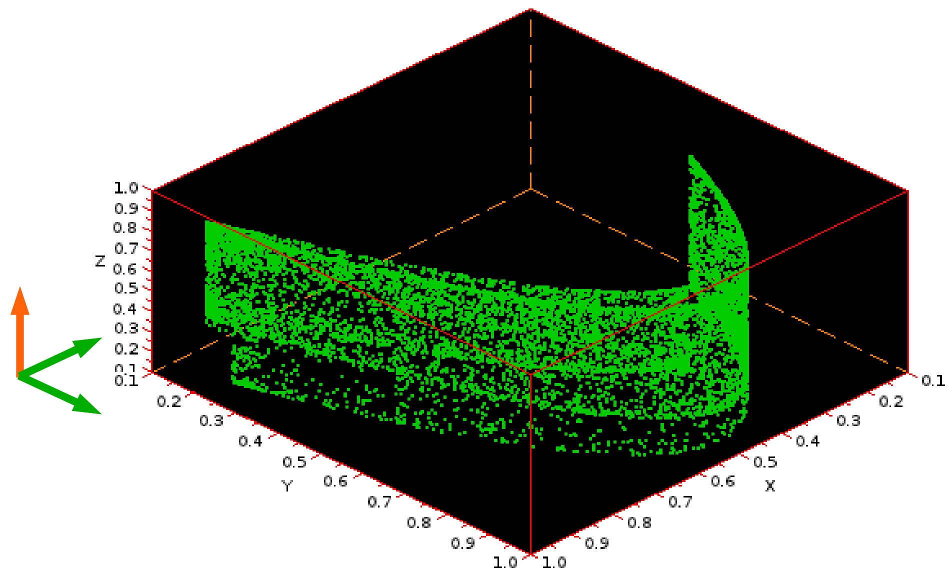

$[y_n;y_{n+1};x_n]$

The cause and the consequence together in the joint space

The cause formed a 1D manifold in its own, but a 2D manifold together with the consequence in the joint state space. The dimensionality increase in the joint state space is the sign of the independence (x contains different information compared to y, thus x does not cause y).

Revealing hidden common cause

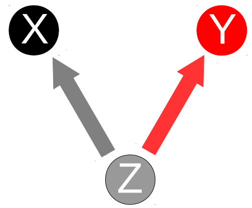

Causal cases and the relations between the single and the joint dimensions:

Independence: $x_t \perp y_t \Rightarrow D_j = D_x + D_y$

Unidirectional causality: $x_t \rightarrow y_t \Rightarrow D_j = D_y < D_x + D_y$

Circular causality: $x_t \leftrightarrow y_t \Rightarrow D_j = D_x = D_y$

Common cause: $x_t \curlyvee y_t \Rightarrow Max(D_x, D_y) < D_j < D_x + D_y$

The type of the causal connection can be revealed by measuring the relations between the joint and the individual dimensions.

How to measure the dimension of the manifold?

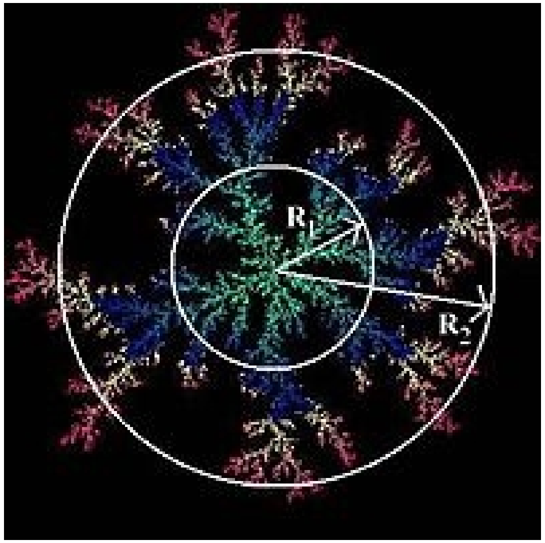

$$N(r) = N_0 \cdot r^D$$

$$D = \frac{Ln\left(\frac{N_i}{N_{i+1}}\right)}{Ln\left(\frac{r_i}{r_{i+1}}\right)}$$

Let’s take two radii and count the number of points within the spheres: the exponent of the increase with respect to the radius gives us the dimension.

Bayesian model: a simplified version

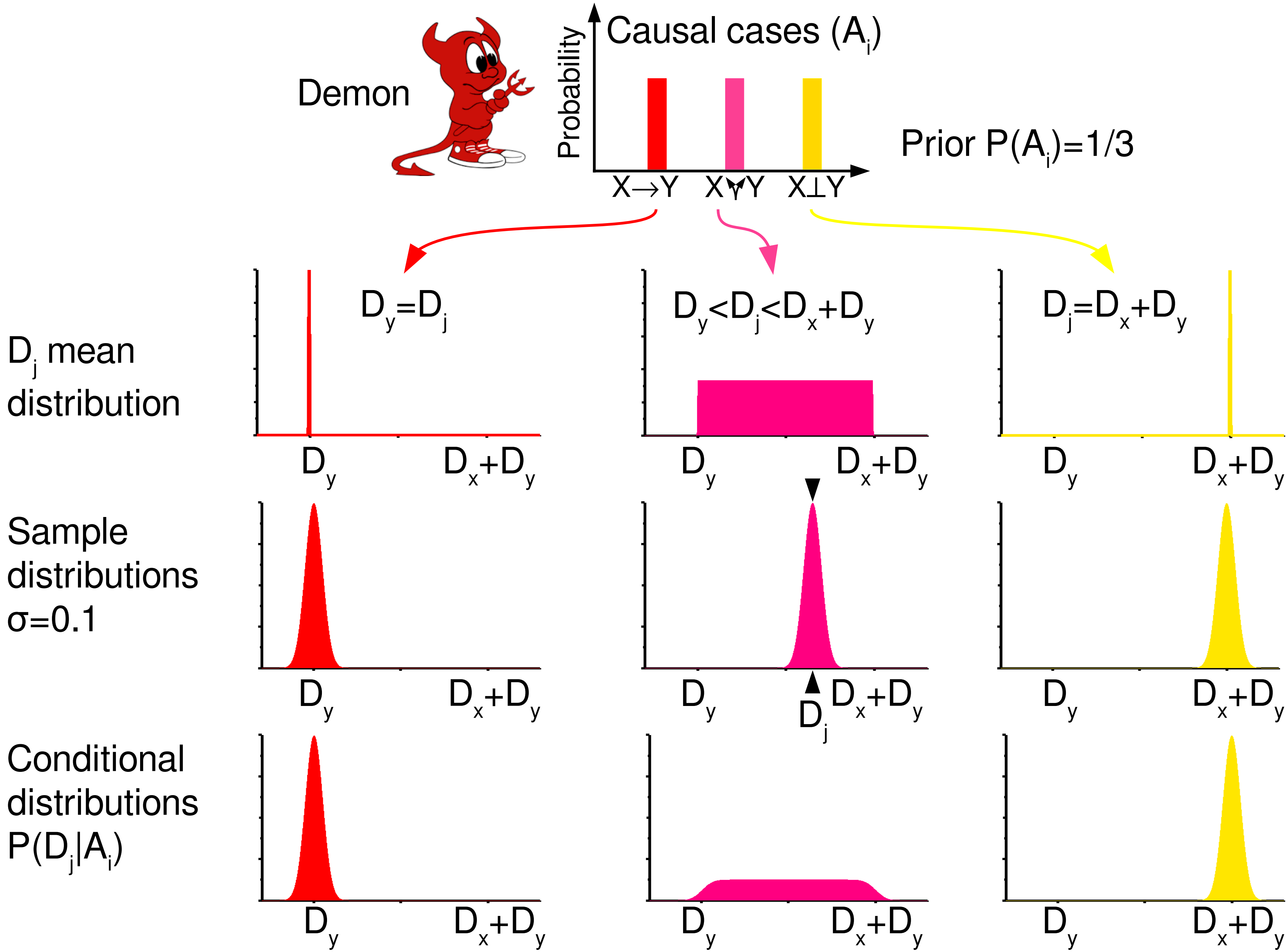

Bayesian inference: a simplified version

Likelihood
$P(D_j|A_i)$

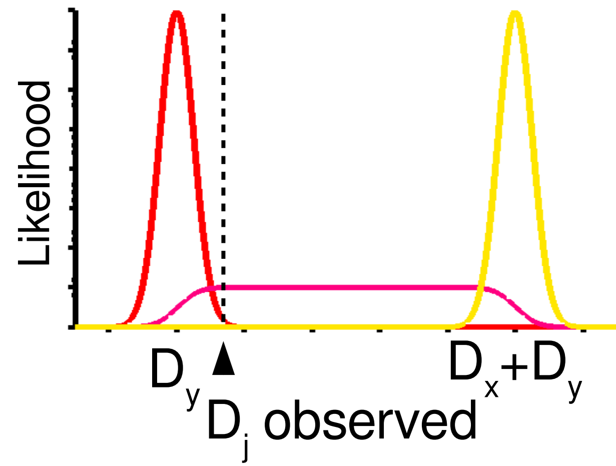

Conditional
posterior
distribution
$P(A_i|D_j)$

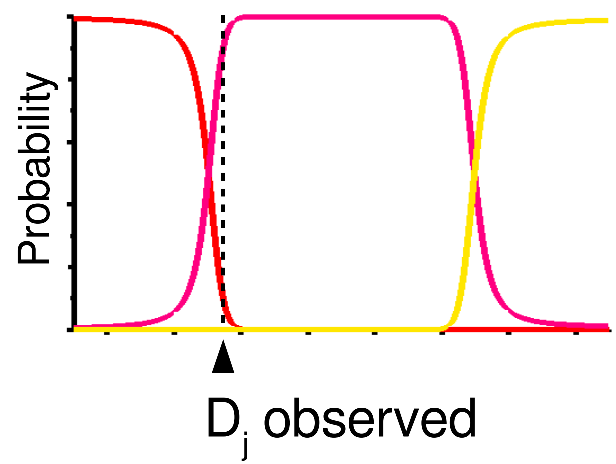

Bayes-theorem

$$P(A_i|D_j) = \frac{P(D_j|A_i)\,P(A_i)}{\sum P(D_j|A_i)\,P(A_i)}$$

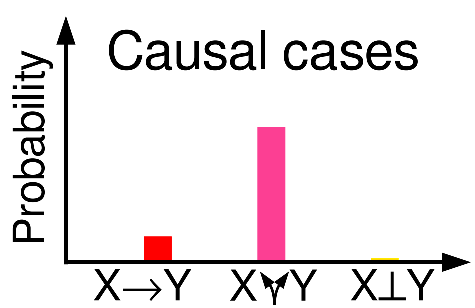

The workflow

1 - Time-delay embedding

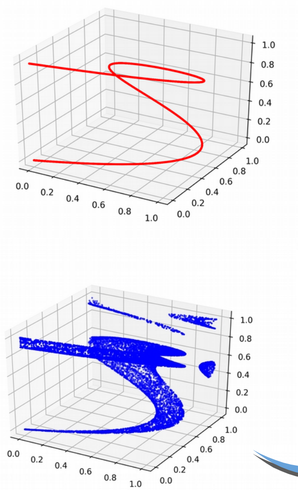

2 - Joining manifolds

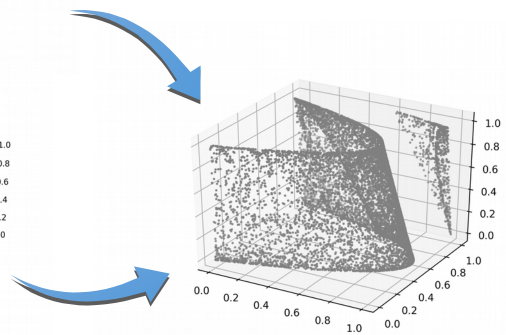

3 - Estimating dimensions

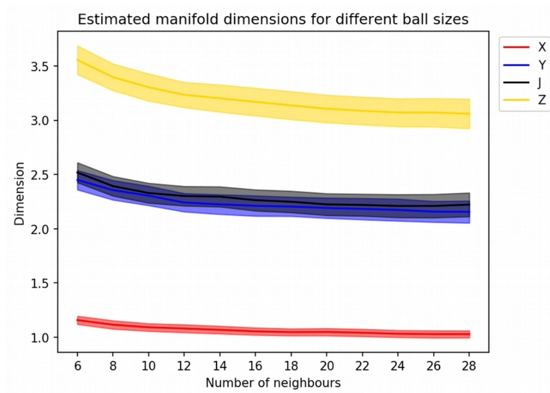

4 - Bootstrapping

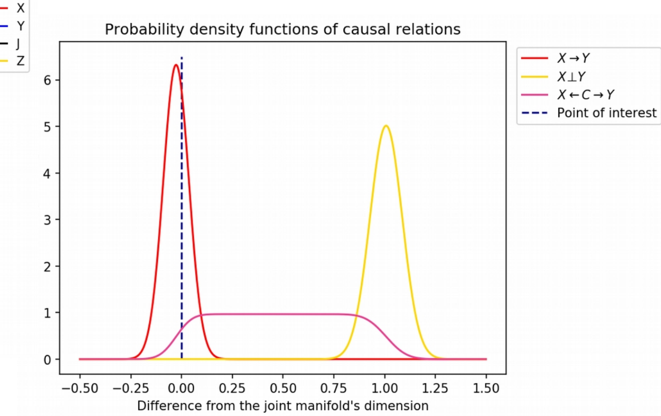

6 – Calculating causal relation probabilities

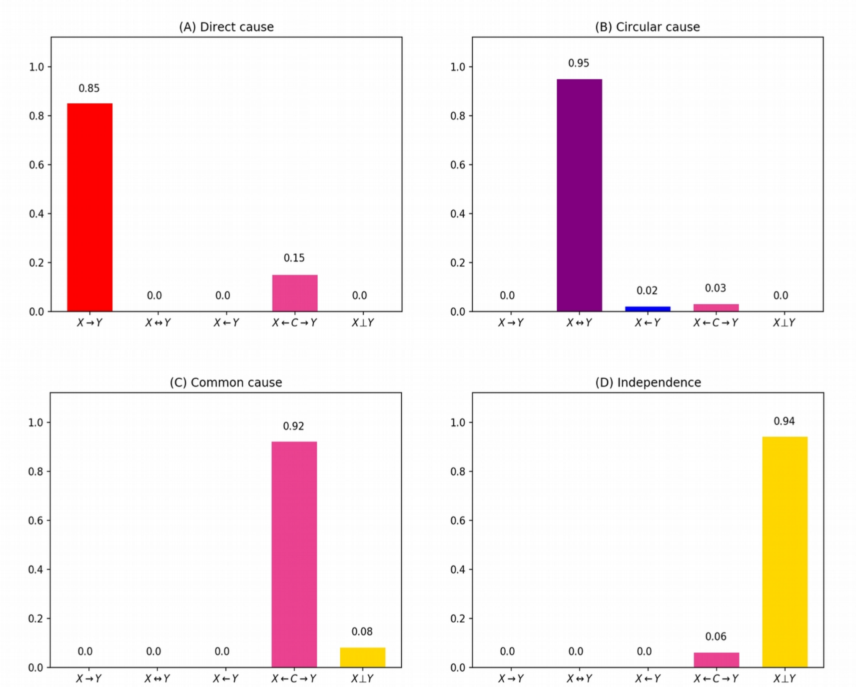

5 - Calculating conditional probabilities

Dimension estimates and probabilities of causal relations for different ball sizes

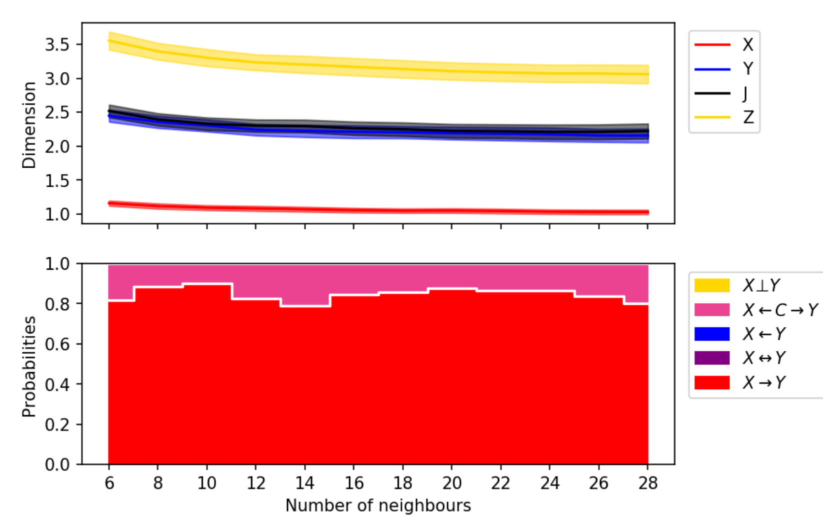

Test I.
Coupled logistic maps

3 Logistic maps coupled in all possible cases.
We used both linear and nonlinear couplings

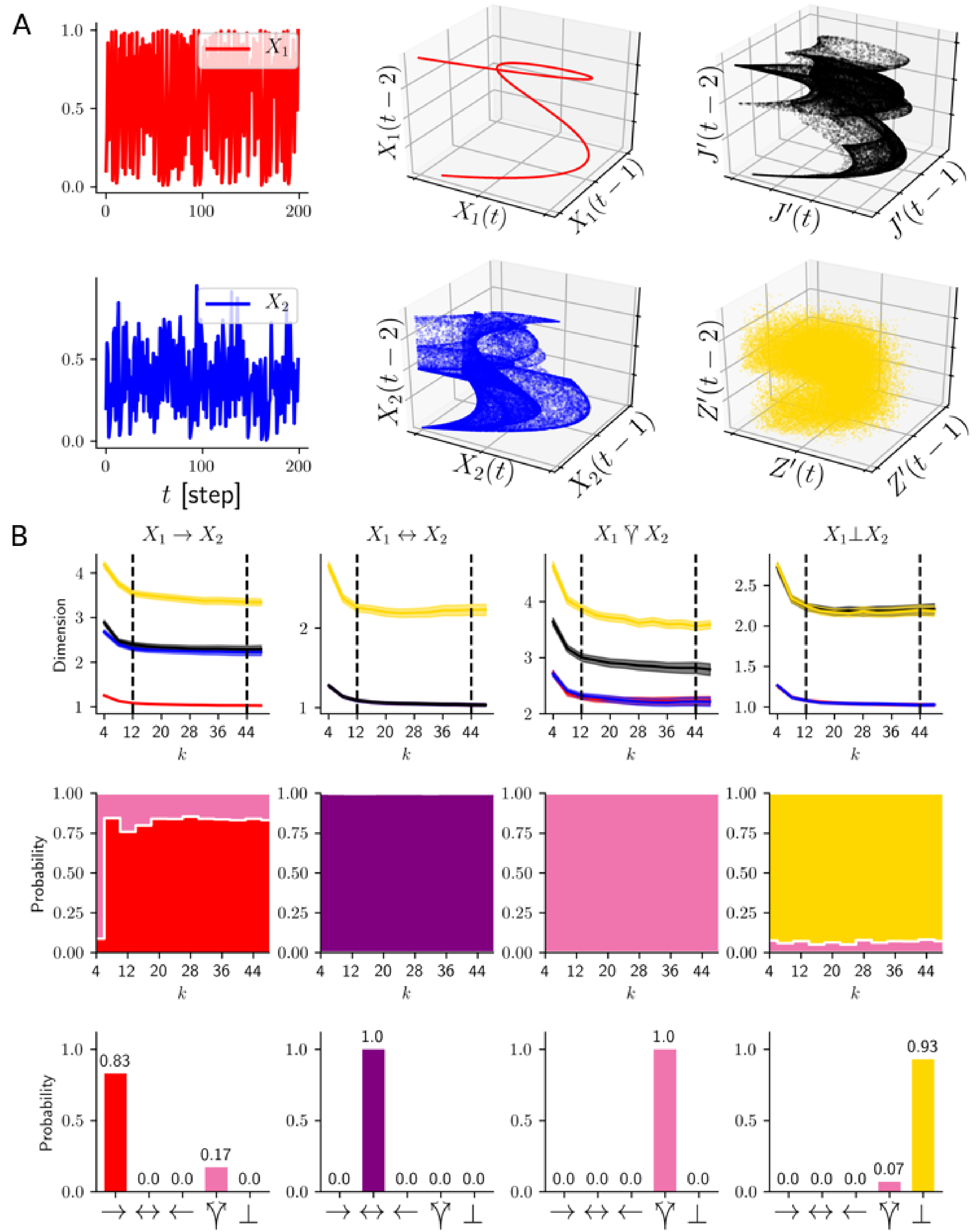

Comparison between 4 methods

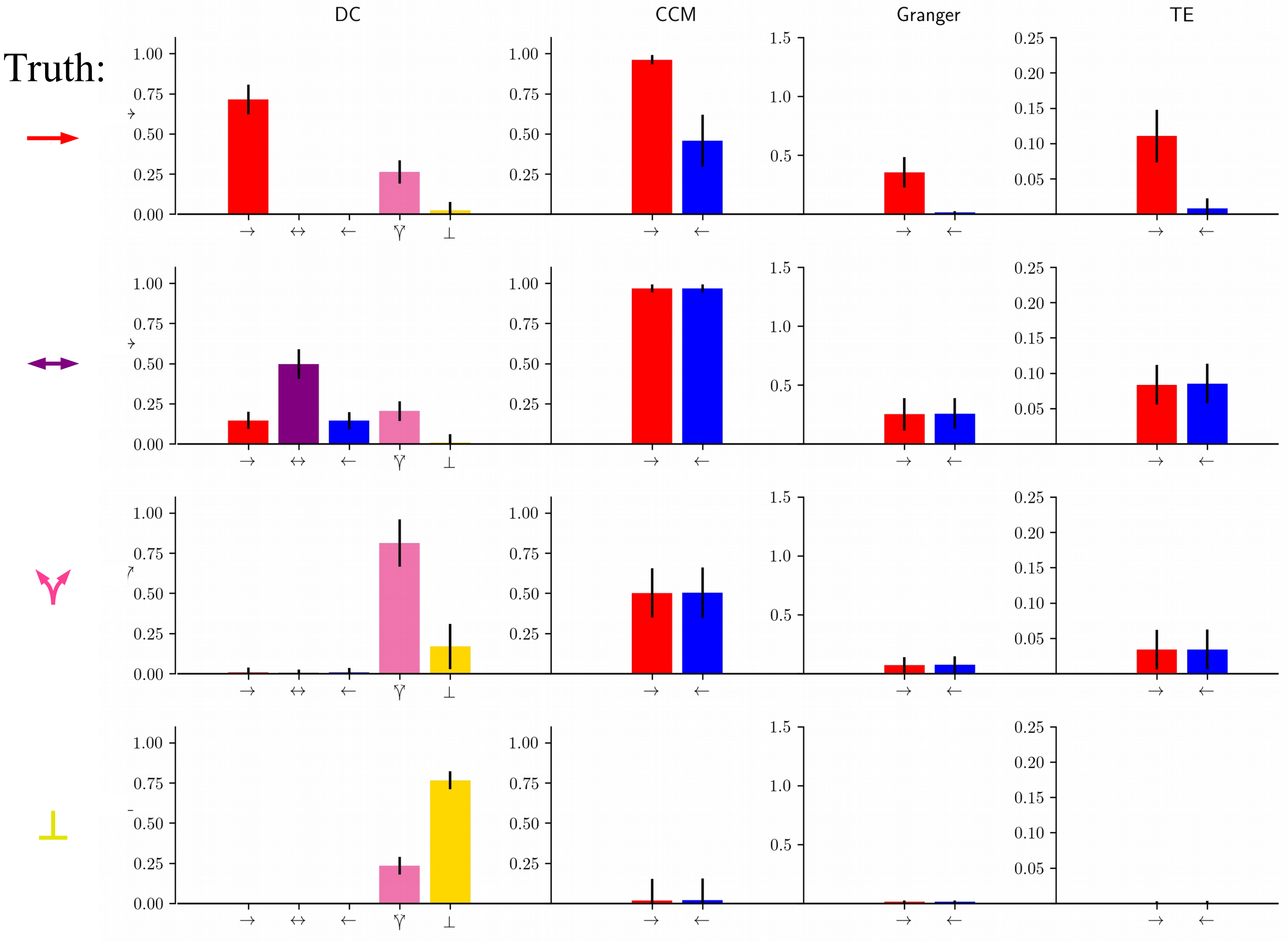

Comparison of the confusion matrices with Granger

Dimensional causality | Granger causality

Nonlinear coupling

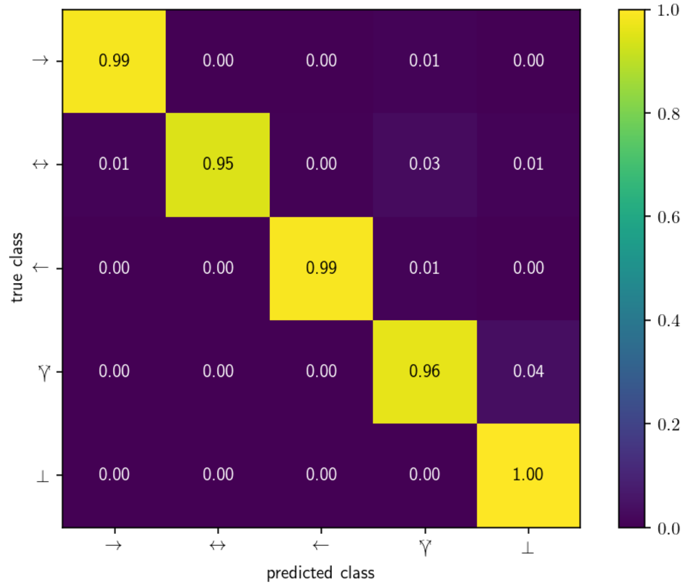

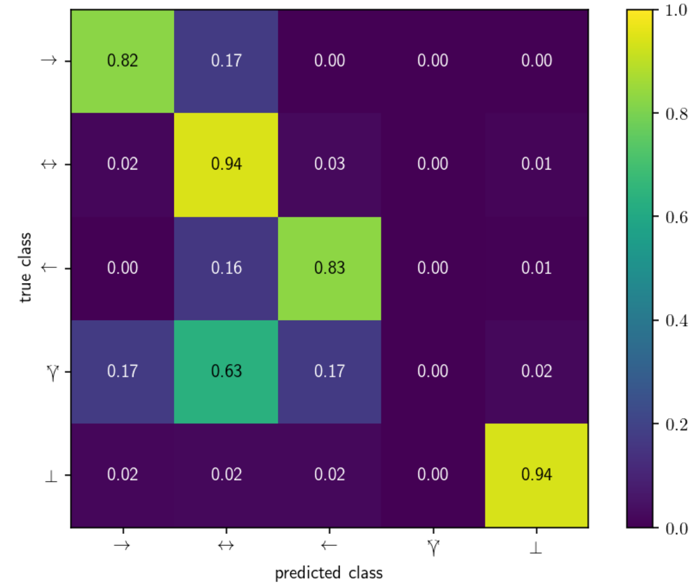

Linear coupling

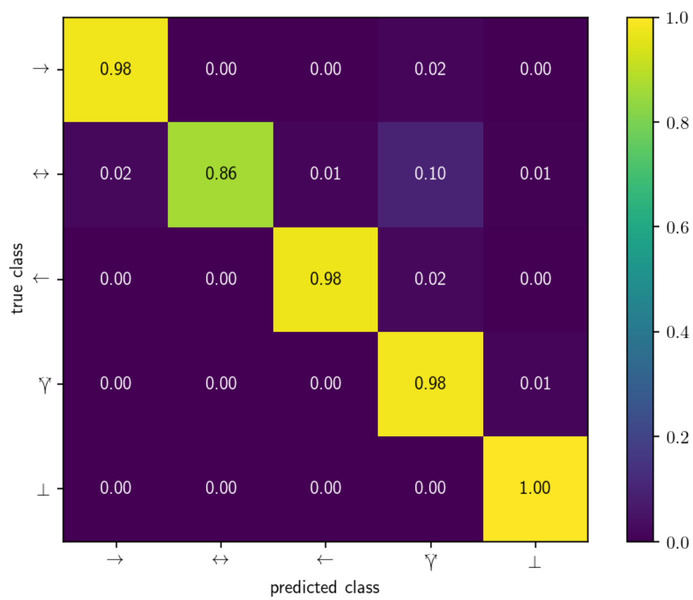

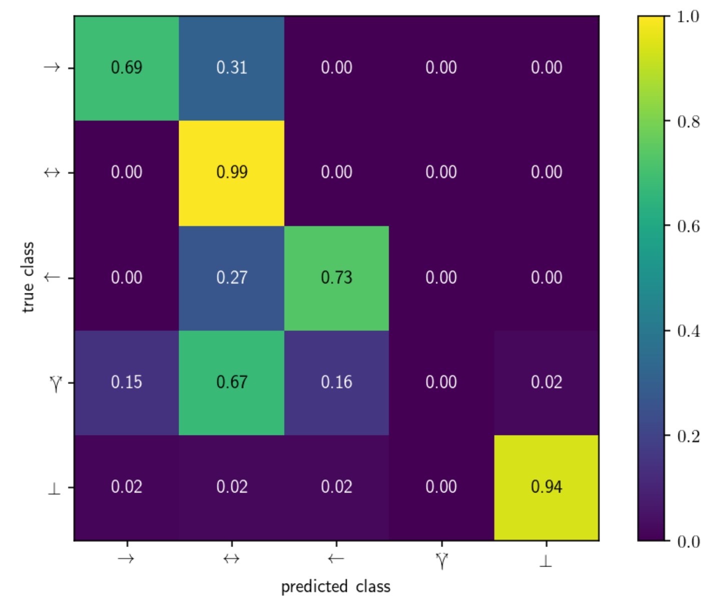

Test II. Coupled Lorentz systems

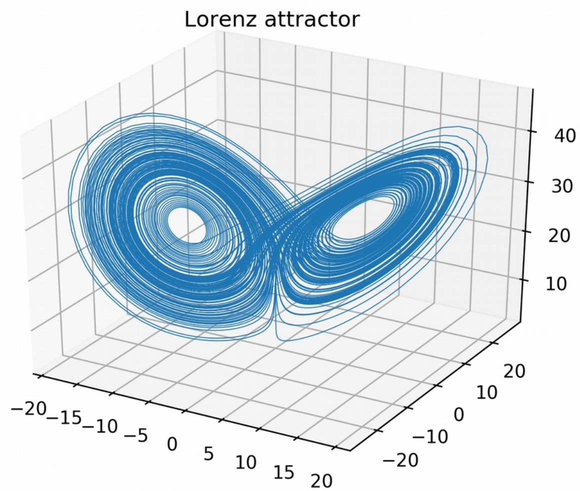

- 3 Lorenz systems: *X, Y, C*
- Each subsystem has 3 coordinates
- They are related through the first coordinates by a coupling

The system is defined by the following differential equations:

$$\dot{x}_1 = \sigma(x_2 - x_1) + m_{y\to x}(x_2 - y_1) + m_{z\to x}(x_2 - z_1)$$
$$\dot{x}_2 = x_1(\rho - x_3) - x_2$$
$$\dot{x}_3 = x_1 x_2 - \beta x_3$$

$$\dot{y}_1 = \sigma(y_2 - y_1) + m_{x\to y}(y_2 - x_1) + m_{z\to y}(y_2 - z_1)$$
$$\dot{y}_2 = y_1(\rho - y_3) - y_2$$
$$\dot{y}_3 = y_1 y_2 - \beta y_3$$

$$\dot{c}_1 = \sigma(c_2 - c_1)$$
$$\dot{c}_2 = c_1(\rho - c_3) - c_2$$
$$\dot{c}_3 = c_1 c_2 - \beta c_3$$

Causal relation probabilities

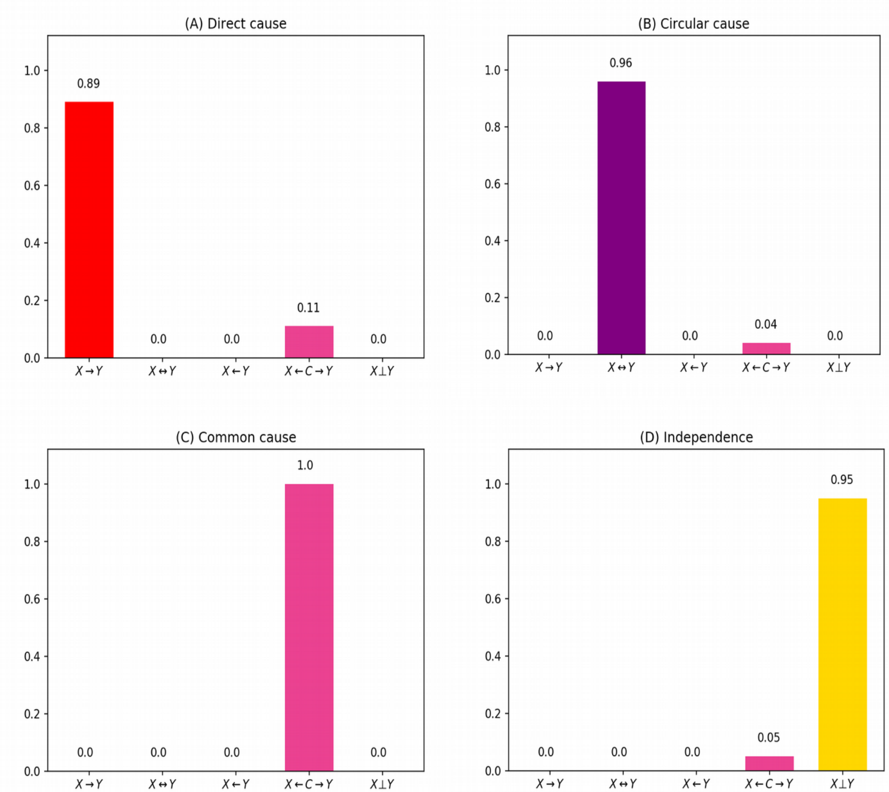

Test III: Hindmarsh-Rose model

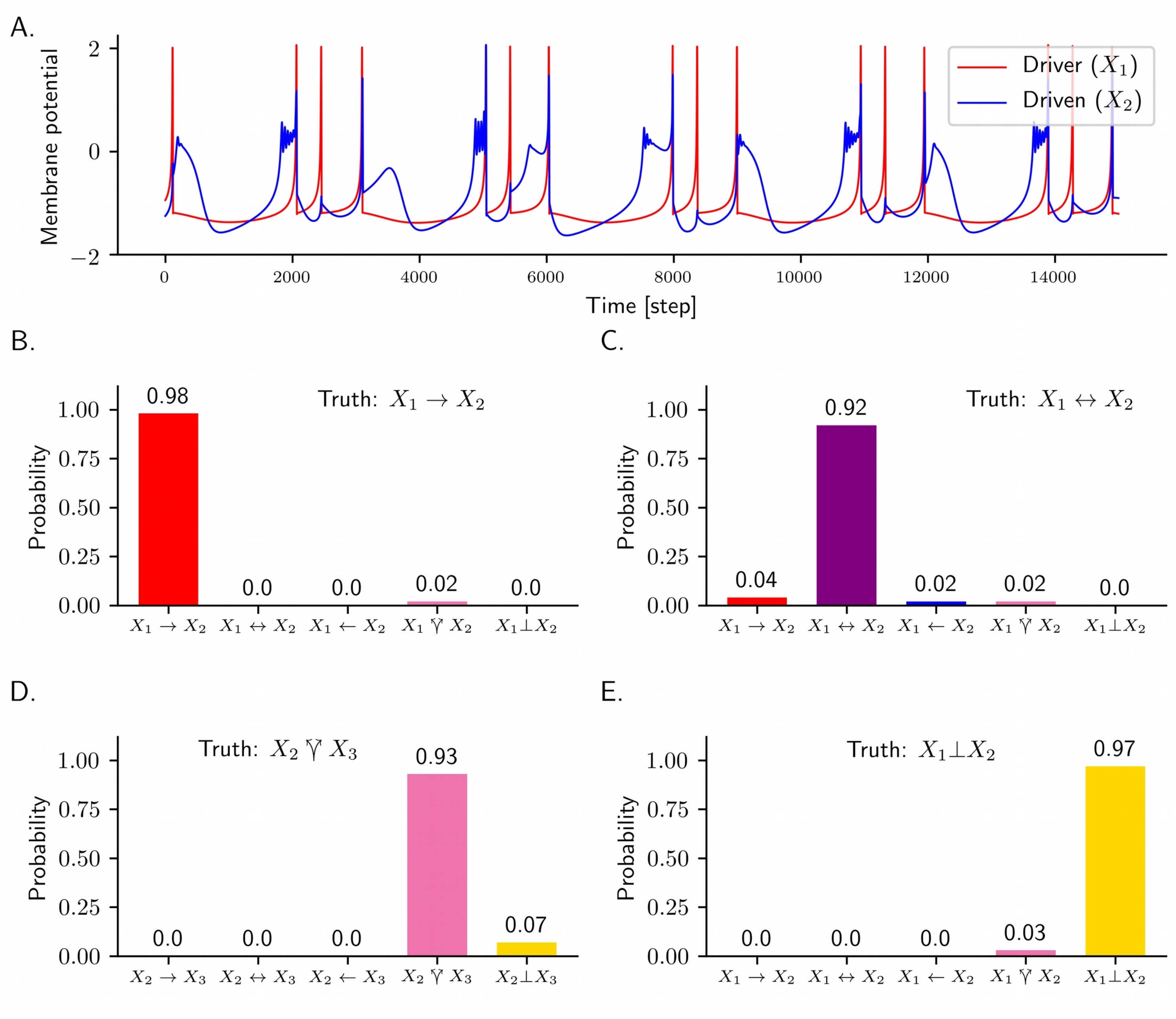

Intra- and inter hippocampal connectivity during seizure

In order to find out the lateralization of the seizure onset, two near-hippocampal electrodes inserted through the foramen ovale into the lateral ventricles.

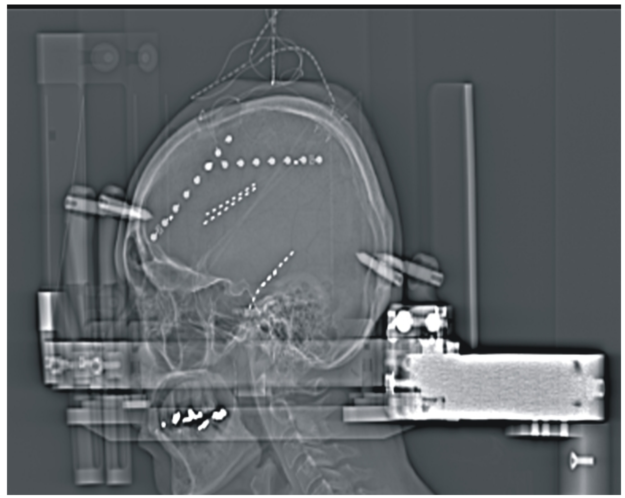

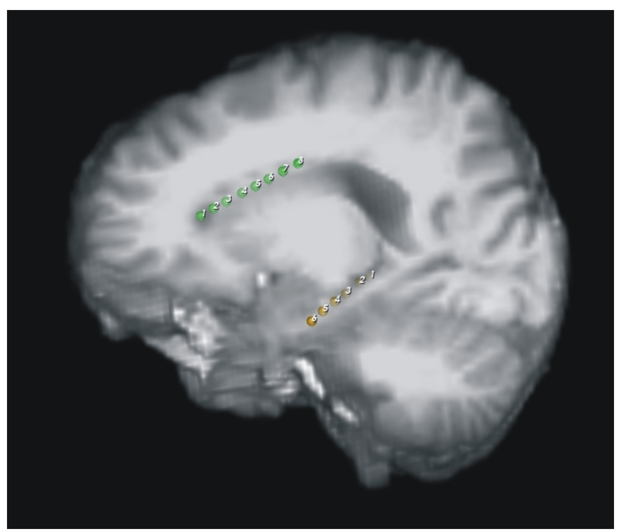

okiti

National Institute of Clinical Neurosiences

Péter Halász

Loránd Eröss

Dániel Fabó

László Entz

Boglárka Hajnal

Emilia Tóth

Márta Virág

Virág Bokodi

Real world test: Analysis of EEG during photostimulation

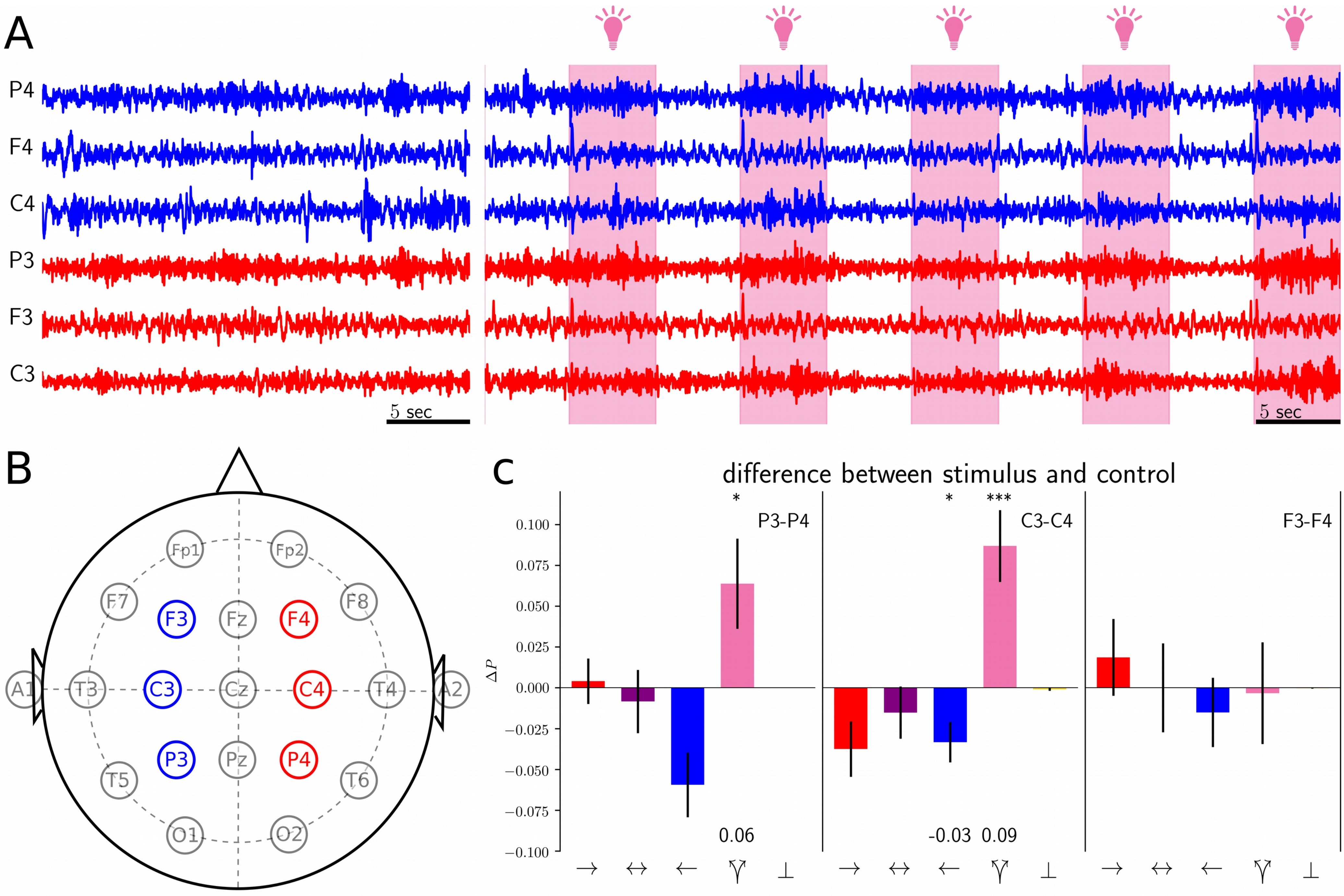

Application: localization the origin of the epilepsy

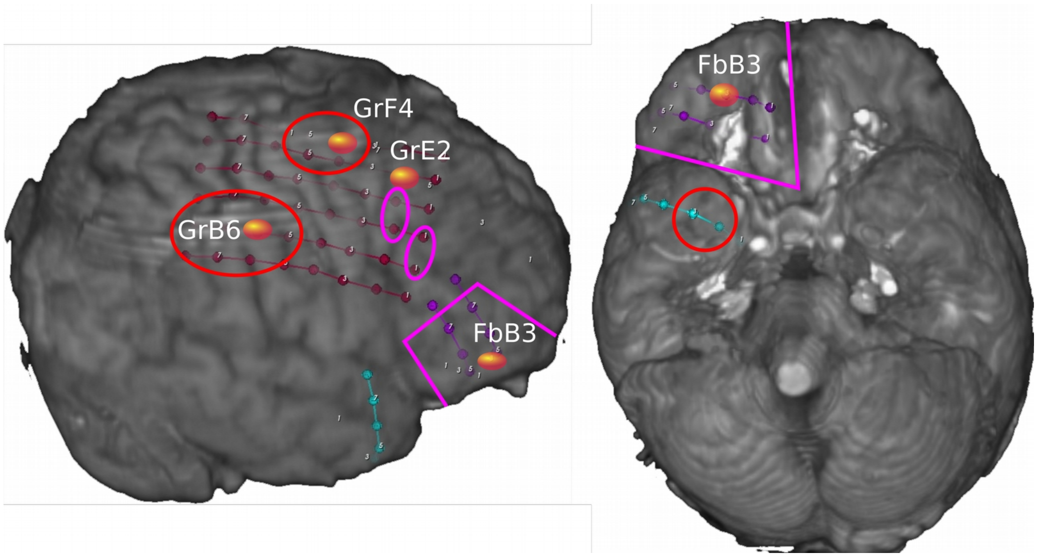

The 20-year-old patient suffered from a drug resistant epilepsy with frequent seizures.

The finding of a cortical dysplasia (at GrF4 electrode site) raised the possibility of the surgical treatment

GrB6 and GrF4 were only slightly involved (red ellipses). Based on the pronounced seizure activity, and the sensitive position of GrB6, only the frontal and orbitobasal parts were cut (purple signs).

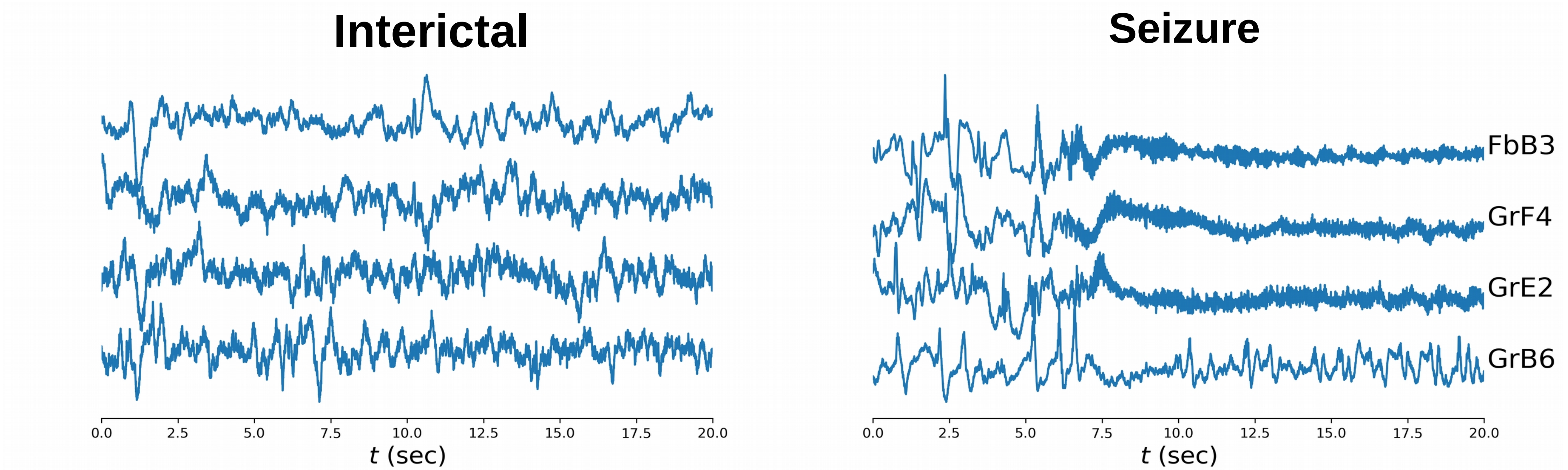

Application: localization the origin of the epilepsy

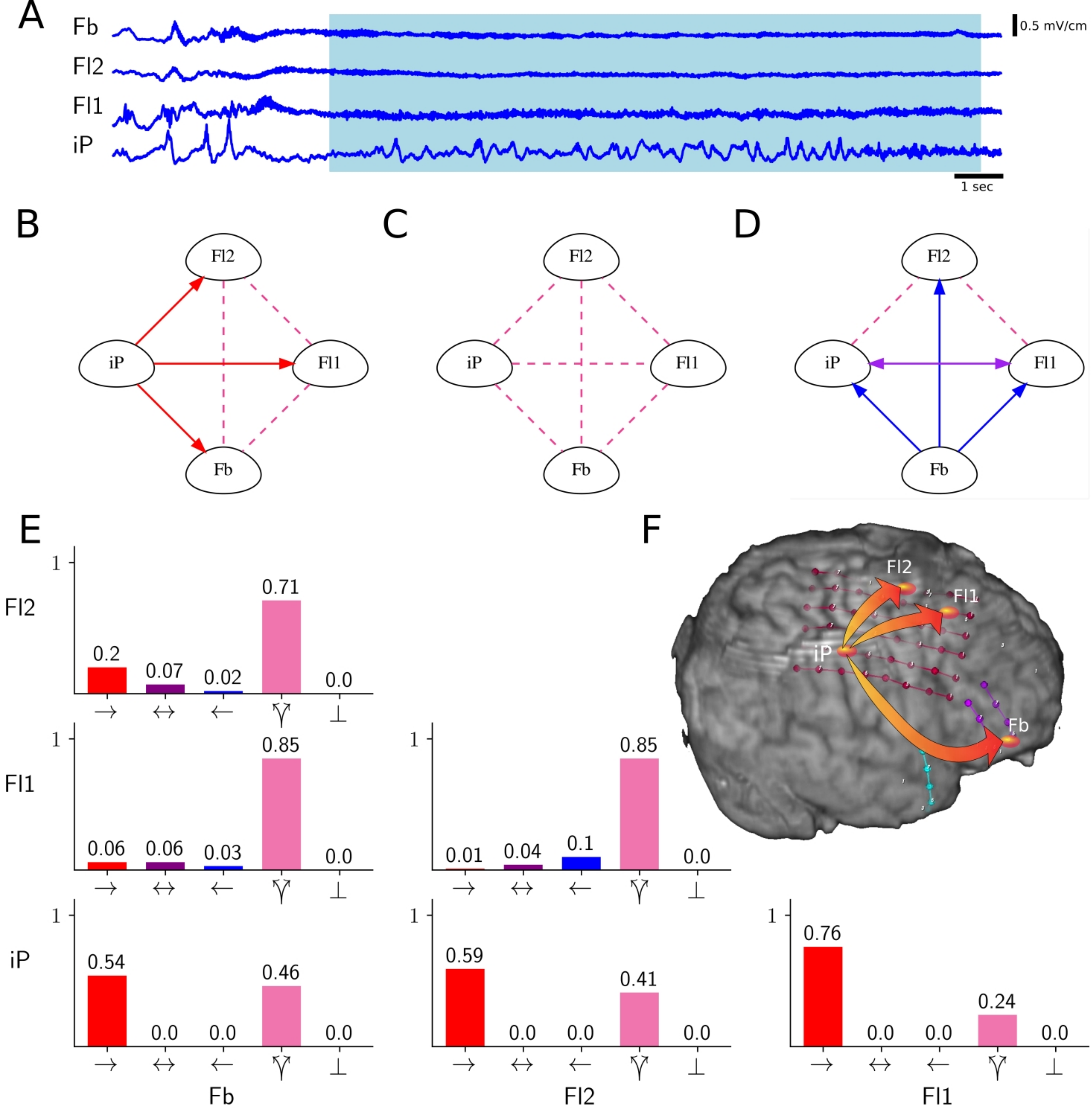

Interictal periods

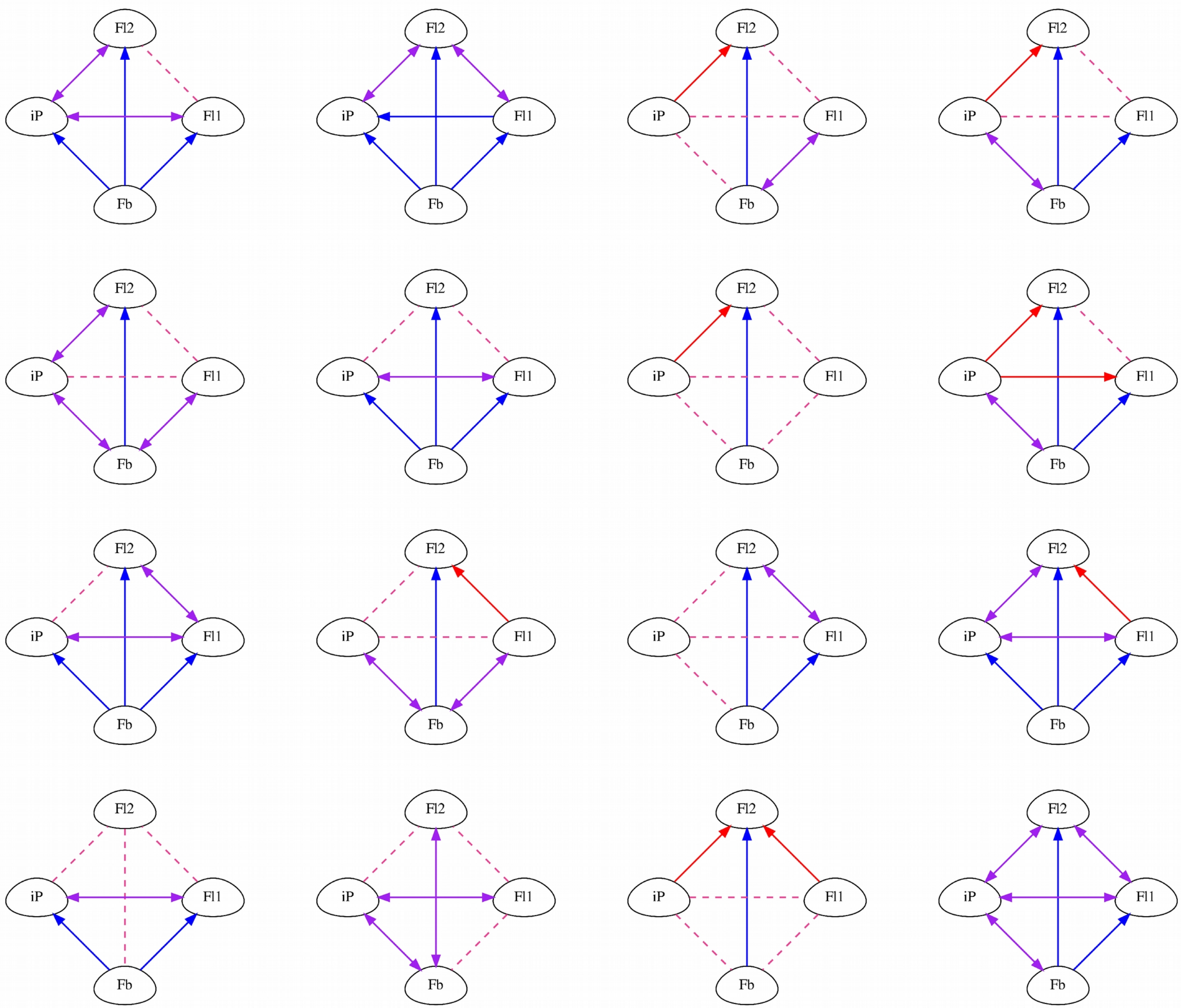

Multiple seizures

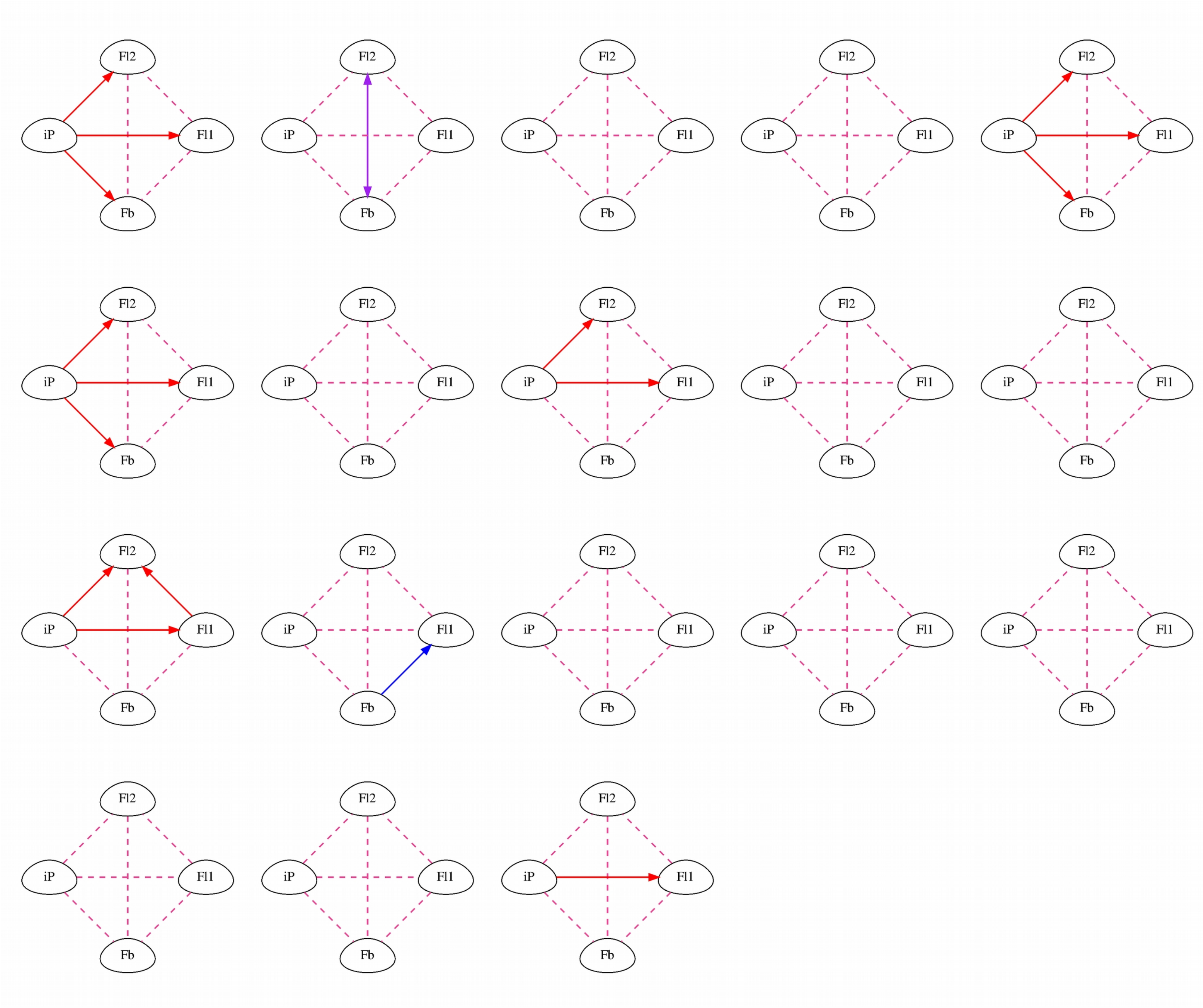

Future directions of methodical development

- Time and Delay dependent Dimensional Causality
- Dimensional Causality between point processes (spike trains) or between a continuous signal and a spike train
- Frequency resolved DC
- Reconstruction of the hidden common cause

Theoretical Neuroscience and Complex Systems Research Group

Acknowledgement

Péter Érdi

Fülöp Bazsó

László Négyessy

Marcell Stippinger

Dorottya Cserpán

László Zalányi

Zsigmond Benkő

Bálint File

This research was supported by grants NKFIH K113147

HUNGARIAN BRAIN RESEARCH PROGRAM
NEMZETI AGYKUTATÁSI PROGRAM

KTIA_ NAP_13-1-2013-0001

HBP CANON NKFIH NN118902

Thank you for your attention!